

REVIEW

Open Access



# Addressing the challenges of infectious bone defects: a review of recent advances in bifunctional biomaterials

Huaiyuan Zhang<sup>1†</sup>, Wenyu Qiao<sup>3†</sup>, Yu Liu<sup>4†</sup>, Xizhou Yao<sup>1</sup>, Yonghua Zhai<sup>2\*</sup> and Longhai Du<sup>1\*</sup>

## Abstract

Infectious bone defects present a substantial clinical challenge due to the complex interplay between infection control and bone regeneration. These defects often result from trauma, autoimmune diseases, infections, or tumors, requiring a nuanced approach that simultaneously addresses infection and promotes tissue repair. Recent advances in tissue engineering and materials science, particularly in nanomaterials and nano-drug formulations, have led to the development of bifunctional biomaterials with combined osteogenic and antibacterial properties. These materials offer an alternative to traditional bone grafts, minimizing complications such as multiple surgeries, high antibiotic dosages, and lengthy recovery periods. This review examines the repair mechanisms in the infectious microenvironment and highlights various bifunctional biomaterials that foster both anti—infective and osteogenic processes. Emerging design strategies are also discussed to provide a forward-looking perspective on treating infectious bone defects with clinically significant outcomes.

## Highlights

- Discussed the mechanisms of pathogenesis in infectious bone defects.
- Bifunctional biomaterials coordinate anti-infection and osteogenesis.
- Focused on the design of several bifunctional biomaterials.
- Explored the challenges and future prospects in the design and application of bifunctional biomaterials.

**Keywords** Infectious bone defects, Bifunctional materials, Bone tissue engineering, Antibacterial properties, Osteogenesis

<sup>†</sup>Huaiyuan Zhang, Wenyu Qiao and Yu Liu have contributed equally to this work.

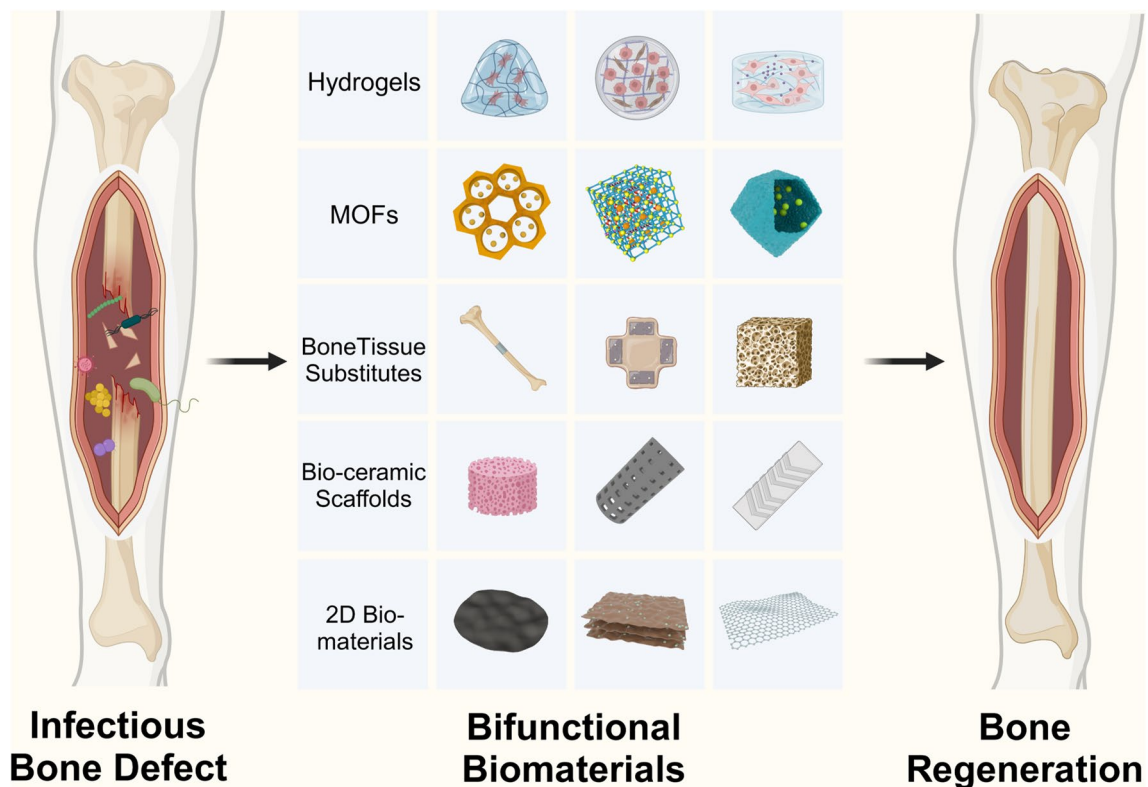
\*Correspondence:

Yonghua Zhai  
zhaiyonghua1201@126.com  
Longhai Du  
longhaidu123@163.com

Full list of author information is available at the end of the article



© The Author(s) 2025. **Open Access** This article is licensed under a Creative Commons Attribution 4.0 International License, which permits use, sharing, adaptation, distribution and reproduction in any medium or format, as long as you give appropriate credit to the original author(s) and the source, provide a link to the Creative Commons licence, and indicate if changes were made. The images or other third party material in this article are included in the article's Creative Commons licence, unless indicated otherwise in a credit line to the material. If material is not included in the article's Creative Commons licence and your intended use is not permitted by statutory regulation or exceeds the permitted use, you will need to obtain permission directly from the copyright holder. To view a copy of this licence, visit <http://creativecommons.org/licenses/by/4.0/>.

**Graphical Abstract****Introduction**

Bone tissue, a vital component of the human body, supports movement, protects organs, and serves as a primary site for hematopoiesis within bone marrow [1]. Structurally, bone is a dynamic composite material composed of organic and inorganic elements, containing living cells, extracellular matrix (ECM), blood vessels, and immune components, which together provide its remarkable regenerative capacity [2].

Bone defects caused by acute trauma (such as fractures), inflammatory diseases (including autoimmune and infectious diseases), age-related degenerative changes, and tumors are very common in clinical practice [3]. Although bone tissue possesses a certain degree of regenerative capacity, this ability is limited (commonly referred to as critical bone defects). For large bone defects that exceed the self-repair capability of bone tissue, bone grafting is typically required to achieve effective treatment outcomes [4]. Bone grafting primarily includes autologous and allogeneic bone grafts, as they possess fundamental properties that stimulate new bone growth, such as osteogenic capability, bone inductive

activity, and bone conductivity [5]. However, autologous bone grafting has limitations related to donor site availability and the risk of donor site injury, while allogeneic bone grafting carries risks of immune rejection and secondary infections [6]. Furthermore, the treatment strategies for bone defects arising from different pathological conditions also exhibit significant variations [7].

The difficulties in traditional treatment strategies lie in controlling infection and reconstructing bone defects, with antibacterial treatment being a prerequisite for bone regeneration [8]. When bone defects are complicated by infection, it can lead to disturbances in microenvironment regulation, repeated infections, and even progressive exacerbation, which can hinder tissue repair. This condition can easily develop into severe osteomyelitis, bone necrosis, and even trigger septicemia, posing a threat to the patient's life [9]. Intravenous administration often makes it difficult for local antibiotics to reach effective therapeutic concentrations. Prolonged systemic administration not only produces significant toxic side effects but also facilitates the development of resistant bacteria. Although antibiotic-impregnated spacers can

enhance local drug concentrations and promote grafting through membrane induction, they require a second surgery approximately six weeks post-operation to remove the spacers [10, 11]. Bone transport techniques are an effective approach for treating bone defects; however, the treatment duration is lengthy, typically exceeding 10 months [12–14]. Additionally, traditional bone repair materials have been widely applied in clinical settings. However, their clinical performance remains unsatisfactory, such as poor mechanical properties, rapid absorption rates, and limited bone induction capabilities [15–17]. Therefore, there is an urgent need to develop new bone substitute materials to meet the clinical demands of bone repair. These materials must possess the following properties: osteogenic capacity, bone induction, bone conduction, biocompatibility, and biodegradability [18]. Osteogenic capacity refers to the ability of host and donor cells contained in the materials to synthesize new bone. Bone induction refers to the ability of materials to promote the differentiation of primitive pluripotent stem cells into mature osteoblasts. Bone conduction indicates the capacity of osteogenic and pre-osteogenic cells to attach to the implanted materials and migrate and grow within the three-dimensional space of the materials [19]. Furthermore, during the process of filling bone defects, new materials should also be able to mimic the structural, mechanical, and biological characteristics of natural bone, which may improve clinical outcomes for patients with bone defects and alleviate their suffering and economic burden in clinical practice [16, 20]. Consequently, the repair of inflammatory bone defects has remained a major challenge in orthopedic treatment, which not only leads to lasting physical and psychological harm for patients but also imposes a significant economic burden [21].

As mentioned earlier, if anti-infection therapy and the promotion of bone defect repair cannot be balanced, the therapeutic effect will be significantly reduced [22, 23]. Thus, dual-function biomaterials—combining antibacterial and osteogenic properties—offer promising solutions for treating infectious bone defects. These materials not only prevent infection at the defect site but also promote the regeneration of bone tissue, representing a significant advancement in bone defect repair [24–27]. For example, bioactive glasses (BGs) are multifunctional biomaterials that induce osteogenesis and angiogenesis [28]. A study by Kittipat et al. developed mesoporous bioactive glass composites loaded with antibacterial cinnamaldehyde (CIN), which demonstrated significant antibacterial activity against *Staphylococcus aureus* (*S. aureus*) and *Escherichia coli* (*E. coli*), while promoting bone tissue regeneration without affecting the proliferation of osteoblast-like MG-63 cells [29]. Therefore, the intervention of

dual-function biomaterials will open a new chapter in the repair strategy for infectious bone defects.

In general, the occurrence and healing of bone defects are closely related to inflammatory responses. Excessive acute inflammation caused by infection increases the risk of bone healing [30]. Therefore, to design more targeted dual-function biomaterials, it is essential to have a comprehensive understanding of the mechanisms underlying infectious bone defects and their local microenvironments. In this review, we will analyze the roles of different cells and inflammatory factors in the formation of new bone during the progression of bone defects, providing a theoretical basis for controlling infection and promoting osteogenic therapy. Based on this, we will summarize dual-function biomaterials with antibacterial and osteogenic properties and conduct an in-depth discussion. Finally, we will explore the development potential of future dual-function materials, offering innovative and feasible solutions for the treatment of infectious bone defects, and providing scientific and precise theoretical support and practical guidance for clinical treatment.

### Pathological processes of infectious bone defects

Bone healing is a complex process of reconstruction that occurs after a bone defect [31]. It can be categorized into primary bone healing and secondary bone healing, with primary bone healing being relatively rare. Secondary bone healing consists of three overlapping stages: the inflammatory phase, the repair phase, and the remodeling phase, with the initial inflammatory phase being crucial for bone healing [32]. Each phase involves precise interactions among various immune cells, cytokines, and growth factors, ensuring a coordinated response to injury.

### Physiological processes in bone healing

The process of bone healing can be further subdivided into six minor stages (Fig. 1). Once a bone defect occurs, the inflammatory response begins immediately. Hemorrhage beneath the periosteum and in the soft tissue leads to the formation of a hematoma. The microenvironment of the hematoma is initially characterized by localized hypoxia, acidity, and lower temperatures, with a high concentration of calcium and lactic acid [34]. During this process, the hematoma serves as a scaffold to recruit inflammatory cells and various factors to initiate a cascade reaction. Numerous inflammatory cytokines and growth factors are involved in this stage, including interleukin-1 (*IL-1*), interleukin-6 (*IL-6*), interleukin-11 (*IL-11*), and tumor necrosis factor- $\alpha$  (*TNF- $\alpha$* ), which promote the migration of inflammatory cells (such as neutrophils and macrophages) to the fracture site and induce angiogenesis [35, 36]. The secretion of these

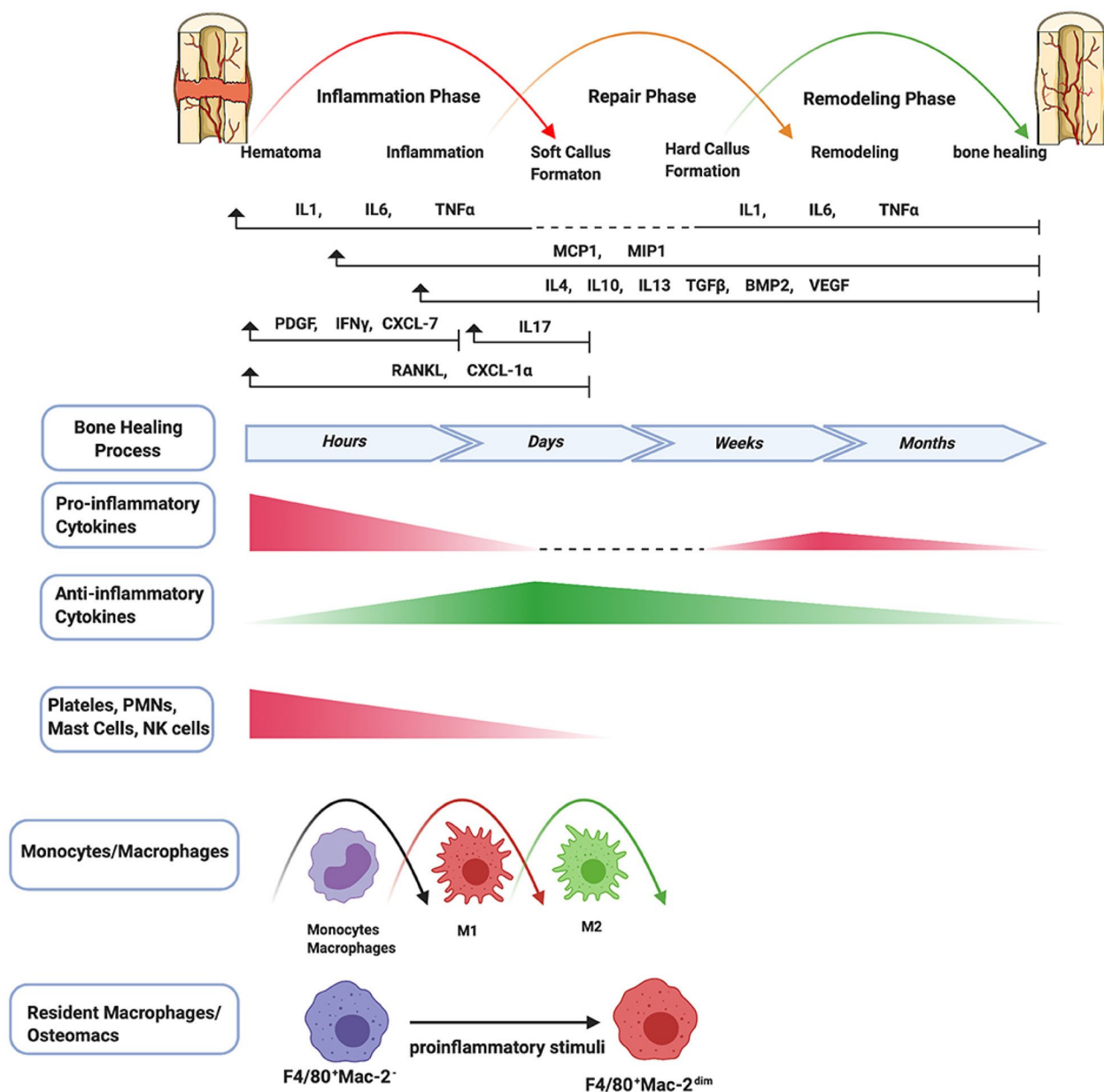


**Fig. 1** This describes the various stages of the bone healing process, as well as the expression patterns of related immune cells and cytokines/growth factors. Bone healing consists of three phases: inflammation, repair, and remodeling, which include six steps: hematoma formation, inflammatory response, soft (fibrocartilaginous) and hard callus formation, remodeling, and final healing. In the inflammatory phase, immune cells (like neutrophils, natural killer cells, mast cells, and platelets) are activated and release cytokines and chemokines to recruit monocytes and macrophages, essential for healing. Key pro-inflammatory cytokines such as *IL-1*, *IL-6*, and *TNF-α* play significant roles throughout the phases. *TNF-α* levels rise during the repair phase and remain elevated during remodeling, while the inflammatory response subsequently shifts to an anti-inflammatory state marked by *IL-4*, *IL-10*, and *IL-13*, which are crucial for fracture healing. Copyright © 2020 Maruyama, Rhee, Utsunomiya, Zhang, Ueno, Yao and Goodman [33]

factors typically peaks around 24 h and is completed in about 7 days [37]. Among the interleukins, *IL-1* is the most important cytokine in bone healing and is primarily produced by macrophages. *IL-1* has functions such as inducing osteoblasts to produce *IL-6*, promoting the

generation of bone healing tissue, and facilitating angiogenesis at the injury site (achieved by activating *IL-1RI* or *IL-1RII*) [38, 39]. *IL-6* is produced only during the acute phase, stimulating angiogenesis, the production of vascular endothelial growth factor (*VEGF*), and the

differentiation of osteoblasts and osteoclasts [40–42]. Meanwhile, macrophages polarize towards the *M1* phenotype, and the immune response shifts to adaptive immunity, primarily characterized by the infiltration of lymphocytes. At the same time, fibroblasts also begin to gather at the site of injury [43]. Additionally, *TNF- $\alpha$*  has been demonstrated through multiple experiments to induce the osteogenic differentiation of mesenchymal stem cells (*MSCs*), which is crucial for subsequent bone healing [44]. Platelets and perivascular cells release several cytokines, such as platelet-derived growth factor (*PDGF*) and transforming growth factor-beta (*TGF- $\beta$* ), which help promote angiogenesis and osteogenic differentiation [45]. During the resolution of inflammation, macrophages transform into *M2* phenotype under the induction of anti-inflammatory cytokines (*IL-4*, *IL-10*, and *IL-13*).

To promote stable bone regeneration, it is crucial to recruit sufficient bone marrow-derived mesenchymal stem cells (*BMSCs*) to the defect site [46]. *BMSCs*, known for their pluripotency and self-renewal capabilities, play a pivotal role in osteogenesis [47, 48]. Factors such as *TNF- $\alpha$*  and stromal cell-derived factor 1 (*SDF-1*) have been shown to attract *BMSCs* to injury sites [49, 50].

Currently, a large number of studies have shown that *SDF-1* and its G protein-coupled receptor *CXCR-4* form an axis (*SDF-1/CXCR-4*), which is an important regulatory factor for the recruitment and homing of *BMSCs* to the injury site [51–55]. Under the influence of pro-inflammatory cytokines, anti-inflammatory cytokines, *TGF- $\beta$* , bone morphogenetic proteins (*BMP*), and growth factors (such as *VEGF*, *PDGF*), and fibroblast growth factor-2 (*FGF-2*), immune cells and *BMSCs* participate in the intercellular regulation to initiate the processes of osteogenesis and angiogenesis [56, 57].

Subsequently, the injury site enters the repair phase. The formation of granulation tissue involves two types of processes: intramembranous ossification and endochondral ossification [58]. The former is relatively rare and occurs on the periosteum, where *BMSCs* differentiate into osteoprogenitor cells, which then proliferate and differentiate into osteoblasts, directly forming woven bone. This process is continuous and is commonly observed in flat bones such as those in the skull and the clavicle [59]. The latter is the primary mechanism of bone repair, occurring within the endosteum and bone marrow, where *BMSCs* differentiate into chondrocytes and secrete cartilage matrix to form a cartilage template. Subsequently, chondrocytes undergo hypertrophic differentiation, leading to the mineralization of the surrounding matrix and the formation of cartilage granulation tissue. Ultimately, hypertrophic chondrocytes undergo apoptosis, resulting in vascular invasion and the migration

of osteoblasts. Afterward, the cartilage matrix is transformed into bone matrix [60]. During this stage, the levels of pro-inflammatory factors such as *IL-1* and *IL-6* significantly decrease or are no longer detectable, while *TNF- $\alpha$*  initially decreases but later increases, meticulously regulating the proliferative activities of osteoblasts and shaping the overall healing response [50].

As the chondrocytes in the fracture granulation tissue proliferate, they become hypertrophic, and the ECM begins to calcify. During the period of 10 to 14 days, bone repair enters the stage of primary bone callus formation, with the formation of hard granulation tissue reaching its peak. The calcified cartilage is replaced by woven bone, making the granulation tissue stronger and mechanically stiffer [61]. Although the hard callus is a rigid structure that provides biomechanical stability, it does not fully restore the biomechanical properties of normal bone. To achieve complete restoration, the fracture healing process enters the second absorption phase, where the hard granulation tissue is remodeled into a layered bone structure with a central medullary cavity [62]. This phase is primarily regulated by *IL-1* and *TNF- $\alpha$* , both of which exhibit high expression levels during this stage. Meanwhile, the content of the *BMP* family, represented by *BMP-2*, also increases, while the expression levels of most members of the *TGF- $\beta$*  family decrease [63, 64]. During this period, the trabecular bone in the damaged area undergoes remodeling under the influence of mechanical stress. The combined action of osteoblasts and osteoclasts gradually eliminates the callus outside the stress axis, thereby facilitating bone healing. This process may take several years to achieve complete regeneration of the skeleton; however, in younger patients, the healing process is typically accelerated [65]. The original callus is gradually replaced by solid lamellar bone, completing the creeping substitution process of the new bone. In addition, growth factors such as epidermal growth factor (*EGF*) and fibroblast growth factor (*FGF*) also promote angiogenesis and the maturation of chondrocytes during bone repair and reconstruction [33]. Successful bone remodeling requires adequate blood supply and gradually increasing mechanical stability. If these conditions are not met, atrophic nonunion may occur [66, 67]. Conversely, when the vascular condition is good but fixation is unstable, it can lead to hypertrophic nonunion or pseudarthrosis [68].

As mentioned above, inflammation is the critical first step in bone healing. The absence or suppression of acute inflammation can lead to impaired bone healing [69–71]. Research on *MIF* mice (macrophage migration inhibitory factor gene-deficient mice, *MIF KO*) and immune-compromised *NOD/scid-IL2R $\gamma$*  null mice has shown that deficiencies in immune function can impair bone



healing, highlighting the importance of an intact immune response for effective bone repair [72–76]. Additionally, multiple pro-inflammatory cytokines and chemokines, such as *IL-6*, *IL-17A*, and *TNF- $\alpha$* , play crucial roles in the complex cascade of bone fracture healing [77–79]. For example, *IL-6* signaling is involved in immune cell recruitment, angiogenesis, endochondral ossification, and granulation tissue remodeling [80]. *IL-17A* enhances the activity of osteoblasts involved in bone tissue formation, while *TNF- $\alpha$*  has a biphasic secretion pattern and can enhance the activation of *BMSCs* [49, 81]. Furthermore, prostaglandins like Prostaglandin E2 (*PGE2*) and non-steroidal anti-inflammatory drugs (*NSAIDs*) that block *COX-2* can adversely affect bone healing [82–85]. Glucocorticoids, although powerful anti-inflammatory agents, can delay bone repair and cause osteoporosis [86, 87]. These findings underscore the crucial role of inflammation in bone healing.

### Microenvironment of Infectious Bone Fractures

The microenvironment of infectious bone fractures is complex and often leads to an intense inflammatory response that disrupts normal bone healing [88, 89]. This section will discuss the relationship between local inflammation and bone regeneration, as well as analyze the effects of infection on the ECM, osteoblasts, and osteoclasts.

The most common bacterium responsible for bone infections is *S. aureus*. Its primary infection mechanisms include intracellular infection, osteocyte lacunar canalicular network (OLCN) invasion, biofilm formation, and abscess formation (Fig. 2) [90]. This bacterium can proliferate in various cell types, including but not limited to macrophages, keratinocytes, epithelial cells, endothelial cells, osteoclasts, osteoblasts, and bone cells [91]. After invading the osteoblasts, fibronectin connects the fibronectin-binding proteins A or B (*FnBPA* or *FnBPB*) on the surface of *S. aureus* cells with the  $\alpha 5 \beta 1$  integrin on osteoblasts. This interaction facilitates bacterial internalization [92]. Since osteoblasts are not immune cells, *S. aureus* can survive for a long time within these cells, rendering internalized cells less sensitive and allowing them to evade clearance by the immune system and killing by antibiotics. The infected cells become a reservoir that subsequently releases pathogens, continuing to infect other cells [93, 94]. Research has indicated that osteoblasts can secrete a certain number of antimicrobial peptides; however, without proactive and effective treatment, the damaged area may progress to a chronic infection [95, 96].

Although *S. aureus* has a diameter of approximately 1  $\mu\text{m}$ , it can alter its size to 100–600 nm to invade the

OLCN, which has a diameter of 0.5  $\mu\text{m}$  [97–101]. This submicron-level invasiveness allows the bacteria to evade immune cells and survive long-term in the bone. Additionally, high-dose antibiotics struggle to achieve effective concentrations within the OLCN, highlighting the need for biomaterials that can resist bacterial invasion.

Biofilm formation is another significant challenge. *S. aureus* adheres to bone surfaces using cell wall proteins, adhesins, eDNA, and microbial surface components recognizing adhesive matrix molecules (MSCRAMM). These components interact with proteins and polysaccharides in the bone cell ECM, such as type I collagen and osteopontin, forming binding sites [102–105]. The bacteria then produce extracellular polymeric substances (EPS) that protect and promote their growth, leading to a dense biofilm structure that shields them from antimicrobial agents and immune cells [106, 107]. Therefore, developing materials that can inhibit and eliminate biofilms is essential.

Furthermore, EPS degradation allows free bacteria to colonize new areas and form new biofilms [108]. Persistent *S. aureus* infections can lead to staphylococcal abscess communities (SACs), which affect the bone marrow and surrounding soft tissues of implants [109]. The bacteria form a fibrin pseudo-capsule using coagulase (*CoA*) and von Willebrand factor-binding protein (*vWbp*), attracting immune cells and causing their necrosis, thus creating a barrier that prevents new immune cells from entering and forming a bacterial sanctuary [110–112]. Once an abscess forms, the probability of spontaneous recovery without targeted antibacterial strategies is very low [113]. Developing biomaterials that can disrupt the fibrin pseudo-capsule is a promising approach for treating abscesses.

The balance between bone regeneration and bone resorption is crucial for maintaining local bone mass in the area of bone defects and for reconstructing normal bone tissue structure [114]. At the microscopic level, infectious bone defects exhibit elevated levels of inflammatory cells compared to sterile bone injuries, with various pro-inflammatory factors such as *IL-1 $\beta$*  significantly increased [115]. These factors can enhance the activity of osteoclasts, leading to increased bone resorption, while inhibiting the function of osteoblasts, thereby hindering the biological processes of bone regeneration [116]. Clearly elucidating the molecular interactions between pathogens, immune cells, and various bone cells within the infectious microenvironment, as well as the mechanisms of bone regeneration, holds significant research importance and clinical value. The influence of immune cells on bone regeneration in the infectious microenvironment is particularly noteworthy.

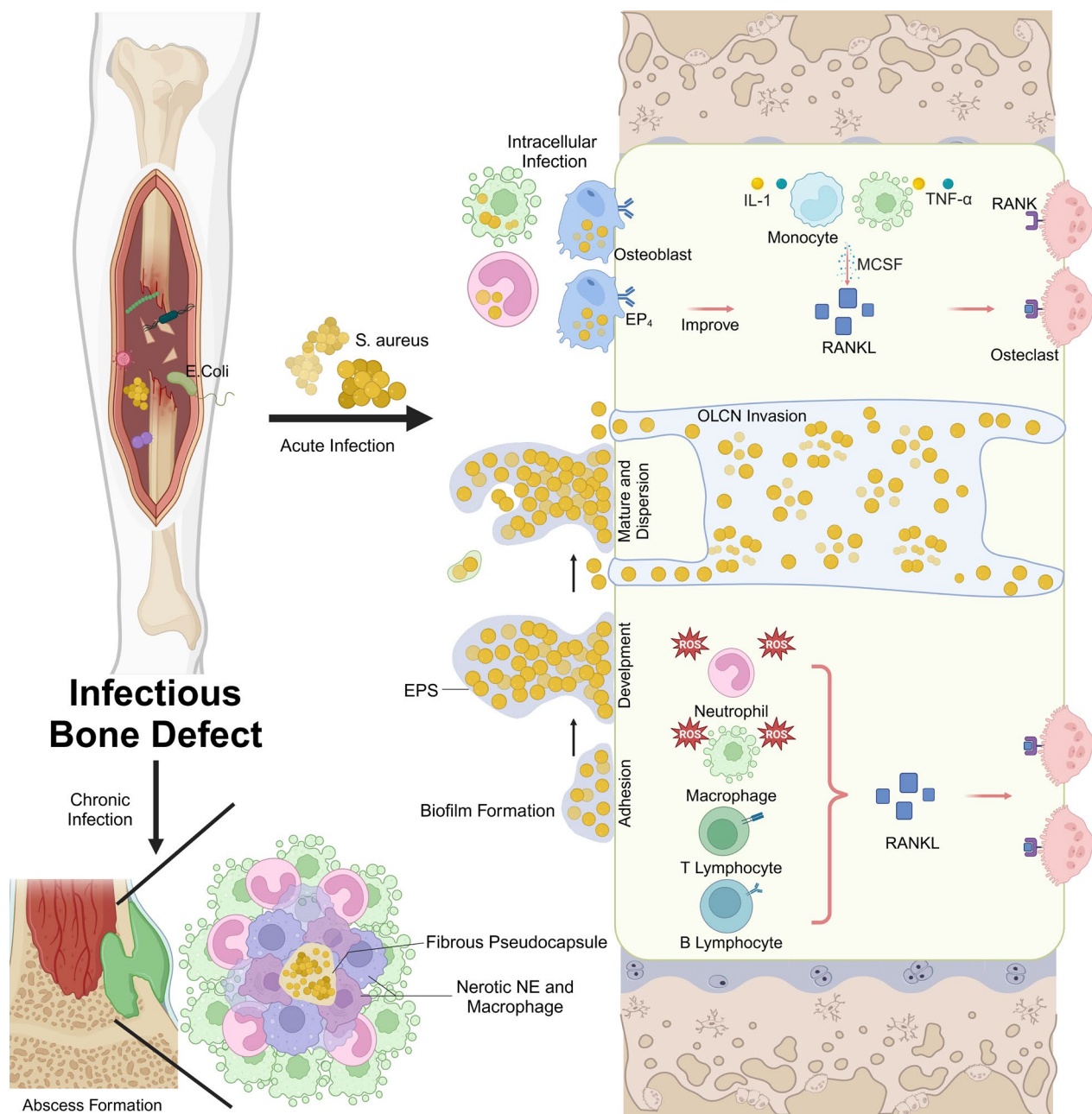


**Fig. 2** Schematic diagram of the key pathogenic mechanisms of infectious microorganisms in bone defects and their partial immune regulatory effects in the bone marrow cavity. (Created with BioRender.com)

Neutrophils (NE) are highly active phagocytic cells that rapidly accumulate during the early stages of pathogen invasion. They migrate to the site of infection through various chemokines, moving through the gaps between endothelial cells to form neutrophil extracellular traps (NETs), where they perform functions such as phagocytosis, reactive oxygen species (ROS) production, and degradation of pathogens by granzyme [117].

However, the excessive accumulation of NE can often lead to side effects such as a high-oxygen environment induced by ROS, resulting in cytotoxicity, bone tissue damage, and bone loss [118, 119]. Additionally, NE expresses elevated levels of receptor activator of nuclear factor- $\kappa$ B ligand (RANKL) in response to stimuli from pathogenic virulence factors like LPS. By binding to the receptor activator of nuclear factor- $\kappa$ B (RANK) on

pre-osteoclasts, *RANKL* induces the differentiation and maturation of osteoclasts, thereby promoting bone resorption [120]. Besides *NE*, macrophages, activated T cells, and B cells are also capable of releasing substantial amounts of *RANKL* in vivo, further inducing bone resorption and bone loss [121].

In addition to *NE*, macrophages also play a role in the early stages of infection. As mentioned earlier, macrophages are a major source of cytokines and release large amounts of *TNF- $\alpha$*  and *IL-1* to activate endothelial cells and lymphocytes to gather at the site of infection. At the same time, macrophages induce endothelial cells to form P-selectin, recruiting *NE* to the infection site to exert immune functions, while also performing phagocytosis and releasing *ROS* to combat the infection [122–124]. However, prolonged inflammation mediated by macrophages can inhibit the formation and maturation of new blood vessels, reduce the rate of bone healing, and suppress the differentiation of osteoblasts. Additionally, the various cytokines released may increase the production of *RANKL*, leading to the side effect of bone resorption [125]. Among these, sustained high levels of *TNF- $\alpha$*  can inhibit the *BMP-2* signaling pathway by promoting the ubiquitination and proteasomal degradation of Smad1 and runt-related transcription factor 2 (*Runx-2*), thereby hindering the bone regeneration process [126, 127].

Osteoclasts differentiate from hematopoietic mononuclear cells/macrophages and are regulated by macrophage colony stimulating factor (*M-CSF*) and *RANKL*. *M-CSF* can also promote the binding of *RANKL* to *RANK* on the surface of osteoclasts, thereby increasing their sensitivity and facilitating osteoclast differentiation [128, 129]. Osteoblasts infected by pathogens can directly or indirectly promote the secretion of *RANKL* through the *EP4* receptor, while simultaneously downregulating the expression of *OPG*, further promoting the generation of osteoclasts [130, 131].

In summary, the infectious microenvironment creates a persistent inflammatory state, enhancing osteoclastic activity and impeding osteogenesis, which collectively disrupts bone healing. Addressing the mechanisms underlying this altered environment is critical for developing effective treatments. Novel biomaterials that can regulate inflammation, disrupt biofilms, and promote osteogenesis represent promising therapeutic strategies for managing infectious bone fractures.

### Design concepts for bifunctional biomaterials

In simple terms, the ideal treatment plan for infectious bone defects is a combination of rapid infection control and bone tissue repair. Consequently, the ideal biomaterials should be designed to release antimicrobial

agents rapidly or exert bactericidal effects in the initial stage. They need to maintain a high concentration for a sufficient duration to effectively control and suppress bacterial proliferation. This is of great significance as uncontrolled infection can lead to further bone destruction and delay the healing process. Importantly, this process should not compromise bone regeneration. On the contrary, it should create a favorable environment for bone repair. Furthermore, these materials should also maintain high biocompatibility and mechanical strength. The high biocompatibility ensures that there are no adverse immune responses, and the mechanical strength provides support for the newly formed bone tissue. This enables osteoblast migration and differentiation on the biomaterial scaffold, promoting the integration of the material with the host bone and the formation of new bone tissue [132–134].

### Selection of antimicrobial materials

For infectious bone defects, antibiotics such as vancomycin (*VAN*), rifampicin, amoxicillin, and levofloxacin remain effective first-line antimicrobial agents. However, they also have some drawbacks, including dose dependence, bacterial resistance arising from high-dose usage, and potential effects on systemic and local cells [135, 136]. In recent years, several new treatments for bone infection, in addition to traditional antibiotics, have also drawn attention.

### Inorganic materials

Most inorganic materials, excluding metals such as  $\text{Ag}^+$ ,  $\text{Zn}^{2+}$ ,  $\text{Cu}^{2+}$ , or  $\text{La}^{3+}$ , that lack antibiotics or functional components generally do not possess antimicrobial properties. They are primarily used to promote bone formation or serve as scaffolding (see Section "Inorganic materials" for details) [137].

Inorganic metal particles represented by gold, silver, zinc, and copper significantly affect bacteria due to their unique physicochemical properties, such as size, zeta potential, surface morphology, and structure [138]. The intermolecular forces between metal particles, such as receptor-ligand interactions, electrostatic interactions, and van der Waals forces, can act on bacterial cell membranes. When they bind with cations, they cause a change in membrane charge, thus breaching the protective biofilm of the bacteria, leading to membrane rupture and bacterial death [139]. Additionally, metal particles can damage the proteins and DNA inside bacteria, affecting various metabolic pathways and hindering biosynthesis, ultimately resulting in bacterial death [140]. Furthermore, metal particles can convert hydrogen peroxide into highly toxic hydroxyl radicals through the



Fenton reaction, leading to the substantial production of ROS and subsequently inducing bacterial death [141].

However, metals are a double-edged sword; while they can kill bacteria, they also exhibit cytotoxicity [142]. Therefore, many researchers have modified metal particles by constructing composite scaffold systems through methods such as blending with scaffold substrates, coating preparation, and material modification grafting. These approaches not only reduce cytotoxicity but also optimize the performance of metal particles, significantly enhancing the selectivity of the materials [143]. For example, Zhang et al. prepared PLA coatings containing different concentrations of  $\text{Cu}^{2+}$  on titanium sheets using a dip-coating method. This coating significantly reduced the biotoxicity of  $\text{Cu}^{2+}$  to BMSCs. At the same time, the  $\text{Cu}^{2+}$  coating promoted healing at the fracture site while significantly reducing infections, achieving a balance among antibacterial effects, bone regeneration, and cellular compatibility. Within 28 days post-surgery, the levels of  $\text{Cu}^{2+}$  in the blood returned to normal [144]. A study applied nano zinc oxide to coat 3D-printed 3Y-ZrO<sub>2</sub> scaffolds. These scaffolds demonstrated high biocompatibility and excellent antibacterial activity in both in vitro and in vivo experiments [145].

### Organic materials

Organic antimicrobial materials are substances composed of organic compounds that possess inherent or potential antimicrobial properties. These materials typically include natural organic antimicrobial materials and synthetic organic antimicrobial materials [146].

When it comes to natural organic antimicrobial materials, chitosan (CS) is the most classic natural cationic polysaccharide. It is mainly obtained through the deacetylation of chitin, which is derived from the exoskeleton of crustaceans. CS has advantages such as non-toxicity, biodegradability, broad-spectrum antibacterial properties, adsorption capacity, and good biocompatibility [132, 147, 148]. Compared to common antimicrobial agents, CS exhibits unique characteristics, such as broad-spectrum efficacy, high bactericidal rates, and effective inhibition of the growth and reproduction of bacteria and fungi [149]. The main mechanisms of antimicrobial action are as follows: 1. Cationic CS molecules react with negatively charged bacterial molecules on the cell surface, altering the cell's permeability, inhibiting bacterial metabolism, and leading to bacterial death [150]. 2. CS can penetrate bacterial cells and bind to DNA, thereby inhibiting protein synthesis related to gene expression in bacteria. Additionally, it can adsorb negatively charged substrates within microbial cells, disrupting their physiological activities and resulting in cell death [151]. 3. CS can

inhibit the absorption of alkaline elements necessary for microbial growth through a metal chelation mechanism, while binding to metal ions required by the microbes to achieve antibacterial effects [152]. 4. High molecular weight CS can adhere to cell walls, reducing the absorption of nutrients from the extracellular environment [153].

Due to the excellent properties of CS, various modification schemes have been extensively studied. For instance, the antibacterial effect of nanoscale CS particles has been significantly enhanced through chemical modification, which increases surface charge density and hydrophobicity, thereby improving antibacterial activity [154–157]. CS loaded with antibiotics has demonstrated synergistic antibacterial effects. Kimna et al. constructed a chitosan-montmorillonite nanoclay material loaded with VAN and gentamicin (GM), achieving encapsulation rates of up to 98% for both VC and GM, with a release duration of up to 30 days. This composite exhibited strong antibacterial activity against gram-positive ( $G^+$ ) *S. aureus* and gram-negative ( $G^-$ ) *E. coli*, while showing no cytotoxic effects on normal cells [158]. In addition to traditional antibiotics, metal chelation, coatings for implant scaffolds, and synthetic hydrogel scaffolds also exhibit good antibacterial effects [159–161]. For example, Yang et al. incorporated graphene oxide/copper nano derivative (GO/Cu) into CS/hyaluronic acid (HA) scaffolds. The constructed composite material demonstrated satisfactory in vivo anti-infection performance by damaging the bacterial membrane, increasing ROS production, and disrupting key enzyme metabolism, which reduced inflammation and maintained acceptable biosafety. Additionally, the GO/Cu material (mass ratio=2:1) exhibited enhanced osteogenic differentiation and promoted bone healing [162].

HA is a linear glycosaminoglycan that is widely used in fields such as trauma, orthopedics, and joint replacement surgery. It primarily exists in the ECM and possesses good biocompatibility, hydrophilicity, and lubricating properties [163]. HA can act as an antibacterial material by disrupting bacterial integrity or serve as a carrier for drugs and coatings for implants [164–166]. For instance, Valverde et al. immobilized HA and CS on the surface of Ti-6Al–4 V alloy to form polyelectrolyte multilayers (PEMs), which exhibited good efficacy against *S. aureus* [167].

Antimicrobial peptides (AMPs), also known as host defense peptides, are components of the innate immune system and exhibit strong antibacterial properties against various microorganisms [168]. Their antibacterial mechanisms mainly include: 1. Disrupting bacterial signal transduction and interfering with biofilm formation to reduce attachment capability; 2. Blocking the synthesis

of products related to bacterial starvation to inhibit biofilm formation; 3. Suppressing the expression of DNA related to bacterial starvation products, thereby fundamentally inhibiting biofilm formation [169]. However, AMPs have a short half-life in vivo and are prone to degradation by proteases or binding with plasma proteins, thereby affecting their biological activity. Consequently, researchers typically combine AMPs with bioactive materials, with strategies mainly including physical mixing and encapsulation, nanoparticle construction, and bio-coating, to improve these drawbacks [170, 171]. He et al. constructed a mineralized collagen scaffold loaded with two AMPs (*Pac-525* and *KSL-W*) using poly (lactic-co-glycolic acid) (PLGA) [172]. In antibacterial experiments, this scaffold exhibited excellent antibacterial efficacy for the long-term inhibition of *S. aureus* and *E. coli*. This is due to the interaction of the antimicrobial peptide with the bacterial cell membrane. *Pac-525* and *KSL-W* disrupt the membrane integrity through electrostatic interactions, leading to bacterial death. Cell proliferation and alkaline phosphatase assays also demonstrated its good osteogenic capacity. The mineralized collagen component of the scaffold provided excellent osteoconductivity and osteoinductivity, promoting cell adhesion, proliferation, and osteogenic differentiation. The porous structure of the scaffold facilitated cell infiltration and nutrient transport. The mechanical properties of the scaffold were sufficient to support bone regeneration, and the PLGA microspheres ensured the sustained release of antimicrobial peptides, maintaining an effective concentration for long-term antibacterial activity. This study provided a broad prospect for the treatment of infectious bone defects. To address potential resistance, protein antibacterial materials inspired by AMPs have been developed, consisting of other amino acids linked at different positions via peptide bonds to disrupt the structure and function of bacteria [173].

Most synthetic organic materials are typically not utilized as antibacterial agents in the treatment of infectious bone defects [174]. Well-researched antibacterial materials can be categorized into over twenty types based on their molecular structure, including quaternary ammonium salts, biguanides, alcohol aldehyde esters, ethers, phenols, and imidazoles. Among these, antibacterial materials from the quaternary ammonium salt category are used more extensively [175]. Polymethyl methacrylate (PMMA) bone cement is a widely used synthetic organic bone repair material that has been clinically applied extensively over the past few decades. Various antibiotics, such as gentamicin and VAN, have been incorporated into PMMA to address bacterial infections [176, 177]. To extend the antibacterial spectrum to drug-resistant bacteria and viruses, and to enhance the release of

antibacterial agents, Wang et al. developed a quaternary ammonium salt-modified antibacterial PMMA bone cement. This material exhibits high mechanical strength and sustained release of antibacterial agents, showing good antibacterial efficacy against both  $G^+$  and  $G^-$  bacteria, with stronger antibacterial activity against  $G^-$  bacteria [178]. However, in the treatment of infectious bone defects, quaternary ammonium salts are typically used to modify CS to enhance its antibacterial properties [179]. Therefore, these materials have significant research potential.

## Selection of bone repair promoting materials

### Inorganic materials

Bone tissue contains a variety of metal elements that play an indispensable role in bone regeneration at both molecular and cellular levels [180]. Consequently, metal particles may provide more direct signals for bone regeneration. For example, ions such as  $Ca^{2+}$ ,  $Mg^{2+}$ ,  $Sr^{2+}$ ,  $Zn^{2+}$ ,  $Li^+$ ,  $Mn^{2+}$ ,  $Cu^{2+}$ ,  $Co^{2+}$ ,  $Ce^{3+}$ ,  $Fe^{3+}$ , and  $Ag^+$  are used in bone regeneration. These elements regulate multiple metabolic processes, including the differentiation and activity of osteoblasts and osteoclasts, bone mineralization, vascular regeneration, and immune modulation [1]. Different metal ions exert distinct effects in these areas.

The most abundant  $Ca^{2+}$  in the bones provides strength and supports movement, while also participating in various signaling pathways. Optimal fluid concentrations can stimulate the proliferation, migration, and mineralization of osteoblasts, enhance their adhesion capacity, and induce macrophages to polarize towards the *M2* phenotype [181–183].  $Mg^{2+}$  is the fourth most abundant mineral in the human body, primarily found in the bones, and is a fundamental element of bone tissue [184]. It plays a role in the following three areas: (1) Promoting the osteogenic differentiation and adhesion of *BMSCs*, facilitating the migration of osteoblasts and inhibiting the generation of osteoclasts [185–187]; (2) Inducing macrophages to polarize towards the *M2* phenotype, eliminating oxidative stress in LPS-induced macrophages [188, 189]; and (3) Promoting the angiogenic differentiation of *BMSCs* [190].  $Sr^{2+}$  is primarily found in areas of active growth and regeneration of fresh trabecular bone, where it functions to prevent bone resorption and stimulate bone formation. It promotes vascularization of bone tissue by activating the *PDGF-BB/PI3K/AKT* signaling pathway [191, 192]. Additionally,  $Sr^{2+}$  and its modified materials exhibit anti-inflammatory properties, capable of regulating the polarization of neutrophils, leading to the production of anti-inflammatory cytokines, and thereby directly or indirectly inducing macrophages to polarize towards the *M2* phenotype [193, 194]. Recent studies have found that  $Sr^{2+}$  significantly inhibits the growth of *E.*

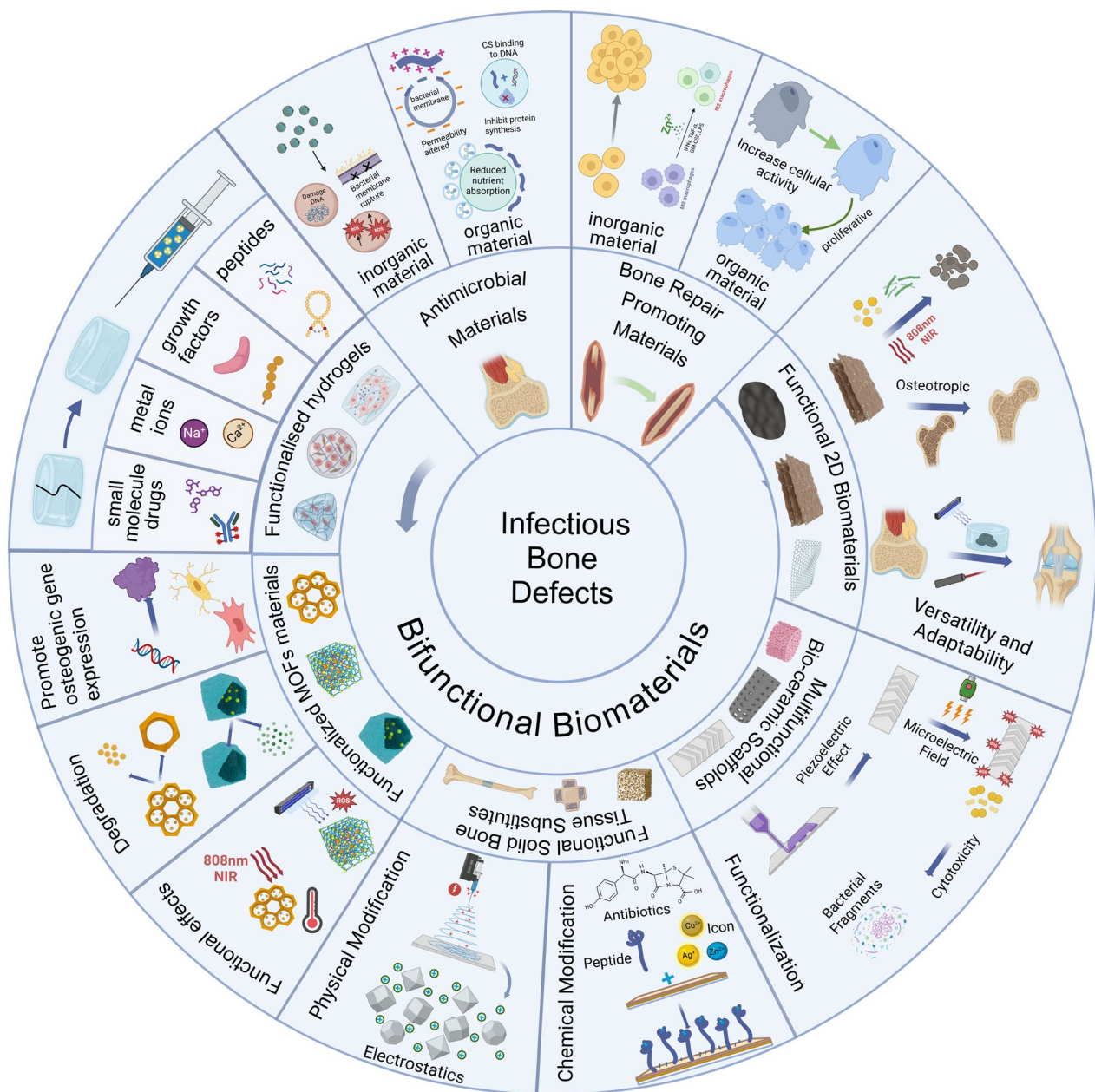


**Fig. 3** Schematic diagram of strategies and mechanisms involving partial bifunctional materials for the treatment of infectious bone defects (Created with BioRender.com)

*coli* and partially suppresses the growth of *S. aureus*, indicating its potential in the treatment of infectious bone defects [195]. Although  $\text{Zn}^{2+}$  constitutes only 30% of the bone, it is an important cofactor for the stability of bone microstructure and the remodeling of bone proteins, playing a critical role in bone growth and stability [196]. It can promote the adhesion, proliferation, and differentiation of osteoblasts, inhibit osteoclasts, regulate the differentiation of inflammatory cells, induce macrophages

to polarize towards the M2 phenotype, and facilitate angiogenesis, while also exhibiting excellent antibacterial properties [197–200]. However, it is important to note that high concentrations of  $\text{Zn}^{2+}$  may enhance the activity of osteoclasts [201]. Other metal ions also play significant roles in bone metabolism. In the application of tissue engineering for promoting bone repair, metal ions are often incorporated into biomaterials to improve their

**Table 1** A partial composite hydrogel strategy for treating infectious bone defects

Categories	Components	Strategy	Assessments of infection	Assessments of bone healing	Year
Gelatin methacrylate (GelMA)	β-TCP; Sodium alginate (Alg); Strontium chloride (Sr <sup>2+</sup> ); MXenes (Ti <sub>3</sub> C <sub>2</sub> )	Photothermal Therapy (PTT) Osteogenic Stimulation	<i>Vitro</i> : Significant inhibition against <i>S. aureus</i> and <i>E. coli</i> (Viability Reduction: 1.4% and 1.1%)	<i>Vitro</i> : mRNA expression levels of <i>Runx2</i> , <i>ALP</i> , and <i>OCN</i> ↑; <i>ALP</i> activities and protein expression levels of <i>ALP</i> and <i>OPN</i> ↑; <i>Vivo</i> : Micro-CT showed Bone volume/Tissue volume (BV/TV) ratio↑; H&E staining: Direct connection of new bone with host bone; Immunohistochemical staining: <i>ALP</i> and <i>OCN</i> ↑	2022[241]
	N-acryloyl glycineamide (NAGA); Molybdenum Disulfide (MoS <sub>2</sub> ); Gadolinium (Gd)	PTT; Tumor Ablation	<i>Vitro</i> : Effective antibacterial activity against <i>S. aureus</i> and <i>E. coli</i> <i>Vivo</i> : Bacterial infections and inflammation↓ ( <i>S. aureus</i> -infected rat tibia defects)	Osteogenic Differentiation: Gd <sup>3+</sup> ions promoted osteogenic differentiation of rat osteoblasts (ROBs); Bone Regeneration: 1. Micro-CT and histological analysis: Significant New bone formation; 2. Quantitative data: BV/TV (11.83%); 3. Fluorochrome-labeling: 6.85% (12 weeks)	2023[242]
GelMA	Copper ion-modified germanium phosphorus nanosheets (GeP@Cu); Gd	Conductivity and Biodegradability	Antibacterial rates of 95.51%±2.15% ( <i>E. coli</i> ) and 94.28%±4.16% ( <i>S. aureus</i> ); ROS Generation	1. Osteogenic Differentiation of <i>BMSCs</i> , <i>ALP</i> activity and mineralized matrix formation↑; 2. Neurogenic Differentiation and Angiogenesis↑; 3. Micro-CT: BV/TV and trabecular number ( <i>Tb.N</i> ) after 12 weeks↑	2023[243]
GelMA	Proanthocyanidin; Amikacin; Boronate Complexes	Dual Delivery System; pH and ROS Responsiveness;	Antibacterial rates of <i>S. aureus</i> and <i>E. coli</i> were 87.4% and 78.4%; Bacterial Morphology: Damaged bacterial morphology	<i>ALP</i> activity and gene expression levels of <i>Alp</i> , <i>Runx2</i> , <i>OCN</i> , and <i>Col1</i> ↑	2024[244]
Carboxymethyl Chitosan (CMCS); GelMA	<i>BMP-2</i> ; PLGA; GO; Antisense <i>yycF</i> (AS <i>yycF</i> )	Photo-crosslinking; Spring Structure	Antibacterial property of composite hydrogel 20 times higher; Biofilm formation ( <i>S. aureus</i> ) ↓;	<i>Vitro</i> : <i>ALP</i> (7 days) and Alizarin Red staining (14 days) ↑; <i>Vivo</i> : 1. Large amounts of new osteotylus formation and effective infection control (8 weeks); 2. Micro-CT: nearly complete healing of the bone defect; 3. Histopathological Analysis: Deposition of collagen and new bone formation	2023[245]
CS Sulfated-(SCS)	Oxidized HA; β-Sodium Glycerophosphate (β-GP); Cu-Sr Doped Mesoporous Bioactive Glass (CuSrMBG)	Dual-Network Formation	1. <i>Vitro</i> : Number of <i>E. coli</i> and <i>S. aureus</i> ↓ (> 95%); 2. <i>M1</i> → <i>M2</i>	Osteogenic Differentiation: <i>ALP</i> and mineral deposition↑; Bone Regeneration: BV/TV, bone mineral density ( <i>BMD</i> ), trabecular structure↑	2024[246]



Table 1 (continued)

Categories	Components	Strategy	Assessments of infection	Assessments of bone healing	Year
Aldehyde hyaluronic acid (AHA); Carboxymeth-yl chitosan (NOCC)	PCL; Van; Mesoporous silica nanoparticles (MSNs); Fingolimod (FTY720)	Dual-Drug Delivery; Structural Support	<i>Vitro</i> : Scaffolds showed strong growth inhibition against <i>S. aureus</i> and <i>E. coli</i>	1. The scaffold supported <i>BMSCs</i> growth; 2. <i>ALP</i> activity and calcium nodule formation↑ 3. <i>Vivo</i> : BV/TV and Trabecular Thickness (Tb.Th)↑	2023[247]
	HAp; Chlorhexidine	Injectable Delivery System	Significant inhibition of <i>S. aureus</i> biofilm formation was observed at a concentration of 50 mg/mL; Lower bacterial colony counts in infectious bone defects	New Bone Formation at 4,8 weeks↑; Micro-CT: Value of BV/TV were $0.32 \pm 0.11$ (4 weeks) and $0.49 \pm 0.13$ (8 weeks) Histological Analysis: Defect areas largely consisted of blue-stained newly formed woven bone, indicating active bone regeneration	2022[248]
Polyethylene Glycol Diacrylate (PEGDA)	Copper (Cu)-Strontium (Sr) Peroxide Nanoparticles (CSp NPs)	Dual Metal Peroxides; pH-Responsive Release (Ph = 5.5: Antibacterial activity pH= 7.4: Osteogenesis)	<i>Vitro</i> : IC50 of <i>S. aureus</i> was $25 \pm 0.796$ µg/mL; A killing rate of 99.94% at 50 µg/mL <i>Vivo</i> :	Proliferation and Osteogenic Differentiation of <i>BMSCs</i> ↑; Expression of <i>Alp</i> , <i>Bsp</i> , and <i>OCN</i> ↑; Bone Regeneration: Complete filling of bone defects with new bone (21 d), BV/TV and BMD↑	2024[249]

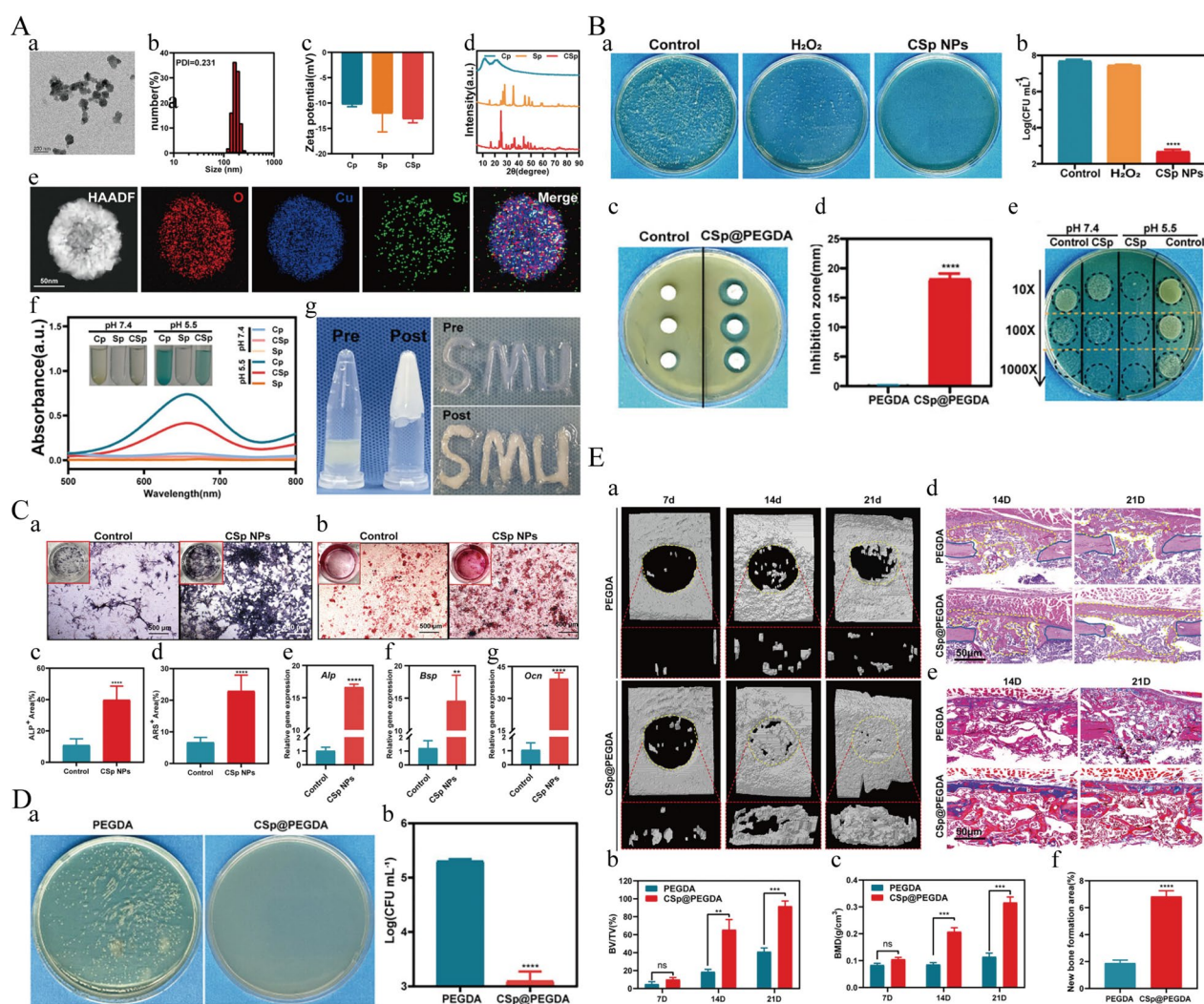


**Fig. 4** A schematic illustration highlights the synergistic antimicrobial and osteogenic effects of the CSp@PEGDA hydrogel. **A** Characterization of CSp@PEGDA. (a) TEM images, (b) Hydrodynamic diameter, (c) Zeta potential, (d) XRD patterns of CSp NPs. (e) HAADF image and element-mapping. (f) Absorption spectra of TMB oxidized by Cp, Sp and CSp NP at different pH. (g) Rapid gelation and plasticity of CSp@PEGDA under blue light irradiation (405 nm) for 30 s. **B** (a,b) Graphs and quantitative analysis of bacterial colony counts on TSA plates treated with CSp NPs. (c) Graph and (d) Quantitative analysis of inhibition zones of CSp@PEGDA composite on TSB agar plate. (e) Graph of bacterial colonies treated with CSp NPs at different pH conditions. **C** In vitro proliferative and osteogenic effect of CSp NPs on BMSCs. (a, c) ALP staining images of BMSCs co-cultured with CSp NPs for 7 days and their corresponding quantitative analysis. (b, d) ARS staining images of BMSCs co-cultured with CSp NPs for 21 days and their corresponding quantitative analysis. (e–g) Relative mRNA expression levels of osteogenesis-related genes *Alp* (Day 7), *Bsp* (Day 14), and *Ocn* (Day 21). **D** In vivo antimicrobial activity of CSp@PEGDA. Graphs(a) and quantitative analyses(b) of *S. aureus* in bone cavity rinses from CSp@PEGDA and PEGDA treated mice. **E** In vivo osteogenesis experiments. (a) Micro-CT images of mice femurs at days 7, 14, and 21. (b, c) Quantitative analyses of BV/TV and BMD at different time points. (d) H&E-stained sections of mice femurs at days 14 and 21, where yellow dashed lines indicate new bone formation, and blue solid lines mark the edges of bone defects. (e) Masson-stained sections of mice femurs at days 14 and 21. (f) Quantitative analysis of newly formed bone tissue at day 14. Copyright © 2024 Wiley-VCH GmbH [249]

release kinetics, optimize the regulation of bone metabolism, and enhance biocompatibility.

In addition to metals, bioceramics represented by calcium phosphate (CaP) bone cement, hydroxyapatite (HAp), and  $\alpha/\beta$ -tricalcium phosphate ( $\alpha/\beta$ -TCP) are widely used in the preparation of multifunctional scaffold systems for infectious bone defects [202–204].

Bioceramic scaffolds are fabricated as follows: The powders are shaped into desired forms using techniques like dry pressing, slip casting, or 3D printing. The bodies are then subjected to high-temperature sintering to enhance density and mechanical strength, with sintering parameters significantly influencing the final properties. Finally, surface treatments or coatings are applied to optimize

bioactivity, making them suitable for a wide range of applications in orthopedics, dentistry, and cardiovascular medicine [205]. Although they have certain shortcomings in antibacterial performance, their composition is highly similar to the inorganic salts found in human bone tissue. In addition to good biocompatibility, they possess high mechanical strength, which is often lacking in organic materials. Therefore, these materials can serve as carriers for antibacterial agents and bone fillers, combined with various antibacterial mechanisms, showing bright prospects in bone tissue scaffold applications [137].

Wu et al. modified calcium phosphate cements (CPCs) to construct an injectable CPC-chitosan scaffold with strong mechanical properties. This scaffold, combined with penicillin-alginate microspheres, can be completely injected with lower injection force. In vitro experiments demonstrated its effective antibacterial function against *S. aureus* infections, and it possesses strength comparable to that of trabecular bone, allowing for good growth of Human Umbilical Cord Mesenchymal Stem Cells (*hUCMSCs*) within the scaffold. If further validated with in vivo experiments using animal models, this scaffold would hold significant clinical translation potential [206].

A study functionalized magnesium hydroxyapatite (Mg-HAp) with silver nanoparticles (AgNPs) to construct an Ag-Mg-HAp scaffold, which demonstrated good antibacterial properties against *E. coli* and *S. aureus*. However, in the same living environment, the proliferation of human adipose-derived stem cells (*hADSCs*) decreased by 90% on day 24. Consequently, researchers need to further optimize the cytotoxicity [207].  $\beta$ -TCP is an important inorganic component of natural bone tissue, exhibiting excellent bioactivity, osteoconductivity, and osteoinductivity. Compared to PMMA, it can degrade in vivo, providing appropriate space for bone repair [208, 209]. Liu et al. improved the toughness, brittleness, and high elastic modulus deficiencies of the scaffold material using gelatin and encapsulated CS microspheres containing gentamicin (GM). This material not only has good antibacterial activity against *S. aureus* but also shows excellent strength and osteoconductivity at different stages of bone repair in in vivo infection models [210].

### Organic materials

CS exhibits both antibacterial properties and the capability to promote bone regeneration. This is because it is similar to glycosaminoglycans in the natural ECM, creating a favorable local microenvironment for cell growth and supporting the proliferation, differentiation, and mineralization of osteoblasts [211]. Studies have found that the higher the deacetylation degree (DD) of CS, which indicates the number of amino groups, the stronger the cell adhesion capacity. Additionally, the

cations carried by CS can enhance cell activity through methods such as electrical stimulation. Research indicates that both osteoblasts and *MSCs* can proliferate and differentiate well in a CS environment [132, 212]. Due to the excellent compatibility of CS with other materials, it can synergistically enhance bone generation. Oftadeh et al. merged HAp with CS and found that various osteogenic markers, such as osteocalcin, alkaline phosphatase, osteonectin, and *Runx2*, showed significantly upregulated transcription levels in cells, further enhancing osteogenic capability [213]. Combinations with metal ions, graphene oxide (GO), bioglass, and bioactive substances such as growth factors and *BMP-2* also demonstrate considerable potential in bone defect repair [214–219].

Collagen and gelatin possess ideal characteristics for applications in bone tissue engineering and are one of the main protein components in natural bone. Their amino acid sequences contain adhesive ligands-arginine-glycine-aspartic acid (RGD)—which facilitate the attachment of various cells [220, 221]. Furthermore, these components exhibit excellent biocompatibility and can be degraded by recipient enzymes, making them excellent biological carriers for other components [222–224]. Alginate is also a natural polymer derived from algae, known for its good biocompatibility and plasticity. The addition of RGD can promote cell adhesion or confer specific functions through other factors and functional groups [225, 226].

Synthetic organic materials usually do not possess antibacterial properties. However, compared with natural organic materials, they offer more possibilities for chemical modifications and molecular changes, making them excellent carriers for drugs or antibacterial materials. In the field of biological carrier treatment for bone infections, poly lactic-co-glycolic acid (PLGA) is a classic synthetic organic material. It is a copolymer of polylactic acid (PLA) and polyglycolic acid (PGA), featuring excellent biocompatibility and biodegradability, with adjustable mechanical properties, thus offering significant advantages as a carrier for the in vivo delivery of antibiotics [227, 228]. Joaquin et al. developed a PLGA microsphere modified with daptomycin and VAN in Palacos R cement, which demonstrated good antibacterial properties in a model of infectious bone defects, while preserving the normal structure of the surrounding bone and reducing damage to the bone tissue [229]. Materials such as PMMA, polycaprolactone (PCL), and polyetheretherketone (PEEK) also play important roles in the treatment of infectious bone defects [230–232]. Next, we will introduce several types of composite materials.

**Table 2** Strategies for the management of infectious bone defects employing MOFs

Categories	Components	Characteristics of MOFs	Assessments of infection	Assessments of bone healing	Year
Porphyrin- Zr -based (HN25 Sonosensitizer)	Alendronate	Morphology: diamond Zeta: 34.64 mV Surface Area: 1273.47 m <sup>2</sup> /g	Against <i>MRSA</i> : 98.97%; Animal models: Significant reduction in bacterial infection and abscess formation	CT and histological evaluations: Significant new bone formation and reduced bone defects; Osteogenic markers ( <i>OPN</i> , <i>Runx2</i> , <i>OCN</i> ) & <i>ALP</i> and <i>ARS</i> staining↑;	2024[269]
MOF-801 Zr -based	Ti + hydrofluoric acid (HF)	Coating thickness: Zr-MOF0, Zr-MOF1, and Zr-MOF2 were 5.38 μm, 9.63 μm, and 14.13 μm	The fluorine-doped Zr-MOF2 exhibited a bacterial inhibition rate of 79.43% and 66.28% against <i>S. aureus</i> and <i>E. coli</i>	Zr-MOF2 promoted <i>MC3T3-E1</i> proliferation and differentiation and induces macrophage transition to <i>M2</i>	2022[270]
UIO-66 Zr -based	Fosfomycin (FOS) CS-based scaffolds	Size: 130 ± 28 nm	Antibacterial Activity: Complete bactericidal activity against <i>S. aureus</i> ; Bacterial Attachment↓	Osteogenic Differentiation : Related genes ( <i>Runx2</i> , <i>COL-1</i> , and <i>OCN</i> ) and ECM mineralization in <i>MC3T3-E1</i> pre-osteoblasts↑; Gene Expression: <i>COL-1</i> *2 times, <i>OCN</i> *2.6–3.5 times↑; <i>ALP</i> Activity↑	2022[271]
Zn-base ZIF-8	Ag <sup>+</sup> PEEK	Size: 300 nm Zeta: −19.4 mV	Colony Forming Units and Bacterial Growth Curve of SPZA indicated complete bactericidal effect	SPZA showed 85.0% cell viability against L929 mouse fibroblast cells	2021[272]
Zn-base ZIF-8	CS	Rhombic Dodecahedron Size: 60 ± 20 nm Encapsulation Efficiency (VAN) : 99.3%	pH = 5.4 (70% of VAN released with 8 h), pH = 7.4 (55%) Inhibition zones: 8–10 mm and a reduction index of ≥ 3	<i>MC3T3-E1</i> preosteoblasts showed high proliferation and osteogenic activities; <i>ALP</i> Activity and Calcium Deposition↑	2019[273]
Cu-base	SiO <sub>2</sub> -CaO AgNPs	Surface Area: 230 m <sup>2</sup> /g Pore Volume: 0.10 cm <sup>3</sup> /g	Antimicrobial Activity: inhibition zones between 8–10 mm and a reduction index of ≥ 3 MIC and MBC: 62.5 μg /mL to 125 μg/mL	Bioactivity: HAp formation after 7 days Cytotoxicity: No significant cytotoxic effects Cell Migration: Ability similar to control assays	2024[274]
Co-base ZIF-67	Osteogenic Growth Peptide (OGP), Titanium Dioxide Nanotubes (TNTs)	Rhombic Dodecahedron Size: 189 ± 21 nm pH-sensitive property: rapid dissolution under acidic conditions	<i>E. coli</i> and <i>S. aureus</i> antibacterial ratios reached 94.9% and 94.5%, respectively; In vivo Antibacterial Efficacy (rat): fewer residual bacteria after 3 days of implantation	Osteointegration: a new bone formation area percentage of 42.6% and a bone-implant contact (BIC) ratio of 56.3% after 4 weeks; <i>M0</i> → <i>M2</i> , <i>TNF-α</i> and <i>IL-1β</i> ↓, <i>IL-10</i> and <i>IL-1</i> ↑	2021[275]
Mg-base	Calcium Sulfate, Calcium Citrate, Dicalcium Hydrogen Phosphate Anhydrous (DCPA)	Block structure 10–15 μm in size UV Absorption Peak: Characteristic peak at 259 nm	Antibacterial Activity: <i>S. aureus</i> survival rate ≤ 10% within 4 h Inhibition Zone: 17.75 mm and 20.59 mm ( <i>S. aureus</i> and <i>E. coli</i> )	Mechanical Strength: increased cement strength from 27 to 32 MPa Osteogenic Differentiation: Promoted <i>mBMSC</i> proliferation and differentiation; Increased expression of <i>Runx2</i> , <i>BMP2</i> , <i>OCN</i> , <i>OPN</i> , and <i>COL-1</i> Inflammation Regulation: Reduced <i>IL-6</i> and increased <i>IL-10</i>	2023[276]



### Bifunctional biomaterials

Composite biomaterials present promising biomimetic solutions that effectively address significant challenges within this field, owing to their performance often surpassing that of their individual constituents. The main strategies include incorporating nanoparticles as fillers into biodegradable biological carriers or constructing polymers using covalent bonds and other methods [233]. Many of the studies mentioned earlier are based on these innovative findings. Bioactive ceramics and glass particles are capable of enhancing the mechanical strength of polymers while concurrently promoting bone tissue regeneration [234]. Additionally, some bioactive materials can provide polymers with extra functions, such as shape memory (for example, injectable and self-healing hydrogels) and photothermal effects (like black phosphorus, BP) (Fig. 3) [235–237].

### Hydrogels with antibacterial function for promoting bone defect repair

Hydrogels are polymers with a three-dimensional network structure that can be formed into various shapes and sizes [238]. Additionally, these materials contain a high degree of hydrophilic groups, allowing them to effectively capture and retain large amounts of moisture or biological fluids [239]. Simultaneously, hydrogels are similar in morphology and function to natural extracellular matrices, providing a favorable environment for cells to support nutrient delivery, cell proliferation, and differentiation, while minimizing damage to biological tissues during this process [240]. In addition to utilizing the inherent properties of hydrogels to repair infectious bone defects, they can also promote therapeutic effects by loading peptides, growth factors, metal ions, or small molecule drugs (Table 1).

GelMA is a representative hydrogel formulation that has been widely applied in various biomedical fields. It is a gelatin modified with double bonds, able to substitute artificial basement membranes due to its excellent biocompatibility, low antigenicity, and cellular response characteristics. More importantly, GelMA contains RGD (Arg-Gly-Asp) and MMP sequences, which play key roles in tissue repair and wound closure [250]. Additionally, GelMA can promote bone formation and angiogenesis [251]. As a photosensitive hydrogel, it undergoes cross-linking and solidification when irradiated with ultraviolet (UV) or visible light, providing numerous advantages, including good injectability and rapid gelation, making it highly suitable for bone tissue engineering [252]. Hydrogels typically exhibit relatively weak mechanical strength. To address this issue, bioceramic  $\beta$ -TCP has been widely utilized to optimize the mechanical properties and bioactivity of GelMA hydrogels [253]. Nie et al. incorporated

$\beta$ -TCP and sodium alginate into GelMA hydrogels as the base material for 3D printing. The introduced MXenes (a novel type of transition metal carbide/nitride/carbonitride) can effectively disrupt bacterial membranes through direct physical contact, thereby killing both  $G^+$  and  $G^-$  suspended bacteria and microbial biofilms, significantly enhancing antibacterial performance. This capability is further amplified under near-infrared (NIR) irradiation (808 nm). The authors filled 3D-printed GTAM scaffolds with rat *BMSCs*, which exhibited excellent biocompatibility and osteogenic capabilities in the presence of bacterial infection [241].

$Cu^{2+}$  not only exhibits excellent antibacterial properties but also serves as a bioinorganic ion that promotes angiogenesis, primarily inducing vessel formation through the *VEGF* and *HIF- $\alpha$*  pathways [254]. Based on this, Xu et al. developed a GelMA hybrid hydrogel, namely GelMA/GeP@Cu, which enhances vascularization during the bone regeneration process. Its core component is GeP nanosheets modified with  $Cu^{2+}$ , which not only support neurovascular regeneration but also possess antimicrobial properties. Experimental results indicate that this novel biocomposite hydrogel scaffold can continuously and slowly release  $Cu^{2+}$ , inhibiting bacterial infection while promoting osteogenic cell differentiation and angiogenesis, thus facilitating bone tissue regeneration in infectious bone defect models [243]. A research team led by Guan et al. developed a composite hydrogel composed of copper-strontium peroxide nanoparticles (CSp NPs) and polyethylene glycol diacrylate (PEGDA) for the treatment of infectious bone defects. This innovative material leverages the pH-responsive release of hydroxyl radicals from  $Cu^{2+}$  within the hydrogel to achieve a 99.94% bacterial killing rate against *S. aureus*. Additionally, the hydrogel releases  $Sr^{2+}$  to enhance osteogenesis, resulting in complete bone defect repair in *IAOM* mice model within 21 days. This dual-functional strategy represents a significant advancement in non-antibiotic therapies for bone infections and regeneration, providing a promising clinical approach to combat drug resistance and promote bone healing (Fig. 4) [249].

In addition to the dual-functional study, Huang et al. constructed a hydrogel that integrates anticancer, antibacterial, MRI, and osteogenic functions [242]. They utilized the luminescence imaging advantage of Gd by incorporating Gd compounds and  $MoS_2$  into GelMA. The MRI effect of Gd allows for monitoring the location and degradation of the hydrogel.  $MoS_2$  endows the hydrogel with excellent photothermal capability, resulting in outstanding antibacterial and anticancer performance. As a rare earth element, Gd possesses an ionic radius similar to that of calcium ions and demonstrates good osteogenic ability in infectious bone defect

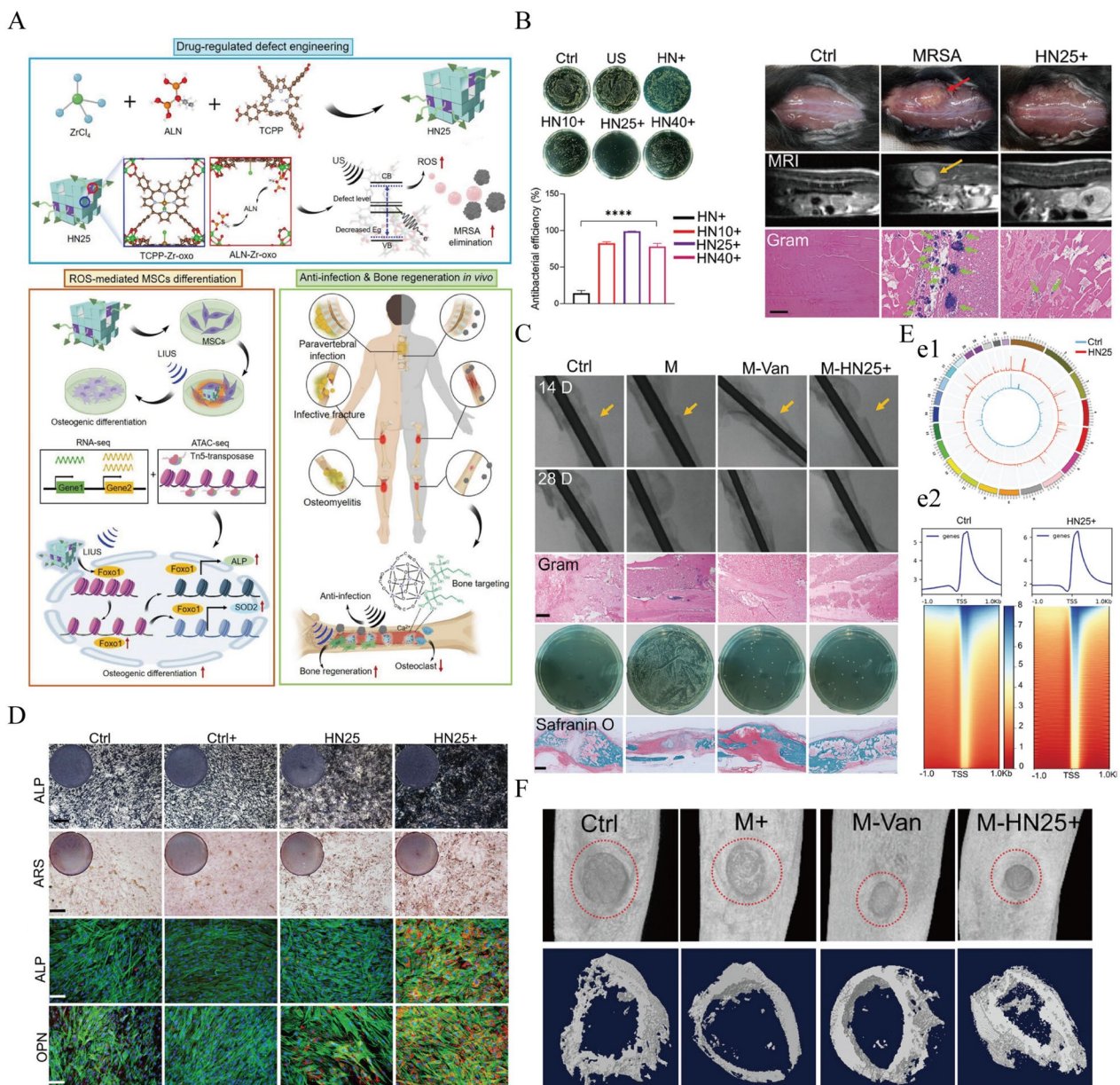


**Fig. 5** **A** This schematic illustrates the targeted repair of infectious bone tissue by the ALN-mediated defective MOF (HN25) through Sono-epigenetic modulation of chromatin accessibility, highlighting the dual role of HN25 in enhancing sonodynamic antibacterial activity and promoting bone regeneration under low-power ultrasound irradiation. **B** Antimicrobial efficiency of HN25 against MRSA under ultrasonic irradiation. **C** Micro-CT, Gram staining (Scale bar = 100  $\mu$ m), spread plate of MRSA and Safranin O and fast green staining (Scale bar = 1 mm) of bone fracture sites after 14 and 28 d. **D** OPN (D1), ALP (D2) and ARS (D3) staining results demonstrate the ability of HN25 to promote osteogenic differentiation of *hMSCs*. **E** Osteogenesis mechanism. (e1) Genome-wide chromatin accessibility of *MSCs* after HN25 under US irradiation treatment and control. (e2) Heatmap of ATAC-seq signals enrichment at TSS regions in *MSCs* cells. **F** Illustration of anti-infection and bone regeneration of HN25. Copyright © 2023 Wiley–VCH GmbH [269]

models, presenting significant clinical translational value.

However, hydrogels have relatively weak mechanical strength, which may lead to damage and structural failure when used in bone tissue engineering due to daily

activities. This can cause the loaded drugs to be released too quickly or to lose efficacy, thereby reducing treatment effectiveness [255]. Therefore, hydrogels with short-term self-healing capabilities improve this deficiency, extending their lifespan and enhancing safety [256].

Chen et al. combined the potent chemokine *SDF-1*, which can recruit bone marrow-derived osteoprogenitor cells, with exosomes secreted by *M2* macrophages and 4% HA, which exhibits strong antibacterial activity against *S. aureus*, *E. coli*, and methicillin-resistant *Staphylococcus aureus* (MRSA), to synthesize a self-healing adhesive hydrogel that is injectable, termed HA@SDF-1 $\alpha$ /M2D-Exos. This hydrogel can restore itself in just 5 min after being divided into two parts, providing an effective solution to the problem of mechanical strength. The positively charged quaternary ammonium groups in the 4% HA effectively eliminated over 95% of MRSA and over 99% of both *S. aureus* and *E. coli*, while various osteogenic-related cells showed no significant cell death. In bone defect models, treatment with this hydrogel significantly enhanced angiogenesis and osteogenesis [257].

In addition to serving as the main component of composite materials, hydrogels can also play a significant role in collaboration. Three-dimensional (3D) printed metallic implants can be customized according to the clinical treatment needs of bone defects and the actual anatomy, aiming to restore the functionality of the original anatomical structure as much as possible [258]. For example, the surface micro-porous structure of porous titanium alloy (pTi) is more compatible with the host bone tissue, promoting angiogenesis and inducing inward bone growth. However, the porous structure may also become a breeding ground for bacteria, presenting significant vulnerabilities in the treatment of infectious bone defects [259]. Additionally, the ability of metal implants to induce cell proliferation and differentiation is relatively weak [260]. Therefore, Qiao modified the surface of pTi with an antibacterial hydrogel composed of sodium tetraborate (Na<sub>2</sub>B<sub>4</sub>O<sub>7</sub>), polyvinyl alcohol (PVA), AgNPs, and tetraethyl orthosilicate (TEOS). In vitro and in vivo studies that examined the inhibition of bacteria and the induction of BMSCs differentiation and mineralization indicated that this composite is an ideal candidate for promoting new bone formation in infected defects [261].

### Functionalized MOFs materials

In recent years, Metal Organic Frameworks (MOFs) with outstanding performance have shown great application potential in biological functional materials. MOFs are a class of porous inorganic–organic hybrid materials, synthesized through coordination between metal ions or clusters and organic ligands, also known as coordination polymers. They possess the rigidity of inorganic materials and the flexibility of organic materials [262–264]. MOFs exhibit high tunability, and their high specific surface area and adjustable pore structures allow for the encapsulation of a large number of functional molecules, facilitating in vivo transport

and enabling their roles in delivery and catalysis [265]. Some MOFs materials demonstrate catalytic properties, such as peroxide catalysis, radiation sensitization, microwave heating, and photocatalysis [266, 267]. In addition, these materials can combine with other substances to form coatings or 3D structures, enabling a wider range of applications [268]. In the treatment of infectious bone defects, MOFs with good biocompatibility exhibit unique effects (Table 2).

In response to the demand for various antibacterial strategies, MOFs through ion mediation, or based on physical methods, particularly showing good efficacy against antibiotic-resistant bacterial infections [277]. Among them, Zn-based MOF materials are excellent choices for treating infectious bone defects. Biocompatible ZIF-8, which has acid-responsive degradation properties, can degrade in response to acidic metabolites produced by bacteria. The released Zn<sup>2+</sup> ions can penetrate the bacterial membrane through ion channels, thereby interfering with the bacteria [273]. Based on its favorable internal space, Han et al. incorporated VAN into ZIF-8 and deposited it onto 3D-printed bioglass scaffolds to bestow the composite material with bone repair functionality. This combination demonstrates a faster release rate of VAN and shows significant inhibitory effects on *S. aureus*. Furthermore, additional studies indicate that the scaffolds promote the expression of MSCs and osteogenic genes [278].

Research on MOFs materials using ion release strategies to combat infections and promote bone repair is quite abundant [270, 279]. Tao et al. coated ZIF-67 (Co-MOF) loaded with osteogenic growth peptides onto the surface of Ti to enhance its antibacterial properties and performance [275]. Due to the inert surface of PEEK limiting its clinical applications, Xiao et al. used a polydopamine (PDA) interlayer to bond Zn-Mg MOF-74 to PEEK, followed by loading Dex. This composite PEEK exhibits good hydrophilicity and stability, inducing an alkaline microenvironment on the surface through the release of Mg<sup>2+</sup> and Zn<sup>2+</sup>, demonstrating strong antibacterial activity against *S. aureus* and *E. coli*. Additionally, the metal ions, in conjunction with Dex, synergistically promote the biological activity and osteogenic differentiation of rat bone marrow mesenchymal stem cells, while Mg<sup>2+</sup> can also induce vascular differentiation of human umbilical vein endothelial cells. In rat subcutaneous infection models, chicken chorioallantoic membrane models, and rat femoral drilling models, this composite material shows good performance, providing new insights for the clinical translation of PEEK [279].

In addition to the previously mentioned photosensitive MOFs that convert O<sub>2</sub> into ROS, some MOFs also possess photothermal effects, such as Prussian blue



**Table 3** Composite Bioceramics scaffold design schemes for the treatment of infectious bone defects

Categories	Components	Strategy	Assessments of infection	Assessments of bone healing	Year
Mesoporous Bioactive Glass (MBG)	DOX; Bioink; PCL	DOX-Controlled BMP2 Expression;	<i>Vitro</i> : Significantly reducing bacterial adhesion and proliferation; <i>Vivo</i> : No bacterial fluorescence signals at 3 days	<i>Vitro</i> : ALP and Alizarin Red staining; Osteogenic differentiation of <i>BMSCs</i> ↑; <i>Vivo</i> : X-ray, micro-CT, and histopathologic analysis: Significant ectopic bone formation; BMP2 Secretion↑	2020[294]
MSNs	Levofloxacin; HAP; Polyurethane (PU)	Controlled Release	Significant inhibition of <i>E. coli</i> and <i>S. aureus</i> ; a visible zone of inhibition ( <i>S. aureus</i> )	Osteogenic Differentiation: Expression of ALP, OCN, and <i>OPN</i> ↑; <i>MC3T3-E1</i> cells ↑; Cells were more in S and G2 phases (Cell Cycle Analysis)	2019[295]
HAP	PLGA; Linezolid	3D Printing	<i>Vitro</i> : Significant inhibition against <i>MRSA</i> (up to 28 days) <i>Vivo</i> : Viable bacteria in rabbit model↓	Micro-CT: Significant healing at the defect area, Bone trabeculae↑; H&E and Masson staining: Tissue destruction and Pus cell accumulation↓; Expression of osteogenic genes ( <i>Runx2</i> , <i>OCN</i> , and <i>COL-1</i> ) ↑	2024[296]
HAP; Calcium Sulfate (CaS)	Rifampicin (RFP)	Local Drug Delivery; Osteogenic Potential	Colony-forming units (CFUs) of <i>S. aureus</i> ↓;	Micro-CT: BV/TV ↑; Histological Analysis: H&E and Masson staining indicated osteoconduction and bone regeneration ↑	2020[297]
β-TCP	Nanosized Silver (NSAg)	Controlled Silver Ion Release	Significant inhibition of <i>S. aureus</i> and <i>E. coli</i> growth;	Mechanical Strength: 7.74±0.19 MPa; Histological Analysis: New bone formation rates per unit area were 18.6±10.3%	2020[298]
β-TCP; S53P4 Bioactive Glass (BG)	Tea Tree Oil (TTO)	3D Printing; Coating Procedures	Significant antibacterial effects against <i>S. aureus</i>	Compressive strength of the scaffold was 2.4±1.0 MPa; Viability of MG-63 cells↑	2023[299]
β-TCP	Gelatin; CS; Gentamycin	Sustained Release	Inhibited the growth of <i>S. aureus</i> (in a dose-dependent manner)	The scaffold fused with bone tissues, and new tissues were formed in defect areas without any infection	2022[210]
α/β-Tricalcium Phosphate (α/β-TCP)	Tea Polyphenol-Magnesium (TP-Mg); Gelatin; Polyvinyl Alcohol (PVA)	Low-Temperature 3D Printing	<i>Vitro</i> : Inhibition rates of over 70% for <i>S. aureus</i> and nearly 60% for <i>E. coli</i> ; <i>Vivo</i> : A significant reduction in bacterial colonies in a rat model of infectious bone defects; <i>M1</i> → <i>M2</i>	<i>Vitro</i> : Osteogenic differentiation of <i>BMSCs</i> ↑; <i>Vivo</i> : Micro-CT showed BV/TV and <i>BMD</i> ↑ (6 and 12 weeks)	2024[300]



Table 3 (continued)

Categories	Components	Strategy	Assessments of infection	Assessments of bone healing	Year
Silicocarnotite ( $\text{Ca}_5(\text{PO}_4)_2\text{SiO}_4$ CPS)	Germanium dioxide ( $\text{GeO}_2$ )	Ultrasound-assisted aqueous precipitation method	Effectively inhibited the proliferation of <i>E. coli</i> / <i>S. aureus</i> ; Colony Counting Assay: $\text{GeO}_2\uparrow$ , Colonies↓; An inhibition ratio of <i>S. aureus</i> and <i>E. coli</i> were 72.1% and 76.4%, separately	Cell viability of <i>BMSCs</i> ↑; Bone tissue regeneration and integration↑	2023[301]

nanoparticles (PBNPs) [280, 281]. Han et al. proposed an innovative idea by mixing PBNPs with CS to create a novel hydrogel. Under the electrostatic adsorption of this hydrogel, bacteria are captured and killed through the photothermal effect stimulated by 808 nm NIR. However, there are certain limitations in the tissue penetration capability of light, which poses challenges for clinical translation [282]. Some sterilization materials using sonodynamic therapy based on MOFs have been reported, and their penetration is comparatively stronger than that of PTT. Ma et al. developed a novel composite material, HN25, which exhibits strong ultrasound-responsive antibacterial properties (Fig. 5). This material demonstrated significant antibacterial activity against *MRSA*, achieving an antibacterial rate of over 98.97% for *MRSA* within 4 h. Furthermore, HN25 has been shown to stimulate bone regeneration by promoting the osteogenic differentiation of mesenchymal stem cells, as evidenced by the increased expression of key bone-related genes and proteins such as *Runx2*, *OCN*, and *OPN*. Additionally, the composite exhibited biocompatibility with human dermal fibroblasts and the capacity to modulate inflammatory responses, positioning it as a promising candidate for bone repair applications without the need for surgical intervention or antibiotics [269].

In summary, the dual functions of antibacterial activity and osteogenesis in functionalized MOFs-based biomaterials are achieved through various properties of MOFs, including biodegradability, drug delivery, ion release, and their combined utilization. Moreover, the increase in antibacterial capacity aids in promoting osteogenesis, as inhibiting and eliminating infections in bone tissue contributes to repair [283]. Regardless of the antibacterial strategy employed, controlled characteristics must be achieved, such as sustained release of ions and drugs, as well as modulation of photothermal effects. Although many studies have demonstrated good antibacterial efficacy and osteogenic capability, there are still some issues regarding the controllability of antibacterial actions, particularly concerning the stability of the MOFs used in functionalized biomaterials [284, 285]. Therefore, further research and exploration of the biodegradability of MOFs are needed to better achieve the functionalization

of biomaterials, endowing them with the dual functions of infection resistance and promotion of bone repair.

### Functional solid bone tissue substitutes

Infectious bone defects often lead to an expansion of the defect space during debridement, necessitating filling materials to withstand the stresses at both ends of the defect. Solid scaffolds typically possess characteristics such as shape stability, complex structures, and diverse functions, with the most important being mechanical properties similar to those of bone tissue. Therefore, 3D printing technology can create patient-specific biomimetic bone repair scaffolds through precise design. However, the implants generated by 3D printing often have relatively limited functions, requiring modifications to meet the demands of bacterial infection control and bone regeneration [286]. Some experimental design ideas have already been discussed previously, and the following will provide a more systematic description of this technology.

Modification of implants includes the application of physical and chemical methods to alter their surfaces. For example, physical modification significantly affects hydrophobicity, van der Waals forces, and electrostatic interactions, thereby influencing the adhesion of bacteria to the implant surface. Nanofibers, tubes, and needles can penetrate bacterial cell membranes and induce cell death, while also imparting responsive functionalities to the materials [287, 288]. For instance, Mo et al. used argon plasma to create inclined and vertical nanostructures on semi-crystalline PEEK, both of which can physically kill the bacteria that come into contact with them. The sharp edges of vertically arranged nanosheets can directly penetrate and damage bacterial membranes, while inclined nanosheets capture the adhered bacteria through high affinity, using strong shear forces to cause severe deformation or even rupture of the bacteria. Comparisons through bone regeneration experiments indicated that inclined nanosheets create favorable conditions for the attachment, proliferation, and osteogenic differentiation of bone cells, thereby promoting the integration of bone implants [289].

Chemical modification is typically achieved through coatings and chemical bonding, such as incorporating

(See figure on next page.)

**Fig. 6** **A** Representative image of the scaffold. **B** SEM images of the scaffold showing (a) the top view and (b) the cross-sectional view. **C** Mineralization performance of the scaffold in simulated body fluid on days 7 and 14. **D** SEM image of *BMSCs* cultured with the scaffold for 7 days. **E** Fluorescence images showing live/dead bacteria of the scaffold against (a) *S. aureus* and (b) *E. coli*. **F** qRT-PCR analysis of the mRNA expression of osteogenesis-related genes *Runx2*, *OCN*, *ALP*, *OPN*, *BMP-2*, and *Col-1* on days 3, 7, and 14 of culture. **G** Western blot analysis of the expression of *M1* marker iNOS and *M2* marker ARG-1 in RAW264.7 macrophages cultured with the scaffold. **H** In vivo anti-infection and osteogenic capabilities: (a) Images of infected tissues at different time points; (b) Micro-CT images of rat calvaria after 6 and 12 weeks of treatment; (c) Quantitative analysis of BV/TV, (d) *BMD*, and (e) *Tb. Sp.* Copyright © 2024 The Author(s). Small published by Wiley-VCH GmbH [300]

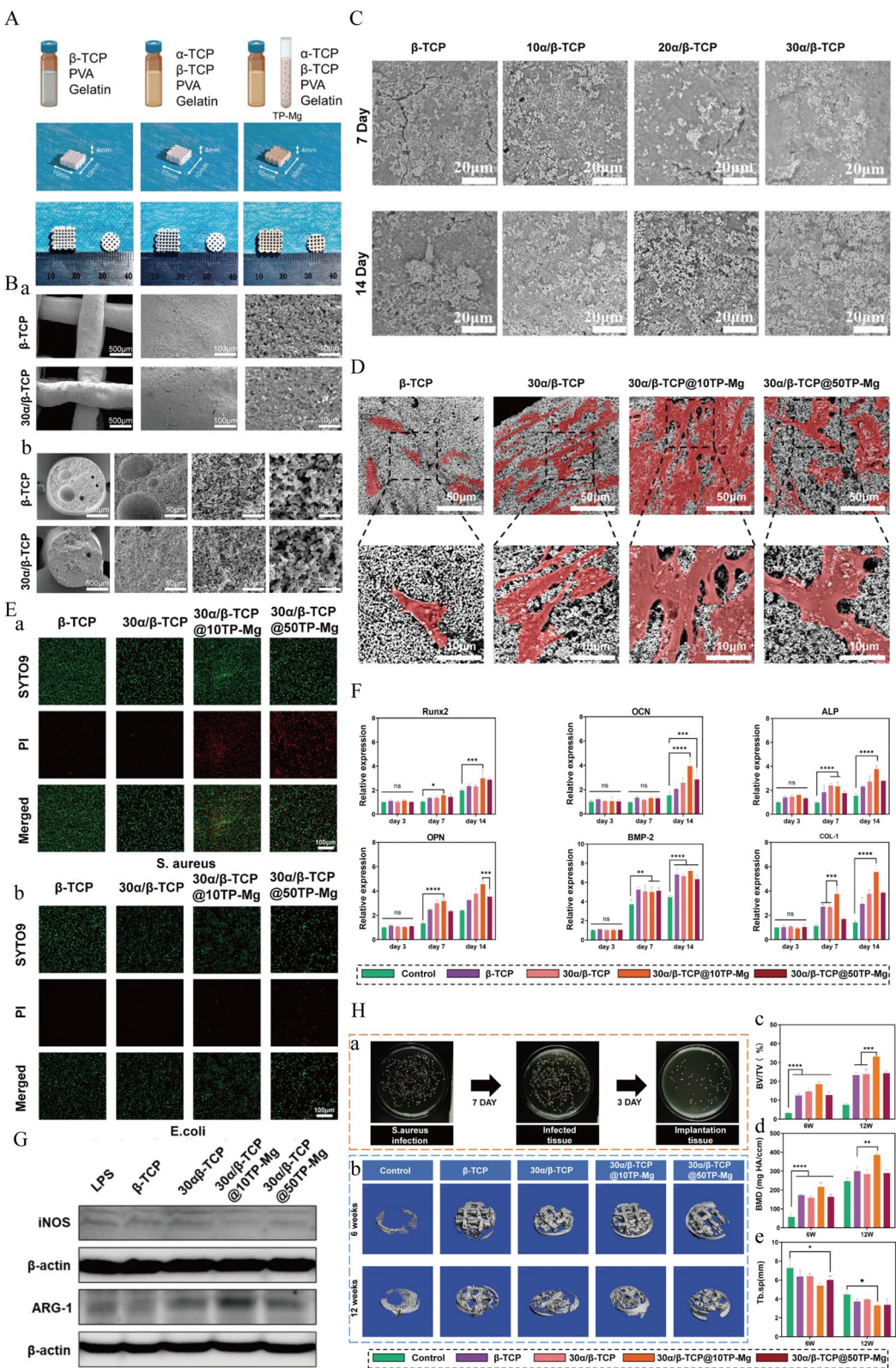


**Fig. 6** (See legend on previous page.)

**Table 4** Research on the application of 2D materials in the treatment of infectious bone defects

Categories	Components	Strategy	Assessments of infection	Assessments of bone healing	Year
MXenes (Ti <sub>3</sub> C <sub>2</sub> )	Berberine (BBR); Biphasic Calcium Phosphate (BCP); Solidum Alginate (SA)	Photothermal Therapy (PTT);	<i>Vitro</i> Assay: Complete bactericidal activity against <i>S. aureus</i> after 96 h	Expression of osteogenic genes ( <i>OCN</i> , <i>OPN</i> , <i>ALP</i> ) <sup>↑</sup> ; Superior BV/TV; Histological Analysis: H&E and Masson's staining revealed more new bone formation and tissue regeneration in 1 and 4 months	2024[312]
	Vanadium Tetrasulfide (VS <sub>4</sub> ): A semiconductor sonosensitizer (capable of generating ROS)	Ultrasound-Responsive Sonodynamic Therapy (SDT)	An antibacterial efficiency of 94.03% against <i>MRSA</i> ; Inflammation <sup>↓</sup>	Expression of osteogenic genes ( <i>OPN</i> and <i>ALP</i> ) <sup>↑</sup> ; Alizarin Red S (ARS) Staining: Richest Mineralized nodes; Bone Regeneration ( <i>Vivo</i> ): Significant new bone growth and mineralization;	2024[313]
MXenes (Ti <sub>3</sub> C <sub>2</sub> )	Peek + H <sub>2</sub> SO <sub>4</sub> = SPEEK; PDA; Calcium Peroxide (CaO <sub>2</sub> ): Provided hydrogen peroxide (H <sub>2</sub> O <sub>2</sub> ) and Ca <sup>2+</sup>	PTT and Photodynamic therapy (PDT)	Against <i>MRSA</i> : 100%; Against <i>S. aureus</i> and <i>E. coli</i> : Similar high antibacterial rates; Eradicated Biofilm	Osteogenic Differentiation: <i>ALP</i> and mineral ECM <sup>↑</sup> ; Osseointegration strength <sup>↑</sup> ; Micro-CT revealed new bone regeneration around implants; Increased collagen deposition and new bone formation	2024[314]
	PMMA Polyethyleneimine (PEI) PDA	PTT	<i>Vitro</i> : 1. Antibacterial Efficiency: <i>MRSA</i> (94.03%), <i>E. coli</i> (96.25%) 2. Lactate dehydrogenase (LDH) cytotoxicity assay: Severe bacterial membrane damage <i>Vivo</i> : No observable bacteria in Gram staining	<i>Vitro</i> : Osteogenic genes ( <i>ALP</i> , <i>Col1</i> , <i>BMP2</i> , <i>Runx2</i> ) and mineralization <sup>↑</sup> ; <i>Vivo</i> : 1. CT showed more new bone formation after 4 and 8w 2. Histological evaluation (H&E and Masson): Less inflammation and more new bone formation	2023[315]
BP BP@Mg (Magnesium-modified black phosphorus)	GelMA	PDT PTT	<i>Vitro</i> : Antibacterial efficiencies against <i>E. coli</i> and <i>S. aureus</i> > 94% (NIR 5 min) <i>Vivo</i> : Antibacterial efficiencies of <i>S. aureus</i> > 96.22% (rat model) H&E and Giemsa staining: Inflammatory cells and bacteria <sup>↓</sup> (1 week)	Micro-CT: BV/TV <sup>↑</sup> (8 week) Masson's trichrome staining: Substantial new bone formation with numerous osteoblasts around the bone tissue Immunofluorescence Staining: Nerve growth factor (NGF), calcitonin gene-related peptide (CGRP), and <i>OCN</i> <sup>↑</sup>	2023[316]
	Zinc sulfonate ligand (ZnL <sub>2</sub> ) HAp	Sequential Photothermal Mediation: 1. < 50 °C: Antibacterial therapy 2. 40–42 °C: Bone regeneration	<i>Vitro</i> : 99.8 ± 0.2% and 99.7 ± 0.1% sterilization efficiency against <i>S. aureus</i> and <i>E. coli</i> <i>Vivo</i> : 98.53% ± 0.42% antibacterial efficiency against <i>S. aureus</i>	Osteogenic Gene Expression: <i>ALP</i> , <i>OCN</i> , <i>OPN</i> , <i>Runx2</i> <sup>↑</sup> <i>ALP</i> Activity and ECM Mineralization <sup>↑</sup> <i>Vivo</i> : BV/TV, Tb.N and Tb.Sp <sup>↑</sup>	2021[317]



Table 4 (continued)

Categories	Components	Strategy	Assessments of infection	Assessments of bone healing	Year
BP pBP(protected by PDA)	Poly (aryl ether nitrile ketone) (PPENK) GelMA/ Dopamine Methacrylate (DMA)	PDT Antitumor therapy	<i>Vitro</i> : Antibacterial rate of 85% against <i>E. coli</i> and over 70% against <i>S. aureus</i> Antitumor Model: Tumor volume↓	Osteogenic Differentiation: Expression of <i>ALP</i> , <i>COL-1</i> , <i>Runx2</i> ↑ Bone Regeneration: Micro-CT showed BV/TV↑ Biomechanical Testing: The bonding strength↑	2023[318]
Graphene	PEEK Hap Stearyltrimethylammonium Chloride (STAC) Cisplatin	Chemo-PTT Sequential Treatment	Bactericidal Rate: Near-total eradication ( <i>MRSA</i> and <i>E. coli</i> under NIR irradiation)	<i>Vitro</i> : Expressions of <i>ALP</i> , <i>OPN</i> , <i>OCN</i> , and <i>Col1a1</i> ↑ <i>Vivo</i> : Micro-CT Showed BV/TV and Tb.N↑ Histological Analysis: New bone formation and larger areas of new bone tissue	2021[319]
GO	Alginate Sericin nHAp	Immunomodulation	Macrophage Polarization: induced M2 polarization; Inflammation↓ and osteoimmune microenvironment↑; <i>Vivo</i> Inflammation↓	<i>Vitro</i> : ALP activity and mineralization nodule formation↑; <i>Vivo</i> : BV/TV↑ and Fibrous Tissue Formation↓ Micro-CT: bone defect repair↑	2023[320]
GO	Alginate Antisense DNA Oligonucleotides (ASOs): Inhibited transcription of <i>S. aureus</i>	Photothermal Conversion; Targeted Antibacterial Action; Injectable and Degradable Hydrogel	<i>Vitro</i> : A zone of inhibition of 10 mm <i>Vivo</i> : Bacterial load and inflammation↓ (Mouse model)	Growth and proliferation of human umbilical cord-derived mesenchymal stem cells ( <i>hUMSCs</i> )↑; Bone Regeneration: High antibiofilm performance and good biocompatibility	2022[321]
MoS <sub>2</sub>	Carbon Nanotubes (CNTs)	Microwave Thermal Therapy (MTT); Microwave Dynamic Therapy (MDT)	<i>Vitro</i> : Antibacterial rates of <i>S. aureus</i> and <i>E. coli</i> were 99.97%; Live/Dead Bacteria Staining: Significant number; SEM and TEM Analysis: Severe rupture and excitation of internal material	Wright and H&E Staining: Bacteria, lymphocytes, Multinucleated cells↓; Masson and Alizarin Red Staining: Osteoblasts and mature bone tissue↑; X-ray Analysis: No significant periosteum reaction or bone spots; Blood Routine and Biochemical Tests: Good anti-inflammatory ability and biocompatibility	2024[322]

substances with antibacterial and anti-inflammatory properties, including antibiotics, peptides, and metal ions [290]. Yavari et al. first employed selective laser melting technology to fabricate a biomimetic topological 3D titanium scaffold, which was then covered with CS and gelatin containing cationic and anionic groups, followed by the coating of *BMP-2* and *VAN* on the scaffold surface. In vitro drug release experiments demonstrated that this multilayer coating method allows for a sustained release of *BMP-2* and *VAN* for approximately 3 weeks, with the adhered bacteria completely eliminated by day 7 [291]. Furthermore, some studies have loaded *MSCs* into scaffolds, with the most common and effective method being the use of 3D scaffolds to guide the proliferation, differentiation, and secretion of cells, thereby promoting various signaling pathways [292]. Wang et al. encapsulated peripheral blood-derived mesenchymal stem cells (*PBMSCs*) and endothelial progenitor cells (*PEPCs*) in a 75:25 ratio within 3D printed biphasic calcium phosphate (BCP) scaffolds, and coated the scaffold surface with a layer of highly active nano-hydroxyapatite (nHA), constructing a composite scaffold (nHA/BCP-PBEP/ PBMSC). This combination maximized the expression of osteogenic and angiogenic markers. Microfil angiography was performed on experimental model rabbits at 6 and 12 weeks, revealing the formation of abundant neovasculature around the scaffolds. Furthermore, histological analysis indicated a significant increase in new bone formation and mineralization, demonstrating excellent quality potential [293].

#### Multifunctional bioceramics scaffolds

Previous descriptions have highlighted the excellent performance of bioceramics in promoting osteogenesis; however, almost all types lack antibacterial properties. Therefore, external antibacterial strategies must be employed to address infections related to bone implants. Currently, various composite bioceramic scaffolds have been developed and utilized for the treatment of infectious bone defects (Table 3).

For instance, Wang et al. loaded doxycycline (*DOX*) into mesoporous bioglass (MBG) and then mixed it with molten PCL. Release experiments indicated that

*DOX* rapidly released 150 µg on the first day, followed by a slow release, with concentrations reaching 400 µg and 600 µg on days 7 and 21, respectively. This composite scaffold significantly inhibited bacterial activity and enhanced its broad-spectrum antibacterial capability. Additionally, it also achieved notable improvements in promoting the differentiation of osteoblasts, which may be related to research showing that *DOX* at a dosage of 1000 ng/mL significantly stimulates *BMP-2* expression [294]. Furthermore, antibiotics such as levofloxacin, gentamicin, chlorhexidine, berberine, and rifampicin have also been extensively studied in functionalized Bioceramics scaffolds, achieving favorable therapeutic effects [295, 297, 302–304]. Hu et al. developed a multifunctional biomimetic bone scaffold using 3D printing, which is made of  $\alpha/\beta$ -TCP, Gelatin, PVA and loaded with TP-Mg nanoparticles. This scaffold exhibits significant antibacterial activity against *S. aureus* and promotes the polarization of macrophages from the pro-inflammatory *M1* phenotype to the anti-inflammatory *M2* phenotype. Additionally, the scaffold demonstrates excellent osteogenic effects through the synergistic action of  $Mg^{2+}$  and  $Ca^{2+}$ . The study successfully developed a biomimetic bone scaffold that integrates anti-inflammatory, antibacterial, and osteogenic induction functions. This scaffold can regulate the early microenvironment and promote bone regeneration and healing, showing promising potential for the treatment of infectious bone defects (Fig. 6) [300].

In addition to the most commonly used antibiotics, other drugs, ion release, and physical effects (such as light, heat, and sound waves) have also become research hotspots [298, 305, 306]. The ions most commonly used for ion release include  $Ag^+$ ,  $Zn^{2+}$ ,  $Cu^{2+}$ ,  $La^{3+}$ , and related oxidizers. These ions are incorporated into and coated onto bioceramics. The key point is that these excellent dopants are biocompatible with normal cells, while exhibiting lethal effects on drug-resistant bacteria, and they do not interfere with the effective osteogenesis of the scaffold [307–309]. Under the piezoelectric effect, ceramics can generate positive charges, thereby inducing antibacterial activity. Sugimoto et al. have developed a lead-free piezoelectric material (Ba, Ca) (Ti, Zr)  $O_3$  (BCTZ50) for bone tissue engineering to enhance

(See figure on next page.)

**Fig. 7** **A** (a) Schematic illustration of the synthesis of SP-MC. (b) Diagram of the anti-infection mechanism of SP-MC. **B** TEM images of (a) MXenes, (b) CaO, and (c) MC. **C** Photothermal and photodynamic performance of SP-MC. Under NIR laser irradiation, the temperature changes of different materials in (a) air and (b) PBS. (c) Temperature changes of SP-MC under different laser intensities. (d) Photothermal images of SP, SP-M, SP-C, and SP-MC. (e) Photothermal cycling curves of SP-MC. **D** In vitro antibacterial performance. Images and quantitative analysis of bacterial treatment with different materials: (a, b) *S. aureus*, (c, d) *E. coli*, and (e, f) *MRSA*. **E** Osteogenesis performance. (a) ALP staining and ARS staining results after the treatment with different implants. (b) The corresponding quantitative analysis of (I) ALP and (II) ARS. **F** Photos of infected wounds after different treatments. **G** In vivo osteogenesis performance assessed by Micro-CT. (a) Reconstructed images of newly formed bone on implants at 8 week, (b) Tb.Th, and (c) trabecular separation (Tb.Sp). Copyright © 2024 Wiley-VCH GmbH [314]

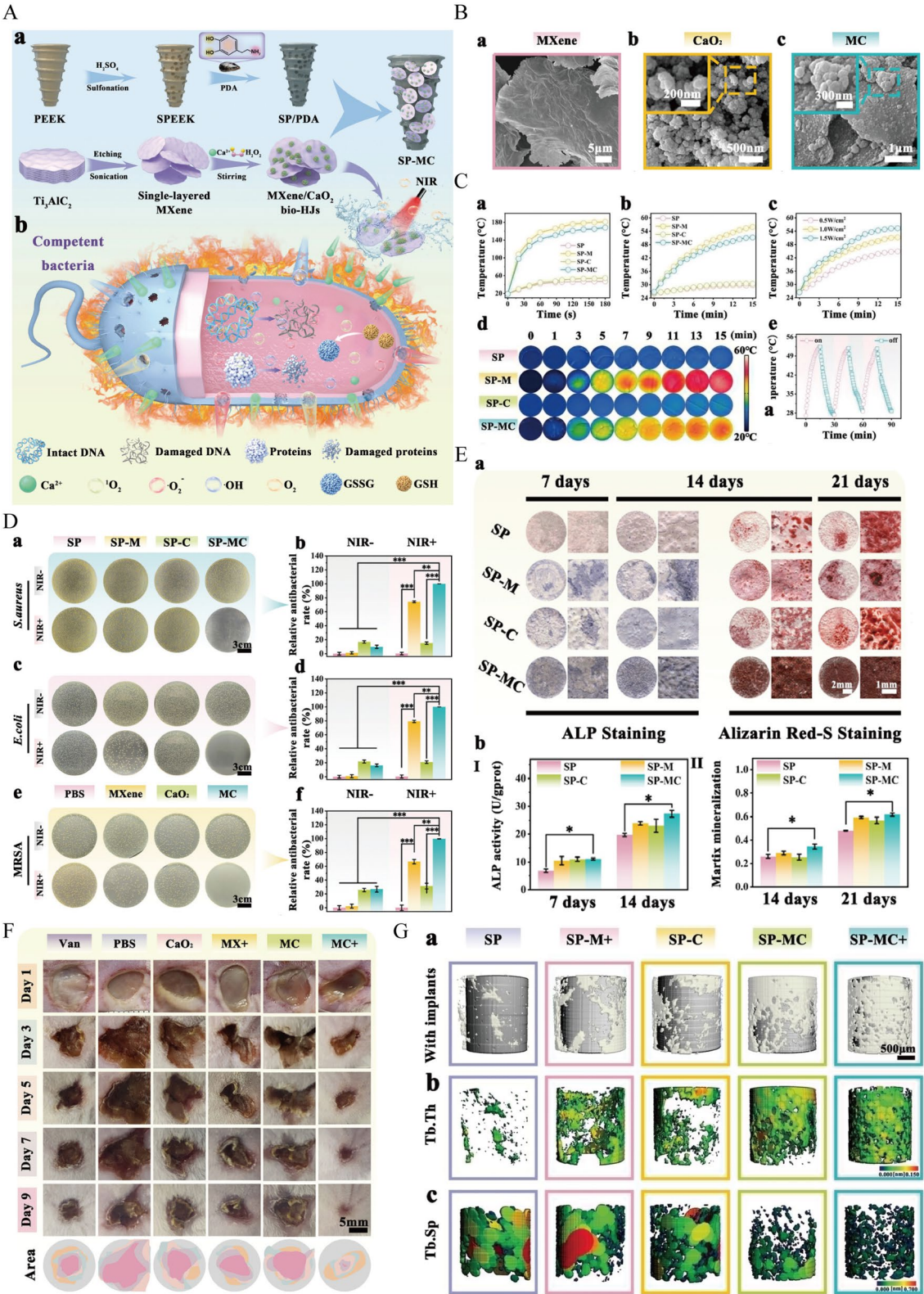


Fig. 7 (See legend on previous page.)



antibacterial performance. This material can generate a microelectric field, stimulating the surrounding liquid to decompose and produce *ROS*, thereby exerting a bactericidal effect [310].

#### Functional two-dimensional (2D) biomaterials

2D nanomaterials possess ultra-thin structures and unique properties, providing new approaches for the treatment of infectious bone defects. Their thickness is only a few angstroms or nanometers, while their length and width can reach the micrometer level. This structure endows them with certain characteristics that 3D materials lack, such as a larger specific surface area, high thermal conductivity, and unique optical properties, including broad light absorption and efficient photothermal conversion [311]. Among these, materials like graphene and its derivatives, MXenes, BP, hexagonal boron nitride (hBN), and transition metal dichalcogenides (TMDs) have been extensively studied for treating bone diseases (Table 4).

MXenes exhibit good antibacterial activity, primarily due to their hydrophilic and anionic surfaces, which enhance interactions with bacterial cell membranes. The hydrogen bonds between their functional groups and lipopolysaccharide molecules hinder bacteria from absorbing nutrients, thereby inhibiting bacterial growth [323]. Yin et al. loaded tobramycin (TOB) into MXene-GelMA hydrogels, and the composite material showed significant destructive effects and promoted osteogenesis against *S. aureus*, maintaining this effect for over 24 h [324]. In one study, researchers functionalized MXenes with PDA to construct an alginate hydrogel that can harness NIR to control the photothermal heating behavior of the hydrogel. During the experiments, it was found that the composite material could regulate the conversion of *M1/M2* macrophages, thereby controlling inflammation and accelerating bone regeneration [325]. Huang et al. designed a nanostructure based on the MXene/ $\text{CaO}_2$  bio-heterojunction (MC bio-HJs), which possesses the functions of PTT and PDT. Under NIR irradiation, it can efficiently generate *ROS*, exhibiting nearly 100% antibacterial efficiency against *MRSA*, *S. aureus*, and *E. coli* (Fig. 7). Furthermore, the study revealed that MC bio-HJs achieves outstanding antibacterial effects by inhibiting bacterial energy metabolism and protein synthesis, thereby disrupting bacterial membrane function and metabolic processes. Both in vivo and in vitro experimental results further confirmed that MC bio-HJs significantly promotes the healing of infected skin wounds and bone repair, offering a novel therapeutic strategy to

address the challenge of regenerative treatment for infectious bone defects [314].

BP is another promising 2D material for the repair of infectious bone defects, with related applications briefly mentioned in the previous sections. Recently, the fusion of BP with GelMA has also garnered widespread attention. Some studies have incorporated  $\text{Mg}^{2+}$  into black phosphorus nanosheets (BPNS) via electrostatic attraction, followed by merging with GelMA hydrogels. This approach validated the optimal concentration that significantly reduces the number of inflammatory cells and bacteria while promoting robust bone tissue regeneration [316]. Li et al. found that PDA significantly enhances the photothermal effect of BP hydrogels. Additionally, the controllability of drug release and encapsulation efficiency have also been optimized [318]. Wu et al. cleverly incorporated BPNS with zinc sulfonate ligands ( $\text{ZnL}_2$ ) into HA scaffolds. The research results show that under mild photothermal conditions below 50 °C, it can effectively eliminate more than 99% of bacteria. The bactericidal mechanism may be due to the synergistic effect between  $\text{ZnL}_2$  and positively charged BP, as well as the generation of *ROS*, leading to the destruction of intracellular biomolecules. Furthermore, the study also observed that the sustained release of  $\text{Zn}^{2+}$  combined with the presence of  $\text{PO}_4^{3-}$  jointly promotes the osteogenic process [317].

Other 2D nanosheets have also shown significant potential for clinical applications. Jin et al. utilized a heterojunction composite material composed of  $\text{MoS}_2$  and CNTs. This  $\text{MoS}_2$ /CNTs composite demonstrated enhanced microwave absorption, which facilitated effective heat and *ROS* generation, enabling rapid bacterial clearance. Both in vitro and in vivo studies confirmed the composite's superior antibacterial activity, excellent biocompatibility, and ability to promote bone healing. These findings underscore its potential as a non-invasive treatment option for infectious bone defects [322].

Overall, a reasonable combination of various materials is the best approach to enhance the effectiveness of bone tissue engineering in treating infectious bone defects. This is also the direction that the majority of researchers are currently pursuing.

#### Discussion

Bone infection is a complex process driven by interactions among various factors. In recent years, advanced diagnostic technologies have markedly improved early detection reliability. For example,  $\alpha$ -defensin, an antibacterial peptide released by neutrophils upon activation, offers a biomarker for early infection identification



[326]. Additionally, magnetic resonance imaging and nuclear medicine (such as technetium-99 m bone scans) are widely used to determine the anatomical location of osteomyelitis and the presence of associated abscesses, aiding in image-guided tissue biopsies. Additionally, novel identification technologies like matrix-assisted laser desorption ionization-time of flight mass spectrometry (MALDI-TOF MS) and genomic sequencing provide further insights into pathogen profiles and infection mechanisms [91].

Despite these advancements, treatment strategies for infectious bone defects continue to pose significant challenges (as discussed previously). The dual need for infection control and bone regeneration has driven the development of innovative biomaterial solutions. Bifunctional biomaterials have emerged as a promising alternative, offering enhanced clinical outcomes by supporting both bone regeneration and infection control at the defect site.

These materials typically involve surface modification and drug loading, enabling intelligent drug release through sustained release systems. They can release bioactive ions or molecules to kill bacteria, reduce inflammation, and promote osteoblast proliferation and differentiation, thereby accelerating bone tissue regeneration. As core scaffolds for bone repair, their design must meet mechanical performance requirements and possess good osteogenic activity and local anti-infection capabilities. In recent years, the development of composites has enhanced antibacterial effectiveness, biocompatibility, and mechanical performance, providing a stable and supportive environment for bone repair. Studies show that these materials can reduce postoperative infection rates, shorten bone healing times, and enhance bone strength.

Based on current research findings and clinical needs, an ideal bifunctional biomaterial should be able to rapidly release antibacterial components in the early stages of infection to inhibit the growth of pathogens. At the same time, it should continuously release factors that promote osteogenesis during the window of bone tissue regeneration to meet the treatment needs of different stages. Such precise temporal and spatial regulation can significantly enhance the effectiveness of infection control and bone healing. However, current research rarely addresses the selection of non-interfering drugs and the design of release modes, which may be a breakthrough point for future studies. Most existing research tends to focus on specific mechanisms, whereas infectious bone defects represent a complex pathological process involving multiple systemic contexts, suggesting that future investigations should consider the connections across various levels. Bifunctional biomaterials also present challenges in synthesis, stability, and large-scale

production. Ensuring consistency and quality during production remains crucial for clinical application. Additionally, biosafety concerns, such as potential thrombosis or vascular injuries, warrant further investigation to ensure long-term viability.

## Conclusion

The advent of bifunctional biomaterials heralds a new era in treatment paradigms. These advanced materials are specifically designed to deliver targeted, phase-dependent antibacterial and osteogenic effects, demonstrating significant potential to markedly improve clinical outcomes for patients suffering from bone infections. We believe that with the continuous development of science and technology, the treatment of bone infections will be more efficient and robust, and these materials will offer more mechanically durable, functionally effective, and personalized solutions.

## Acknowledgements

Not applicable.

## Author contributions

H.Z., W.Q., and Y.L. designed the content and wrote the first draft; L.D., Y.Z. and H.Z. produced the figures; W.Q. and Y.L. produced the table; L.D., Y.Z. and X.Y. revised the manuscript. L.D. and Y.Z. were responsible for supervision of the entire project as the corresponding author.

## Funding

This work did not receive any specific grant from funding agencies in the public, commercial, or not-for-profit sectors.

## Data availability

No datasets were generated or analysed during the current study.

## Declarations

### Ethics approval and consent to participate

Ethics approval and consent to participate do not apply to this review manuscript.

### Consent for publication

All authors of this study agreed to publish.

### Competing interests

The authors declare no competing interests.

### Author details

<sup>1</sup>Department of Orthopedics, Jinshan Hospital, Fudan University, Shanghai 201508, China. <sup>2</sup>Department of Cardiovascular Medicine, Department of Hypertension, Ruijin Hospital and State Key Laboratory of Medical Genomics, Shanghai Key Laboratory of Hypertension, Shanghai Institute of Hypertension, Shanghai Jiao Tong University School of Medicine, 197 Ruijin 2nd Road, Shanghai 200025, China. <sup>3</sup>Department of General Surgery, Jinshan Hospital, Fudan University, Shanghai 201508, China. <sup>4</sup>Research Center for Clinical Medicine, Jinshan Hospital Affiliated to Fudan University, Shanghai 201508, China.

Received: 9 January 2025 Accepted: 4 March 2025

Published online: 29 March 2025

## References

- Micheletti C, Hurley A, Gourrier A, Palmquist A, Tang T, Shah FA, Grandfield K. Bone mineral organization at the mesoscale: a review of mineral ellipsoids in bone and at bone interfaces. *Acta Biomater.* 2022;142:1–13.
- Heng BC, Bai Y, Li X, Lim LW, Li W, Ge Z, Zhang X, Deng X. Electroactive biomaterials for facilitating bone defect repair under pathological conditions. *Adv Sci (Weinh).* 2023;10: e2204502.
- Liu Z, Yuan X, Liu M, Fernandes G, Zhang Y, Yang S, Ionita CN, Yang S. Antimicrobial peptide combined with BMP2-modified mesenchymal stem cells promotes calvarial repair in an osteolytic model. *Mol Ther.* 2018;26:199–207.
- Lopes D, Martins-Cruz C, Oliveira MB, Mano JF. Bone physiology as inspiration for tissue regenerative therapies. *Biomaterials.* 2018;185:240–75.
- Kneser U, Schaefer DJ, Polykandriotis E, Horch RE. Tissue engineering of bone: the reconstructive surgeon's point of view. *J Cell Mol Med.* 2006;10:7–19.
- Zhang J, Jiang Y, Shang Z, Zhao B, Jiao M, Liu W, Cheng M, Zhai B, et al. Biodegradable metals for bone defect repair: a systematic review and meta-analysis based on animal studies. *Bioact Mater.* 2021;6:40274052.
- Wu Z, Pu P, Su Z, Zhang X, Nie L, Chang Y. Schwann cell-derived exosomes promote bone regeneration and repair by enhancing the biological activity of porous Ti6Al4V scaffolds. *Biochem Biophys Res Commun.* 2020;531:559–65.
- Ansari M. Bone tissue regeneration: biology, strategies and interface studies. *Prog Biomater.* 2019;8:223–37.
- Zhang Y, Zhou J, Wu JL, Ma JC, Wang H, Wen J, Huang S, Lee M, et al. Intrinsic antibacterial and osteoinductive stemosomes promote infected bone healing. *J Control Release.* 2023;354:713–25.
- Aragon J, Feoli S, Irujo S, Mendoza G. Composite scaffold obtained by electro-hydrodynamic technique for infection prevention and treatment in bone repair. *Int J Pharm.* 2019;557:162–9.
- Klein C, Monet M, Barbier V, Vanlaeys A, Masquelet AC, Gouyon R, Mentavri R. The Masquelet technique: current concepts, animal models, and perspectives. *J Tissue Eng Regen Med.* 2020;14:1349–59.
- Hu XX, Xiu ZZ, Li GC, Zhang JY, Shu LJ, Chen Z, Li H, Zou QF, et al. Effectiveness of transverse tibial bone transport in treatment of diabetic foot ulcer: a systematic review and meta-analysis. *Front Endocrinol (Lausanne).* 2022;13:1095361.
- Catagni MA, Azam W, Guerreschi F, Lovisetti L, Poli P, Khan MS, Di Giacomo LM. Trifocal versus bifocal bone transport in treatment of long segmental tibial bone defects. *Bone Joint J.* 2019;101-B:162–9.
- Liu K, Zhang H, Maimaiti X, Yusufu A. Bifocal versus trifocal bone transport for the management of tibial bone defects caused by fracture-related infection: a meta-analysis. *J Orthop Surg Res.* 2023;18:140.
- Kashirina A, Yao Y, Liu Y, Leng J. Biopolymers as bone substitutes: a review. *Biomater Sci.* 2019;7:3961–83.
- Wang W, Yeung KWK. Bone grafts and biomaterials substitutes for bone defect repair: a review. *Bioact Mater.* 2017;2:224–47.
- Mohamed KR, Beherei HH, El-Rashidy ZM. In vitro study of nano-hydroxyapatite/chitosan-gelatin composites for bio-applications. *J Adv Res.* 2014;5:201–8.
- Roberts TT, Rosenbaum AJ. Bone grafts, bone substitutes and orthobiologics: the bridge between basic science and clinical advancements in fracture healing. *Organogenesis.* 2012;8:114–24.
- Khan SN, Cammisia FP Jr, Sandhu HS, Diwan AD, Girardi FP, Lane JM. The biology of bone grafting. *J Am Acad Orthop Surg.* 2005;13:77–86.
- Agarwal R, Garcia AJ. Biomaterial strategies for engineering implants for enhanced osseointegration and bone repair. *Adv Drug Deliv Rev.* 2015;94:53–62.
- Zhou J, Zhang Z, Joseph J, Zhang X, Ferdows BE, Patel DN, Chen W, Banfi G, et al. Biomaterials and nanomedicine for bone regeneration: progress and future prospects. *Exploration (Beijing).* 2021;1:20210011.
- Giordani C, Maccacchione G, Giuliani A, Valli D, Scarpa ES, Antonelli A, Sabbatini J, Giachetti G, et al. Pro-osteogenic and anti-inflammatory synergistic effect of orthosilicic acid, vitamin K2, curcumin, polydatin and quercetin combination in young and senescent bone marrow-derived mesenchymal stromal cells. *Int J Mol Sci.* 2023;24:8820.
- Fan Y, Cui C, Rosen CJ, Sato T, Xu R, Li P, Wei X, Bi R, et al. Klotho in *Osx*(+) mesenchymal progenitors exerts pro-osteogenic and anti-inflammatory effects during mandibular alveolar bone formation and repair. *Signal Transduct Target Ther.* 2022;7:155.
- Egawa S, Hirai K, Matsumoto R, Yoshii T, Yuasa M, Okawa A, Sugo K, Sotome S. Efficacy of antibiotic-loaded hydroxyapatite/collagen composites is dependent on adsorbability for treating *Staphylococcus aureus* osteomyelitis in rats. *J Orthop Res.* 2020;38:843–51.
- Alegrete N, Sousa SR, Peleteiro B, Monteiro FJ, Gutierrez M. Local antibiotic delivery ceramic bone substitutes for the treatment of infected bone cavities and bone regeneration: a systematic review on what we have learned from animal models. *Materials (Basel).* 2023;16:2387.
- Mariano LC, Fernandes MHR, Gomes PS. Antimicrobial biomaterials for the healing of infected bone tissue: a systematic review of microtomographic data on experimental animal models. *J Funct Biomater.* 2022;13:193.
- Hempel U, Matthaus C, Preissler C, Moller S, Hintze V, Dieter P. Artificial matrices with high-sulfated glycosaminoglycans and collagen are anti-inflammatory and pro-osteogenic for human mesenchymal stromal cells. *J Cell Biochem.* 2014;115:1561–71.
- Jones JR. Reprint of: review of bioactive glass: from hench to hybrids. *Acta Biomater.* 2015;23(Suppl):S53–82.
- Chotchindakun K, Pekkoh J, Ruangsuriya J, Zheng K, Unalan I, Boccacini AR. Fabrication and characterization of cinnamaldehyde-loaded mesoporous bioactive glass nanoparticles/PHBV-based microspheres for preventing bacterial infection and promoting bone tissue regeneration. *Polymers (Basel).* 2021;13:1794.
- Andrzejowski P, Giannoudis PV. The 'diamond concept' for long bone non-union management. *J Orthop Traumatol.* 2019;20:21.
- Claes L, Recknagel S, Ignatius A. Fracture healing under healthy and inflammatory conditions. *Nat Rev Rheumatol.* 2012;8:133–43.
- Marsell R, Einhorn TA. The biology of fracture healing. *Injury.* 2011;42:551–5.
- Maruyama M, Rhee C, Utsunomiya T, Zhang N, Ueno M, Yao Z, Goodman SB. Modulation of the inflammatory response and bone healing. *Front Endocrinol (Lausanne).* 2020;11:386.
- Walters G, Pountos I, Giannoudis PV. The cytokines and micro-environment of fracture hematoma: current evidence. *J Tissue Eng Regen Med.* 2018;12:e1662–77.
- Bastian O, Pillay J, Alblas J, Leenen L, Koenderman L, Blokhuis T. Systemic inflammation and fracture healing. *J Leukoc Biol.* 2011;89:669–73.
- Segalini AI, Mohamadi A, Dizier B, Lokajczyk A, Brion R, Lanel R, Amiaud J, Charrier C, et al. Interleukin-34 promotes tumor progression and metastatic process in osteosarcoma through induction of angiogenesis and macrophage recruitment. *Int J Cancer.* 2015;137:73–85.
- Cho TJ, Gerstenfeld LC, Einhorn TA. Differential temporal expression of members of the transforming growth factor beta superfamily during murine fracture healing. *J Bone Miner Res.* 2002;17:513–20.
- Li M, Yin H, Yan Z, Li H, Wu J, Wang Y, Wei F, Tian G, et al. The immune microenvironment in cartilage injury and repair. *Acta Biomater.* 2022;140:23–42.
- Carmi Y, Dotan S, Rider P, Kaplanov I, White MR, Baron R, Abutbul S, Huszar M, et al. The role of IL-1beta in the early tumor cell-induced angiogenic response. *J Immunol.* 2013;190:3500–9.
- Coughlin BA, Trombley BT, Mohr S. Interleukin-6 (IL-6) mediates protection against glucose toxicity in human Muller cells via activation of VEGF-A signaling. *Biochem Biophys Res Commun.* 2019;517:227–32.
- Zhang D, Huang Y, Huang Z, Zhang R, Wang H, Huang D. FTY-720P suppresses osteoclast formation by regulating expression of interleukin-6 (IL-6), interleukin-4 (IL-4), and matrix metalloproteinase 2 (MMP2). *Med Sci Monit.* 2016;22:2187–94.
- Komi DEA, Redegeld FA. Role of mast cells in shaping the tumor micro-environment. *Clin Rev Allergy Immunol.* 2020;58:313–25.
- Yang X, Ricciardi BF, Hernandez-Soria A, Shi Y, Pleshko Camacho N, Bostrom MP. Callus mineralization and maturation are delayed during fracture healing in interleukin-6 knockout mice. *Bone.* 2007;41:928–36.
- Nakao Y, Fukuda T, Zhang Q, Sanui T, Shinjo T, Kou X, Chen C, Liu D, et al. Exosomes from TNF alpha-treated human gingiva-derived MSCs enhance M2 macrophage polarization and inhibit periodontal bone loss. *Acta Biomater.* 2021;122:306–24.
- Patil AS, Sable RB, Kothari RM. An update on transforming growth factor-beta (TGF-beta): sources, types, functions and clinical applicability for cartilage/bone healing. *J Cell Physiol.* 2011;226:3094–103.

46. Zhao P, Xiao L, Peng J, Qian YQ, Huang CC. Exosomes derived from bone marrow mesenchymal stem cells improve osteoporosis through promoting osteoblast proliferation via MAPK pathway. *Eur Rev Med Pharmacol Sci*. 2018;22:3962–70.
47. Zhao Q, Zhang Y, Xiao L, Lu H, Ma Y, Liu Q, Wang X. Surface engineering of titania nanotubes incorporated with double-layered extracellular vesicles to modulate inflammation and osteogenesis. *Regen Biomater*. 2021;8:rbab010.
48. Wang C, Inzana JA, Mirando AJ, Ren Y, Liu Z, Shen J, O'Keefe RJ, Awad HA, et al. NOTCH signaling in skeletal progenitors is critical for fracture repair. *J Clin Invest*. 2016;126:1471–81.
49. Su Z, Li J, Lin J, Li Z, Che Y, Zhang Z, Zheng G, Ye G, et al. TNF- $\alpha$ -induced KAT2A impedes BMMSC quiescence by mediating succinylation of the mitophagy-related protein VCP. *Adv Sci (Weinh)*. 2024;11: e2303388.
50. Karnes JM, Daffner SD, Watkins CM. Multiple roles of tumor necrosis factor- $\alpha$  in fracture healing. *Bone*. 2015;78:87–93.
51. Zhang B, Liu N, Shi H, Wu H, Gao Y, He H, Gu B, Liu H. High glucose microenvironments inhibit the proliferation and migration of bone mesenchymal stem cells by activating GSK3 $\beta$ . *J Bone Miner Metab*. 2016;34:140–50.
52. Zhong Q, Wang D, Mai H, Chen R, Xu Y, Lei M, Xie J, Tang Z, et al. Injectable thermo-responsive poloxamer hydrogel/methacrylate gelatin microgels stimulates bone regeneration through biomimetic programmed release of SDF-1 and IGF-1. *Int J Biol Macromol*. 2024;271: 132742.
53. Xu J, Chen Y, Liu Y, Zhang J, Kang Q, Ho K, Chai Y, Li G. Effect of SDF-1/Cxcr4 signaling antagonist AMD3100 on bone mineralization in distraction osteogenesis. *Calcif Tissue Int*. 2017;100: 641652.
54. Yang F, Xue F, Guan J, Zhang Z, Yin J, Kang Q. Stromal-cell-derived factor (SDF) 1- $\alpha$  overexpression promotes bone regeneration by osteogenesis and angiogenesis in osteonecrosis of the femoral head. *Cell Physiol Biochem*. 2018;46:2561–75.
55. Lauer A, Wolf P, Mehler D, Gotz H, Ruzgar M, Baranowski A, Henrich D, Rommens PM, et al. Biofabrication of SDF-1 functionalized 3D-printed cell-free scaffolds for bone tissue regeneration. *Int J Mol Sci*. 2020;21:2175.
56. Toosi S, Behravan J. Osteogenesis and bone remodeling: a focus on growth factors and bioactive peptides. *BioFactors*. 2020;46:326–40.
57. Zhang H, Li X, Li J, Zhong L, Chen X, Chen S. SDF-1 mediates mesenchymal stem cell recruitment and migration via the SDF-1/CXCR4 axis in bone defect. *J Bone Miner Metab*. 2021;39:126–38.
58. Bernhard JC, Marolt Presen D, Li M, Monforte X, Ferguson J, Leinfellner G, Heimel P, Betti SL, et al. Effects of endochondral and intramembranous ossification pathways on bone tissue formation and vascularization in human tissue-engineered grafts. *Cells*. 2022;11:3070.
59. Blumer MJF. Bone tissue and histological and molecular events during development of the long bones. *Ann Anat*. 2021;235: 151704.
60. Kenkre JS, Bassett J. The bone remodelling cycle. *Ann Clin Biochem*. 2018;55:308–27.
61. Qiu M, Li C, Cai Z, Li C, Yang K, Tulufu N, Chen B, Cheng L, et al. 3D biomimetic calcified cartilaginous callus that induces type H vessels formation and osteoclastogenesis. *Adv Sci (Weinh)*. 2023;10: e2207089.
62. Ghiasi MS, Chen JE, Rodriguez EK, Vaziri A, Nazarian A. Computational modeling of human bone fracture healing affected by different conditions of initial healing stage. *BMC Musculoskelet Disord*. 2019;20:562.
63. Wu M, Wu S, Chen W, Li YP. The roles and regulatory mechanisms of TGF- $\beta$  and BMP signaling in bone and cartilage development, homeostasis and disease. *Cell Res*. 2024;34:101–23.
64. Icer MA, Gezmen-Karadag M. The multiple functions and mechanisms of osteopontin. *Clin Biochem*. 2018;59:17–24.
65. Li JJ, Ebied M, Xu J, Zreiqat H. Current approaches to bone tissue engineering: the interface between biology and engineering. *Adv Healthc Mater*. 2018;7: e1701061.
66. Wang L, You X, Zhang L, Zhang C, Zou W. Mechanical regulation of bone remodeling. *Bone Res*. 2022;10:16.
67. Peng Y, Wu S, Li Y, Crane JL. Type H blood vessels in bone modeling and remodeling. *Theranostics*. 2020;10:426–36.
68. Gelalis ID, Politis AN, Arnaoutoglou CM, Korompilias AV, Pakos EE, Vekris MD, Karageorgos A, Xenakis TA. Diagnostic and treatment modalities in nonunions of the femoral shaft: a review. *Injury*. 2012;43:980–8.
69. Foulke BA, Kendal AR, Murray DW, Pandit H. Fracture healing in the elderly: a review. *Maturitas*. 2016;92:49–55.
70. Kim H, Kim DH, Kim DM, Kholinne E, Lee ES, Alzahrani WM, Kim JW, Jeon IH, et al. Do nonsteroidal anti-inflammatory or COX-2 inhibitor drugs increase the nonunion or delayed union rates after fracture surgery?: A propensity-score-matched study. *J Bone Joint Surg Am*. 2021;103:1402–10.
71. Bell JM, Shields MD, Watters J, Hamilton A, Beringer T, Elliott M, Quinlivan R, Tirupathi S, et al. Interventions to prevent and treat corticosteroid-induced osteoporosis and prevent osteoporotic fractures in Duchenne muscular dystrophy. *Cochrane Database Syst Rev*. 2017;1:10899.
72. Sumaiya K, Langford D, Natarajaseenivasan K, Shanmugapriya S. Macrophage migration inhibitory factor (MIF): a multifaceted cytokine regulated by genetic and physiological strategies. *Pharmacol Ther*. 2022;233: 108024.
73. Kobayashi T, Onodera S, Kondo E, Tohyama H, Fujiki H, Yokoyama A, Yasuda K. Impaired fracture healing in macrophage migration inhibitory factor-deficient mice. *Osteoporos Int*. 2011;22:1955–65.
74. Nagasawa Y, Takei M, Iwata M, Nagatsuka Y, Tsuzuki H, Imai K, Imadome KI, Fujiwara S, et al. Human osteoclastogenesis in Epstein-Barr virus-induced erosive arthritis in humanized NOD/Shi-scid/IL2Rg $\gamma$  null mice. *PLoS ONE*. 2021;16: e0249340.
75. Wang H, Han P, Qi X, Li F, Li M, Fan L, Zhang H, Zhang X, et al. Bcl-2 enhances chimeric antigen receptor T cell persistence by reducing activation-induced apoptosis. *Cancers (Basel)*. 2021;13:197.
76. Kovanan PE, Leonard WJ. Cytokines and immunodeficiency diseases: critical roles of the gamma(c) dependent cytokines interleukins 2, 4, 7, 9, 15, and 21, and their signaling pathways. *Immunol Rev*. 2004;202:67–83.
77. Oei L, Rivadeneira F, Zillikens MC, Oei EH. Diabetes, diabetic complications, and fracture risk. *Curr Osteoporos Rep*. 2015;13:106–15.
78. Okamoto K. Regulation of bone by IL-17-producing T cells. *Nihon Rinsho Meneki Gakkai Kaishi*. 2017;40:361–6.
79. Zhang E, Miramini S, Patel M, Richardson M, Ebeling P, Zhang L. Role of TNF- $\alpha$  in early-stage fracture healing under normal and diabetic conditions. *Comput Methods Progr Biomed*. 2022;213: 106536.
80. Lin WM, Yuan Q. Latest research findings on immune microenvironment regulation in jaw bone related diseases. *Sichuan Da Xue Xue Bao Yi Xue Ban*. 2022;53:528–31.
81. Dar HY, Perrien DS, Pal S, Stoica A, Uppuganti S, Nyman JS, Jones RM, Weitzmann MN, et al. Callus gamma delta T cells and microbe-induced intestinal Th17 cells improve fracture healing in mice. *J Clin Invest*. 2023;133: e166577.
82. Lisowska B, Kosson D, Domaracka K. Lights and shadows of NSAIDs in bone healing: the role of prostaglandins in bone metabolism. *Drug Des Devel Ther*. 2018;12:1753–8.
83. Marquez-Lara A, Hutchinson ID, Nunez F Jr, Smith TL, Miller AN. Nonsteroidal anti-inflammatory drugs and bone-healing: a systematic review of research quality. *JBJS Rev*. 2016;4: e4.
84. Lisowska B, Kosson D, Domaracka K. Positives and negatives of non-steroidal anti-inflammatory drugs in bone healing: the effects of these drugs on bone repair. *Drug Des Devel Ther*. 2018;12:1809–14.
85. Geusens P, Emans PJ, de Jong JJ, van den Bergh J. NSAIDs and fracture healing. *Curr Opin Rheumatol*. 2013;25:524–31.
86. Hachemi Y, Rapp AE, Picke AK, Weidinger G, Ignatius A, Tuckermann J. Molecular mechanisms of glucocorticoids on skeleton and bone regeneration after fracture. *J Mol Endocrinol*. 2018;61:R75–90.
87. Okada K, Kawao N, Nakai D, Wakabayashi R, Horiuchi Y, Okumoto K, Kurashimo S, Takafuji Y, et al. Role of macrophages and plasminogen activator inhibitor-1 in delayed bone repair induced by glucocorticoids in mice. *Int J Mol Sci*. 2022;23:478.
88. Goodman SB, Maruyama M. Inflammation, bone healing and osteonecrosis: from bedside to bench. *J Inflamm Res*. 2020;13:913–23.
89. Torres HM, Arnold KM, Oviedo M, Westendorp JJ, Weaver SR. Inflammatory processes affecting bone health and repair. *Curr Osteoporos Rep*. 2023;21:842–53.
90. Luthje FL, Skovgaard K, Jensen HE, Blurup-Plum SA, Henriksen NL, Aalbaek B, Jensen LK. Receptor activator of nuclear factor kappa-B ligand is not regulated during chronic osteomyelitis in pigs. *J Comp Pathol*. 2020;179:7–24.

91. Masters EA, Ricciardi BF, Bentley KLM, Moriarty TF, Schwarz EM, Muthukrishnan G. Skeletal infections: microbial pathogenesis, immunity and clinical management. *Nat Rev Microbiol*. 2022;20:385–400.
92. Wang J, Meng M, Li M, Guan X, Liu J, Gao X, Sun Q, Li J, et al. Integrin  $\alpha 5 \beta 1$ , as a receptor of fibronectin, binds the FbaA protein of group A *Streptococcus* to initiate autophagy during infection. *Smbio*. 2020;11:10.
93. Wen Q, Gu F, Sui Z, Su Z, Yu T. The process of osteoblastic infection by *Staphylococcus aureus*. *Int J Med Sci*. 2020;17:1327–32.
94. Hamza T, Li B. Differential responses of osteoblasts and macrophages upon *Staphylococcus aureus* infection. *BMC Microbiol*. 2014;14:207.
95. Josse J, Velard F, Gangloff SC. *Staphylococcus aureus* vs. osteoblast: relationship and consequences in osteomyelitis. *Front Cell Infect Microbiol*. 2015;5:85.
96. Zhu C, Wang J, Cheng T, Li Q, Shen H, Qin H, Cheng M, Zhang X. The potential role of increasing release of mouse beta-defensin-14 in the treatment of osteomyelitis in mice: a primary study. *PLoS ONE*. 2014;9:e86874.
97. Yu B, Pacureanu A, Olivier C, Cloetens P, Peyrin F. Assessment of the human bone lacuno-canalicular network at the nanoscale and impact of spatial resolution. *Sci Rep*. 2020;10:4567.
98. Masters EA, Salminen AT, Begolo S, Luke EN, Barrett SC, Overby CT, Gill AL, de Mesy Bentley KL, et al. An in vitro platform for elucidating the molecular genetics of *S. aureus* invasion of the osteocyte lacuno-canalicular network during chronic osteomyelitis. *Nanomedicine*. 2019;21:102039.
99. Masters EA, de Mesy Bentley KL, Gill AL, Hao SP, Galloway CA, Salminen AT, Guy DR, McGrath JL, et al. Identification of penicillin binding protein 4 (PBP4) as a critical factor for *Staphylococcus aureus* bone invasion during osteomyelitis in mice. *PLoS Pathog*. 2020;16:e1008988.
100. Zoller SD, Hegde V, Burke ZDC, Park HY, Ishmael CR, Blumstein GW, Sheppard W, Hamad C, et al. Evading the host response: *Staphylococcus* "hiding" in cortical bone canalicular system causes increased bacterial burden. *Bone Res*. 2020;8:43.
101. Masters EA, Muthukrishnan G, Ho L, Gill AL, de Mesy Bentley KL, Galloway CA, McGrath JL, Awad HA, et al. *Staphylococcus aureus* cell wall biosynthesis modulates bone invasion and osteomyelitis pathogenesis. *Front Microbiol*. 2021;12:723498.
102. Schilcher K, Horswill AR. *Staphylococcal* biofilm development: structure, regulation, and treatment strategies. *Microbiol Mol Biol Rev*. 2020;84:10.
103. Masters EA, Trombetta RP, de Mesy Bentley KL, Boyce BF, Gill AL, Gill SR, Nishitani K, Ishikawa M, et al. Evolving concepts in bone infection: redefining "biofilm", "acute vs. chronic osteomyelitis", "the immune proteome" and "local antibiotic therapy." *Bone Res*. 2019;7:20.
104. Moormeier DE, Bayles KW. *Staphylococcus aureus* biofilm: a complex developmental organism. *Mol Microbiol*. 2017;104:365–76.
105. Cui YC, Wu Q, Teh SW, Peli A, Bu G, Qiu YS, Benelli G, Kumar SS. Bone breaking infections—a focus on bacterial and mosquito-borne viral infections. *Microb Pathog*. 2018;122:130–6.
106. Jamal M, Ahmad W, Andleeb S, Jalil F, Imran M, Nawaz MA, Hussain T, Ali M, et al. Bacterial biofilm and associated infections. *J Chin Med Assoc*. 2018;81:7–11.
107. Mangwani N, Kumari S, Das S. Bacterial biofilms and quorum sensing: fidelity in bioremediation technology. *Biotechnol Genet Eng Rev*. 2016;32:43–73.
108. Lister JL, Horswill AR. *Staphylococcus aureus* biofilms: recent developments in biofilm dispersal. *Front Cell Infect Microbiol*. 2014;4:178.
109. Cheng AG, DeDent AC, Schneewind O, Missiakas D. A play in four acts: *Staphylococcus aureus* abscess formation. *Trends Microbiol*. 2011;19:225–32.
110. Malachowa N, Kobayashi SD, Porter AR, Braughton KR, Scott DP, Gardner DJ, Missiakas DM, Schneewind O, et al. Contribution of *Staphylococcus aureus* coagulases and clumping factor a to abscess formation in a rabbit model of skin and soft tissue infection. *PLoS ONE*. 2016;11:e0158293.
111. Farnsworth CW, Schott EM, Jensen SE, Zukoski J, Benvie AM, Refaai MA, Kates SL, Schwarz EM, et al. Adaptive upregulation of clumping factor A (ClfA) by *Staphylococcus aureus* in the obese, type 2 diabetic host mediates increased virulence. *Infect Immun*. 2017;85:10.
112. Kobayashi SD, Malachowa N, DeLeo FR. Pathogenesis of *Staphylococcus aureus* abscesses. *Am J Pathol*. 2015;185:1518–27.
113. Hofstee MI, Riool M, Terjajevs I, Thompson K, Stoddart MJ, Richards RG, Zaat SAJ, Moriarty TF. Three-dimensional in vitro *Staphylococcus aureus* abscess communities display antibiotic tolerance and protection from neutrophil clearance. *Infect Immun*. 2020;88:10.
114. Salhotra A, Shah HN, Levi B, Longaker MT. Mechanisms of bone development and repair. *Nat Rev Mol Cell Biol*. 2020;21:696–711.
115. Johnson CT, Sok MCP, Martin KE, Kalelkar PP, Caplin JD, Botchwey EA, Garcia AJ. Lysostaphin and BMP-2 co-delivery reduces *S. aureus* infection and regenerates critical-sized segmental bone defects. *Sci Adv*. 2019;5:1228.
116. Ho-Shui-Ling A, Bolander J, Rustom LE, Johnson AW, Luyten FP, Picart C. Bone regeneration strategies: engineered scaffolds, bioactive molecules and stem cells current stage and future perspectives. *Biomaterials*. 2018;180:143–62.
117. Szczerba BM, Castro-Giner F, Vetter M, Krol I, Gkoutela S, Landin J, Scheidmann MC, Donato C, et al. Neutrophils escort circulating tumour cells to enable cell cycle progression. *Nature*. 2019;566:553–7.
118. Schneider AH, Taira TM, Publio GA, da Silva D, Donate Yabuta PB, Dos Santos JC, Machado CC, de Souza FF, et al. Neutrophil extracellular traps mediate bone erosion in rheumatoid arthritis by enhancing RANKL-induced osteoclastogenesis. *Br J Pharmacol*. 2024;181:429–46.
119. Iantomasi T, Romagnoli C, Palmieri G, Donati S, Falsetti I, Miglietta F, Aurilia C, Marini F, et al. Oxidative stress and inflammation in osteoporosis: molecular mechanisms involved and the relationship with microRNAs. *Int J Mol Sci*. 2023;24:3772.
120. Sugisaki R, Miyamoto Y, Yoshimura K, Sasa K, Kaneko K, Tanaka M, Ito S, et al. Possible involvement of elastase in enhanced osteoclast differentiation by neutrophils through degradation of osteoprotegerin. *Bone*. 2020;132:115216.
121. Kong L, Smith W, Hao D. Overview of RAW2647 for osteoclastogenesis study: phenotype and stimuli. *J Cell Mol Med*. 2019;23:3077–87.
122. Chen Y, Liu K, Qin Y, Chen S, Guan G, Huang Y, Chen Y, Mo Z. Effects of pereskia aculeata miller petroleum ether extract on complete freund's adjuvant-induced rheumatoid arthritis in rats and its potential molecular mechanisms. *Front Pharmacol*. 2022;13:869810.
123. Kral-Pointner JB, Haider P, Szabo PL, Salzmann M, Brekalo M, Schneider KH, Schrottmaier WC, Kaun C, et al. Reduced monocyte and neutrophil infiltration and activation by P-selectin/CD62P inhibition enhances thrombus resolution in mice. *Arterioscler Thromb Vasc Biol*. 2024;44:954–68.
124. Nightingale TD, McCormack JJ, Grimes W, Robinson C, Lopes da Silva M, White IJ, Vaughan A, Cramer LP, et al. Tuning the endothelial response: differential release of exocytic cargos from Weibel-Palade bodies. *J Thromb Haemost*. 2018;16:1873–86.
125. Mussbacher M, Derler M, Basilio J, Schmid JA. NF-kappaB in monocytes and macrophages—an inflammatory master regulator in multitasked immune cells. *Front Immunol*. 2023;14:1134661.
126. Guo R, Yamashita M, Zhang Q, Zhou Q, Chen D, Reynolds DG, Awad HA, Yanoso L, et al. Ubiquitin ligase Smurf1 mediates tumor necrosis factor-induced systemic bone loss by promoting proteasomal degradation of bone morphogenetic signaling proteins. *J Biol Chem*. 2008;283:23084–92.
127. Deshpande S, James AW, Blough J, Donneys A, Wang SC, Cederna PS, Buchman SR, Levi B. Reconciling the effects of inflammatory cytokines on mesenchymal cell osteogenic differentiation. *J Surg Res*. 2013;185:278–85.
128. McDonald MM, Khoo WH, Ng PY, Xiao Y, Zamerli J, Thatcher P, Kyaw W, Pathmanandavel K, et al. Osteoclasts recycle via osteomorphs during RANKL-stimulated bone resorption. *Cell*. 2021;184(1330–1347):e1313.
129. Kim HJ, Kang WY, Seong SJ, Kim SY, Lim MS, Yoon YR. Follistatin-like 1 promotes osteoclast formation via RANKL-mediated NF-kappaB activation and M-CSF-induced precursor proliferation. *Cell Signal*. 2016;28:1137–44.
130. Jiang W, Jin Y, Zhang S, Ding Y, Huo K, Yang J, Zhao L, Nian B, et al. PGE2 activates EP4 in subchondral bone osteoclasts to regulate osteoarthritis. *Bone Res*. 2022;10:27.
131. Somayaji SN, Ritchie S, Sahraei M, Marriott I, Hudson MC. *Staphylococcus aureus* induces expression of receptor activator of NF-kappaB ligand and prostaglandin E2 in infected murine osteoblasts. *Infect Immun*. 2008;76:5120–6.



132. Tian Y, Wu D, Wu D, Cui Y, Ren G, Wang Y, Wang J, Peng C. Chitosan-based biomaterial scaffolds for the repair of infected bone defects. *Front Bioeng Biotechnol*. 2022;10: 899760.
133. Chi H, Chen G, He Y, Chen G, Tu H, Liu X, Yan J, Wang X. 3D-HA scaffold functionalized by extracellular matrix of stem cells promotes bone repair. *Int J Nanomedicine*. 2020;15:5825–38.
134. Chen Z, Zhang Q, Li H, Wei Q, Zhao X, Chen F. Elastin-like polypeptide modified silk fibroin porous scaffold promotes osteochondral repair. *Bioact Mater*. 2021;6:589–601.
135. Hickok NJ, Shapiro IM. Immobilized antibiotics to prevent orthopaedic implant infections. *Adv Drug Deliv Rev*. 2012;64:1165–76.
136. Zegre M, Barros J, Ribeiro IAC, Santos C, Caetano LA, Goncalves L, Monteiro FJ, Ferraz MP, et al. Poly(DL-lactic acid) scaffolds as a bone targeting platform for the co-delivery of antimicrobial agents against *S. aureus*-*C. albicans* mixed biofilms. *Int J Pharm*. 2022;622:121832.
137. Zhao C, Liu W, Zhu M, Wu C, Zhu Y. Bioceramic-based scaffolds with antibacterial function for bonetissue engineering: a review. *Bioact Mater*. 2022;18:383–98.
138. Sukhanova A, Bozrova S, Sokolov P, Berestovoy M, Karaulov A, Nabiev I. Dependence of nanoparticle toxicity on their physical and chemical properties. *Nanoscale Res Lett*. 2018;13:44.
139. Shaikh S, Nazam N, Rizvi SMD, Ahmad K, Baig MH, Lee EJ, Choi I. Mechanistic insights into the antimicrobial actions of metallic nanoparticles and their implications for multidrug resistance. *Int J Mol Sci*. 2019;20:2468.
140. Slavin YN, Asnis J, Hafeli UO, Bach H. Metal nanoparticles: understanding the mechanisms behind antibacterial activity. *J Nanobiotechnology*. 2017;15:65.
141. Canaparo R, Foglietta F, Limongi T, Serpe L. Biomedical applications of reactive oxygen species generation by metal nanoparticles. *Materials (Basel)*. 2020;14:53.
142. Teixeira ABV, de Castro DT, Schiavon MA, Dos Reis AC. Cytotoxicity and release ions of endodontic sealers incorporated with a silver and vanadium base nanomaterial. *Odontology*. 2020;108:661–8.
143. Spirescu VA, Chircov C, Grumezescu AM, Vasile BS, Andronescu E. Inorganic nanoparticles and composite films for antimicrobial therapies. *Int J Mol Sci*. 2021;22:4595.
144. Zhang C, Li X, Xiao D, Zhao Q, Chen S, Yang F, Liu J, Duan K. Cu(2+) release from polylactic acid coating on titanium reduces bone implant-related infection. *J Funct Biomater*. 2022;13:78.
145. Li C, Ai F, Miao X, Liao H, Li F, Liu M, Yu F, Dong L, et al. "The return of ceramic implants": rosestem inspired dual layered modification of ceramic scaffolds with improved mechanical and anti-infective properties. *Mater Sci Eng C Mater Biol Appl*. 2018;93:873–9.
146. Li S, Dong S, Xu W, Tu S, Yan L, Zhao C, Ding J, Chen X. Antibacterial hydrogels. *Adv Sci (Weinh)*. 2018;5:1700527.
147. Kjalarsdottir L, Dyrkjof A, Dagbjartsson A, Laxdal EH, Orlgysson G, Gislason J, Einarsson JM, et al. Bone remodeling effect of a chitosan and calcium phosphate-based composite. *Regen Biomater*. 2019;6:241–7.
148. Shariatnia Z. Carboxymethyl chitosan: properties and biomedical applications. *Int J Biol Macromol*. 2018;120:1406–19.
149. Ardean C, Davidescu CM, Nemes NS, Negrea A, Ciopec M, Duteanu N, Negrea P, Duda-Seiman D, et al. Factors influencing the antibacterial activity of chitosan and chitosan modified by functionalization. *Int J Mol Sci*. 2021;22:7449.
150. Raafat D, von Barga K, Haas A, Sahl HG. Insights into the mode of action of chitosan as antibacterial compound. *Appl Environ Microbiol*. 2008;74:3764–73.
151. Shi S, Shi W, Zhou B, Qiu S. Research and application of chitosan nanoparticles in orthopaedic infections. *Int J Nanomed*. 2024;19:6589–602.
152. Chung YC, Yeh JY, Tsai CF. Antibacterial characteristics and activity of water-soluble chitosan derivatives prepared by the Maillard reaction. *Molecules*. 2011;16:8504–14.
153. Ke CL, Deng FS, Chuang CY, Lin CH. Antimicrobial actions and applications of chitosan. *Polymers (Basel)*. 2021;13:904.
154. Ganesan S, Alagarasan JK, Sonaimuthu M, Aruchamy K, Alkallas FH, Ben Gouider Trabelsi A, Kusmartsev FV, Poliseti V, et al. Preparation and characterization of salsalate-loaded chitosan nanoparticles: in vitro release and antibacterial and antibiofilm activity. *Mar Drugs*. 2022;20:733.
155. Dai X, Liu X, Li Y, Xu Q, Yang L, Gao F. Nitrogen-phosphorous co-doped carbonized chitosan nanoparticles for chemotherapy and ROS-mediated immunotherapy of intracellular *Staphylococcus aureus* infection. *Carbohydr Polym*. 2023;315: 121013.
156. Haji Hossein Tabrizi A, Habibi M, Foroohi F, Mohammadian T, Asadi Karam MR. Investigation of the effects of antimicrobial and anti-biofilm peptide IDR1018 and chitosan nanoparticles on ciprofloxacin-resistant *Escherichia coli*. *J Basic Microbiol*. 2022;62:1229–40.
157. Zhao D, Yu S, Sun B, Gao S, Guo S, Zhao K. Biomedical applications of chitosan and its derivative nanoparticles. *Polymers (Basel)*. 2018;10:462.
158. Kimna C, Deger S, Tamburaci S, Tihminioglu F. Chitosan/montmorillonite composite nanospheres for sustained antibiotic delivery at post-implantation bone infection treatment. *Biomed Mater*. 2019;14: 044101.
159. Li Y, Liu C, Liu W, Cheng X, Zhang A, Zhang S, Liu C, Li N, et al. Apatite formation induced by chitosan/gelatin hydrogel coating anchored on poly(aryl ether nitrile ketone) substrates to promote osteoblastic differentiation. *Macromol Biosci*. 2021;21: e2100262.
160. Ge J, Li M, Fan J, Celia C, Xie Y, Chang Q, Deng X. Synthesis, characterization, and antibacterial activity of chitosan-chelated silver nanoparticles. *J Biomater Sci Polym Ed*. 2024;35:45–62.
161. Tao J, Zhang Y, Shen A, Yang Y, Diao L, Wang L, Cai D, Hu Y. Injectable chitosan-based thermosensitive hydrogel/nanoparticle-loaded system for local delivery of vancomycin in the treatment of osteomyelitis. *Int J Nanomed*. 2020;15:5855–71.
162. Yang Y, Li M, Luo H, Zhang D. Surface-decorated graphene oxide sheets with copper nano derivatives for bone regeneration: an in vitro and in vivo study regarding molecular mechanisms, osteogenesis, and anti-infection potential. *ACS Infect Dis*. 2022;8:499–515.
163. Iaconis GN, Lunetti P, Gallo N, Cappello AR, Fiermonte G, Dolce V, Capobianco L. Hyaluronic acid: a powerful biomolecule with wide-ranging applications—a comprehensive review. *Int J Mol Sci*. 2023;24:10296.
164. Romano CL, De Vecchi E, Bortolin M, Morelli I, Drago L. Hyaluronic acid and its composites as a local antimicrobial/antiadhesive barrier. *J Bone Jt Infect*. 2017;2:63–72.
165. He R, Sui J, Wang G, Wang Y, Xu K, Qin S, Xu S, Ji F, et al. Polydopamine and hyaluronic acid immobilisation on vancomycin-loaded titanium nanotube for prophylaxis of implant infections. *Colloids Surf B Biointerfaces*. 2022;216: 112582.
166. Yang J, Wang Y, Gao Y, Wang Z, Yin C, Ding X, Yang E, Sun D, et al. Efficient sterilization system combining flavonoids and hyaluronic acid with metal organic frameworks as carrier. *J Biomed Mater Res B Appl Biomater*. 2022;110:1887–98.
167. Valverde A, Perez-Alvarez L, Ruiz-Rubio L, Pacha Olivenza MA, Garcia Blanco MB, Diaz-Fuentes M, Vilas-Vilela JL. Antibacterial hyaluronic acid/chitosan multilayers onto smooth and micropatterned titanium surfaces. *Carbohydr Polym*. 2019;207:824–33.
168. Li G, Lai Z, Shan A. Advances of antimicrobial peptide-based biomaterials for the treatment of bacterial infections. *Adv Sci (Weinh)*. 2023;10: e2206602.
169. Wang G, Cui Y, Liu H, Tian Y, Li S, Fan Y, Sun S, Wu D, et al. Antibacterial peptides-loaded bioactive materials for the treatment of bone infection. *Colloids Surf B Biointerfaces*. 2023;225: 113255.
170. Xiao M, Jasensky J, Foster L, Kuroda K, Chen Z. Monitoring antimicrobial mechanisms of surface immobilized peptides in situ. *Langmuir*. 2018;34:2057–62.
171. Wang C, Hong T, Cui P, Wang J, Xia J. Antimicrobial peptides towards clinical application: delivery and formulation. *Adv Drug Deliv Rev*. 2021;175: 113818.
172. He Y, Jin Y, Ying X, Wu Q, Yao S, Li Y, Liu H, Ma G, et al. Development of an antimicrobial peptide loaded mineralized collagen bone scaffold for infective bone defect repair. *Regen Biomater*. 2020;7:515–25.
173. Zhou H, Zhu Y, Yang B, Huo Y, Yin Y, Jiang X, Ji W. Stimuli-responsive peptide hydrogels for biomedical applications. *J Mater Chem B*. 2024;12:1748–74.
174. Shuaishuai W, Tongtong Z, Dapeng W, Mingran Z, Xukai W, Yue Y, Hengliang D, Guangzhi W, et al. Implantable biomedical materials for treatment of bone infection. *Front Bioeng Biotechnol*. 2023;11:1081446.
175. Luo H, Yin XQ, Tan PF, Gu ZP, Liu ZM, Tan L. Polymeric antibacterial materials: design, platforms and applications. *J Mater Chem B*. 2021;9:2802–15.

176. Matos AC, Ribeiro IA, Guedes RC, Pinto R, Vaz MA, Goncalves LM, Almeida AJ, Bettencourt AF. Key-properties outlook of a levofloxacin-loaded acrylic bone cement with improved antibiotic delivery. *Int J Pharm*. 2015;485:317–28.
177. Gandomkarzadeh M, Moghimi HR, Mahboubi A. Evaluation of the effect of ciprofloxacin and vancomycin on mechanical properties of PMMA cement; a preliminary study on molecular weight. *Sci Rep*. 2020;10:3981.
178. Wang H, Maeda T, Miyazaki T. Preparation of bioactive and antibacterial PMMA-based bone cement by modification with quaternary ammonium and alkoxy silane. *J Biomater Appl*. 2021;36:311–20.
179. Tan H, Ma R, Lin C, Liu Z, Tang T. Quaternized chitosan as an antimicrobial agent: antimicrobial activity, mechanism of action and biomedical applications in orthopedics. *Int J Mol Sci*. 2013;14:1854–69.
180. Luo X, Xiao D, Zhang C, Wang G. The roles of exosomes upon metallic ions stimulation in bone regeneration. *J Funct Biomater*. 2022;13:126.
181. Cho H, Lee J, Jang S, Lee J, Oh TI, Son Y, Lee E. CaSR-mediated hBMSCs activity modulation: additional coupling mechanism in bone remodeling compartment. *Int J Mol Sci*. 2020;22:325.
182. Haag SL, Schiele NR, Bernards MT. Enhancement and mechanisms of MC3T3-E1 osteoblast-like cell adhesion to albumin through calcium exposure. *Biotechnol Appl Biochem*. 2022;69:492–502.
183. Zhang J, Wu Q, Yin C, Jia X, Zhao Z, Zhang X, Yuan G, Hu H, et al. Sustained calcium ion release from bioceramics promotes CaSR-mediated M2 macrophage polarization for osteoinduction. *J Leukoc Biol*. 2021;110:485–96.
184. Garcia E, Shalauova I, Matyus SP, Schutten JC, Bakker SJL, Dullaart RPF, Connelly MA. Nuclear magnetic resonance-measured ionized magnesium is inversely associated with type 2 diabetes in the insulin resistance atherosclerosis study. *Nutrients*. 2022;14:1792.
185. Wang J, Ma XY, Feng YF, Ma ZS, Ma TC, Zhang Y, Li X, Wang L, et al. Magnesium ions promote the biological behaviour of rat calvarial osteoblasts by activating the PI3K/Akt signalling pathway. *Biol Trace Elem Res*. 2017;179:284–93.
186. Choi S, Kim KJ, Cheon S, Kim EM, Kim YA, Park C, Kim KK. Biochemical activity of magnesium ions on human osteoblast migration. *Biochem Biophys Res Commun*. 2020;531:588–94.
187. Zhai Z, Qu X, Li H, Yang K, Wan P, Tan L, Ouyang Z, Liu X, et al. The effect of metallic magnesium degradation products on osteoclast-induced osteolysis and attenuation of NF- $\kappa$ B and NFATc1 signaling. *Biomaterials*. 2014;35:6299–310.
188. Zhang X, Chen Q, Mao X. Magnesium enhances osteogenesis of BMSCs by tuning osteoimmunomodulation. *Biomed Res Int*. 2019;2019:7908205.
189. Qiao W, Wong KHM, Shen J, Wang W, Wu J, Li J, Lin Z, Chen Z, et al. TRPM7 kinase-mediated immunomodulation in macrophage plays a central role in magnesium ion-induced bone regeneration. *Nat Commun*. 2021;12:2885.
190. Qin H, Weng J, Zhou B, Zhang W, Li G, Chen Y, Qi T, Zhu Y, et al. Magnesium ions promote in vitro rat bone marrow stromal cell angiogenesis through notch signaling. *Biol Trace Elem Res*. 2023;201:28232842.
191. Pilmane M, Salma-Ancane K, Loca D, Locs J, Berzina-Cimdina L. Strontium and strontium ranelate: historical review of some of their functions. *Mater Sci Eng C Mater Biol Appl*. 2017;78:1222–30.
192. Sun Y, Li Y, Zhang Y, Wang T, Lin K, Liu J. A polydopamine-assisted strontium-substituted apatite coating for titanium promotes osteogenesis and angiogenesis via FAK/MAPK and PI3K/AKT signaling pathways. *Mater Sci Eng C Mater Biol Appl*. 2021;131:112482.
193. Li T, He H, Yang Z, Wang J, Zhang Y, He G, Huang J, Song D, et al. Strontium-doped gelatin scaffolds promote M2 macrophage switch and angiogenesis through modulating the polarization of neutrophils. *Biomater Sci*. 2021;9:2931–46.
194. Naruphontjirakul P, Li S, Pinna A, Barrak F, Chen S, Redpath AN, Rankin SM, Porter AE, et al. Interaction of monodispersed strontium containing bioactive glass nanoparticles with macrophages. *Biomater Adv*. 2022;133:112610.
195. Baheiraei N, Eyni H, Bakhshi B, Najafloo R, Rabiee N. Effects of strontium ions with potential antibacterial activity on in vivo bone regeneration. *Sci Rep*. 2021;11:8745.
196. Wang S, Li R, Xia D, Zhao X, Zhu Y, Gu R, Yoon J, Liu Y. The impact of Zn-doped synthetic polymer materials on bone regeneration: a systematic review. *Stem Cell Res Ther*. 2021;12:123.
197. Qiao Y, Zhang W, Tian P, Meng F, Zhu H, Jiang X, Liu X, Chu PK. Stimulation of bone growth following zinc incorporation into biomaterials. *Biomaterials*. 2014;35:6882–97.
198. Suzuki M, Suzuki T, Watanabe M, Hatakeyama S, Kimura S, Nakazono A, Honma A, Nakamaru Y, et al. Role of intracellular zinc in molecular and cellular function in allergic inflammatory diseases. *Allergol Int*. 2021;70:190–200.
199. Ye J, Li B, Li M, Zheng Y, Wu S, Han Y. ROS induced bactericidal activity of amorphous Zn-doped titanium oxide coatings and enhanced osseointegration in bacteria-infected rat tibias. *Acta Biomater*. 2020;107:313–24.
200. Liu J, Zhao Y, Zhang Y, Yao X, Hang R. Exosomes derived from macrophages upon Zn ion stimulation promote osteoblast and endothelial cell functions. *J Mater Chem B*. 2021;9:3800–7.
201. Meng G, Wu X, Yao R, He J, Yao W, Wu F. Effect of zinc substitution in hydroxyapatite coating on osteoblast and osteoclast differentiation under osteoblast/osteoclast co-culture. *Regen Biomater*. 2019;6:349359.
202. Zhang H, Cui Y, Zhuo X, Kim J, Li H, Li S, Yang H, Su K, et al. Biological fixation of bioactive bone cement in vertebroplasty: the first clinical investigation of borosilicate glass (BSG) Reinforced PMMA bone cement. *ACS Appl Mater Interf*. 2022;14:51711–27.
203. Bee SL, Bustami Y, Ul-Hamid A, Lim K, Abdul Hamid ZA. Synthesis of silver nanoparticle-decorated hydroxyapatite nanocomposite with combined bioactivity and antibacterial properties. *J Mater Sci Mater Med*. 2021;32:106.
204. Vallet-Regi M, Ruiz-Hernandez E. Bioceramics: from bone regeneration to cancer nanomedicine. *Adv Mater*. 2011;23:5177–218.
205. Punj S, Singh J, Singh K. Ceramic biomaterials: properties, state of the art and future perspectives. *Ceram Int*. 2021;47:28059–74.
206. Wu S, Lei L, Bao C, Liu J, Weir MD, Ren K, Schneider A, Oates TW, et al. An injectable and antibacterial calcium phosphate scaffold inhibiting *Staphylococcus aureus* and supporting stem cells for bone regeneration. *Mater Sci Eng C Mater Biol Appl*. 2021;120:111688.
207. Calabrese G, Petralia S, Franco D, Nocito G, Fabbri C, Forte L, Guglielmino S, Squarizoni S, et al. A new Ag-nanostructured hydroxyapatite porous scaffold: antibacterial effect and cytotoxicity study. *Mater Sci Eng C Mater Biol Appl*. 2021;118:111394.
208. Fahimipour F, Rasouliyanboroujeni M, Dashtimoghaddam E, Khoshroo K, Tahriri M, Bastami F, Lobner D, Tayebi L. 3D printed TCP-based scaffold incorporating VEGF-loaded PLGA microspheres for craniofacial tissue engineering. *Dent Mater*. 2017;33:1205–16.
209. Yu T, Pan H, Hu Y, Tao H, Wang K, Zhang C. Autologous platelet-rich plasma induces bone formation of tissue-engineered bone with bone marrow mesenchymal stem cells on beta-tricalcium phosphate ceramics. *J Orthop Surg Res*. 2017;12:178.
210. Liu Y, Zhao Q, Chen C, Wu C, Ma Y. beta-tricalcium phosphate/gelatin composite scaffolds incorporated with gentamycin-loaded chitosan microspheres for infected bone defect treatment. *PLoS ONE*. 2022;17:e0277522.
211. Pattnaik S, Nethala S, Tripathi A, Saravanan S, Moorthi A, Selvamurugan N. Chitosan scaffolds containing silicon dioxide and zirconia nanoparticles for bone tissue engineering. *Int J Biol Macromol*. 2011;49:1167–72.
212. Zhao X, Li P, Guo B, Ma PX. Antibacterial and conductive injectable hydrogels based on quaternized chitosan-graft-polyaniline/oxidized dextran for tissue engineering. *Acta Biomater*. 2015;26:236–48.
213. Oftadeh MO, Bakhshandeh B, Dehghan MM, Khojasteh A. Sequential application of mineralized electroconductive scaffold and electrical stimulation for efficient osteogenesis. *J Biomed Mater Res A*. 2018;106:1200–10.
214. Kazimierzczak P, Kolmas J, Przekora A. Biological response to macroporous chitosan-agarose bone scaffolds comprising Mg- and Zn-doped nano-hydroxyapatite. *Int J Mol Sci*. 2019;20:3835.
215. Liu S, Li Z, Wang Q, Han J, Wang W, Li S, Liu H, Guo S, et al. Graphene oxide/chitosan/hydroxyapatite composite membranes enhance osteoblast adhesion and guided bone regeneration. *ACS Appl Bio Mater*. 2021;4:8049–59.
216. Ciolek L, Krok-Borkowicz M, Gasinski A, Biernat M, Antosik A, Pamula E. Bioactive glasses enriched with strontium or zinc with different degrees

- of structural order as components of chitosan-based composite scaffolds for bone tissue engineering. *Polymers (Basel)*. 2023;15:3994.
217. Adithya SP, Sidharthan DS, Abhinandan R, Balagangadharan K, Selvamurugan N. Nanosheets incorporated bio-composites containing natural and synthetic polymers/ceramics for bone tissue engineering. *Int J Biol Macromol*. 2020;164:1960–72.
  218. Divband B, Aghazadeh M, Al-Qaim ZH, Samiei M, Hussein FH, Shaabani A, Shahi S, Sedghi R. Bioactive chitosan biguanidine-based injectable hydrogels as a novel BMP-2 and VEGF carrier for osteogenesis of dental pulp stem cells. *Carbohydr Polym*. 2021;273: 118589.
  219. Han S, Yang H, Ni X, Deng Y, Li Z, Xing X, Du M. Programmed release of vascular endothelial growth factor and exosome from injectable chitosan nanofibrous microsphere-based PLGA-PEG-PLGA hydrogel for enhanced bone regeneration. *Int J Biol Macromol*. 2023;253: 126721.
  220. Stuckensen K, Schwab A, Knauer M, Muinos-Lopez E, Ehlicke F, Reboredo J, Granero-Molto F, Gbureck U, et al. Tissue mimicry in morphology and composition promotes hierarchical matrix remodeling of invading stem cells in osteochondral and meniscus scaffolds. *Adv Mater*. 2018;30: e1706754.
  221. Loessner D, Meinert C, Kaemmerer E, Martine LC, Yue K, Levett PA, Klein TJ, Melchels FP, et al. Functionalization, preparation and use of cell-laden gelatin methacryloyl-based hydrogels as modular tissue culture platforms. *Nat Protoc*. 2016;11:727–46.
  222. Sarker B, Zehnder T, Rath SN, Horch RE, Kneser U, Detsch R, Boccaccini AR. Oxidized alginate gelatin hydrogel: a favorable matrix for growth and osteogenic differentiation of adipose-derived stem cells in 3D. *ACS Biomater Sci Eng*. 2017;3:1730–7.
  223. Filippi M, Born G, Chaaban M, Scherberich A. Natural polymeric scaffolds in bone regeneration. *Front Bioeng Biotechnol*. 2020;8:474.
  224. Tamay DG, Dursun Usal T, Alagoz AS, Yucel D, Hasirci N, Hasirci V. 3D and 4D printing of polymers for tissue engineering applications. *Front Bioeng Biotechnol*. 2019;7:164.
  225. Lueckgen A, Garske DS, Ellinghaus A, Mooney DJ, Duda GN, Cipitria A. Enzymatically-degradable alginate hydrogels promote cell spreading and in vivo tissue infiltration. *Biomaterials*. 2019;217: 119294.
  226. Zhao D, Wang X, Cheng B, Yin M, Hou Z, Li X, Liu K, Tie C, et al. Degradation-kinetics-controllable and tissue-regeneration-matchable photocross-linked alginate hydrogels for bone repair. *ACS Appl Mater Interfaces*. 2022;14:21886–905.
  227. Ueng SW, Lin SS, Wang IC, Yang CY, Cheng RC, Liu SJ, Chan EC, Lai CF, et al. Efficacy of vancomycin-releasing biodegradable poly(lactide-co-glycolide) antibiotics beads for treatment of experimental bone infection due to *Staphylococcus aureus*. *J Orthop Surg Res*. 2016;11:52.
  228. Li X, Huang X, Li L, Wu J, Yi W, Lai Y, Qin L. LL-37-coupled porous composite scaffold for the treatment of infected segmental bone defect. *Pharmaceutics*. 2022;15:1792.
  229. Garcia-Garcia J, Azuara G, Fraile-Martinez O, Garcia-Montero C, Alvarez-Mon MA, Ruiz-Diez S, Alvarez-Mon M, Bujan J, et al. Modification of the polymer of a bone cement with biodegradable microspheres of PLGA and loading with daptomycin and vancomycin improve the response to bone tissue infection. *Polymers (Basel)*. 2022;14:888.
  230. He M, Wang H, Han Q, Shi X, He S, Sun J, Zhu Z, Gan X, et al. Glucose-primed PEEK orthopaedic implants for antibacterial therapy and safeguarding diabetic osseointegration. *Biomaterials*. 2023;303: 122355.
  231. Wei S, Jian C, Xu F, Bao T, Lan S, Wu G, Qi B, Bai Z, et al. Vancomycin-impregnated electrospun polycaprolactone (PCL) membrane for the treatment of infected bone defects: an animal study. *J Biomater Appl*. 2018;32:1187–96.
  232. Al Thayer Y, Alotaibi HF, Yang L, Prokopovich P. PMMA bone cement containing long releasing silicabased chlorhexidine nanocarriers. *PLoS ONE*. 2021;16: e0257947.
  233. Koons GL, Diba M, Mikos AG. Materials design for bone-tissue engineering. *Nat Rev Mater*. 2020;5:584–603.
  234. Zhang L, Yang G, Johnson BN, Jia X. Three-dimensional (3D) printed scaffold and material selection for bone repair. *Acta Biomater*. 2019;84:16–33.
  235. Liu S, Han Z, Hao JN, Zhang D, Li X, Cao Y, Huang J, Li Y. Engineering of a NIR-activable hydrogel coated mesoporous bioactive glass scaffold with dual-mode parathyroid hormone derivative release property for angiogenesis and bone regeneration. *Bioact Mater*. 2023;26:1–13.
  236. Li W, Wu Y, Zhang X, Wu T, Huang K, Wang B, Liao J. Self-healing hydrogels for bone defect repair. *RSC Adv*. 2023;13:16773–88.
  237. Qiu M, Tulufu N, Tang G, Ye W, Qi J, Deng L, Li C. Black phosphorus accelerates bone regeneration based on immunoregulation. *Adv Sci (Weinh)*. 2024;11: e2304824.
  238. Seliktar D. Designing cell-compatible hydrogels for biomedical applications. *Science*. 2012;336:11241128.
  239. Jose G, Shalomon KT, Chen JP. Natural Polymers based hydrogels for cell culture applications. *Curr Med Chem*. 2020;27:2734–76.
  240. Wei M, Hsu Y-I, Asoh T-A, Sung M-H, Uyama H. Injectable poly( $\gamma$ -glutamic acid)-based biodegradable hydrogels with tunable gelation rate and mechanical strength. *J Mater Chem B*. 2021;9:3584–94.
  241. Nie R, Sun Y, Lv H, Lu M, Huangfu H, Li Y, Zhang Y, Wang D, et al. 3D printing of MXene composite hydrogel scaffolds for photothermal antibacterial activity and bone regeneration in infected bone defect models. *Nanoscale*. 2022;14:8112–29.
  242. Huang Y, Zhai X, Ma T, Zhang M, Yang H, Zhang S, Wang J, Liu W, et al. A unified therapeutic prophylactic tissue-engineering scaffold demonstrated to prevent tumor recurrence and overcoming infection toward bone remodeling. *Adv Mater*. 2023;35: e2300313.
  243. Xu Y, Xu C, Yang K, Ma L, Li G, Shi Y, Feng X, Tan L, et al. Copper Ion-modified germanium phosphorus nanosheets integrated with an electroactive and biodegradable hydrogel for neuro-vascularized bone regeneration. *Adv Healthc Mater*. 2023;12: e2301151.
  244. Qi H, Wang B, Wang M, Xie H, Chen C. A pH/ROS-responsive antioxidative and antimicrobial GelMA hydrogel for on-demand drug delivery and enhanced osteogenic differentiation in vitro. *Int J Pharm*. 2024;657: 124134.
  245. Qin B, Dong H, Tang X, Liu Y, Feng G, Wu S, Zhang H. Antisense yycF and BMP-2 co-delivery gelatin methacryloyl and carboxymethyl chitosan hydrogel composite for infective bone defects regeneration. *Int J Biol Macromol*. 2023;253: 127233.
  246. Wang S, Lei H, Mi Y, Ma P, Fan D. Chitosan and hyaluronic acid based injectable dual network hydrogels—mediating antimicrobial and inflammatory modulation to promote healing of infected bone defects. *Int J Biol Macromol*. 2024;274: 133124.
  247. Zhang Q, Zhou X, Du H, Ha Y, Xu Y, Ao R, He C. Bifunctional hydrogel-integrated 3D printed scaffold for repairing infected bone defects. *ACS Biomater Sci Eng*. 2023;9:4583–96.
  248. Xu L, Ye Q, Xie J, Yang J, Jiang W, Yuan H, Li J. An injectable gellan gum-based hydrogel that inhibits *Staphylococcus aureus* for infected bone defect repair. *J Mater Chem B*. 2022;10:282–92.
  249. Guan X, Wu S, Ouyang S, Ren S, Cui N, Wu X, Xiang D, Chen W, et al. Remodeling microenvironment for implant-associated osteomyelitis by dual metal peroxide. *Adv Healthc Mater*. 2024;13: e2303529.
  250. Klotz BJ, Gawlitta D, Rosenberg A, Malda J, Melchels FPW. Gelatin-methacryloyl hydrogels: towards biofabrication-based tissue repair. *Trends Biotechnol*. 2016;34:394–407.
  251. Lv B, Lu L, Hu L, Cheng P, Hu Y, Xie X, Dai G, Mi B, et al. Recent advances in GelMA hydrogel transplantation for musculoskeletal disorders and related disease treatment. *Theranostics*. 2023;13:2015–39.
  252. Kurian AG, Singh RK, Patel KD, Lee JH, Kim HW. Multifunctional GelMA platforms with nanomaterials for advanced tissue therapeutics. *Bioact Mater*. 2022;8:267–95.
  253. Mahmoud AH, Han Y, Dal-Fabbro R, Daghrery A, Xu J, Kaigler D, Bhaduri SB, Malda J, et al. Nanoscale beta-TCP-laden GelMA/PCL composite membrane for guided bone regeneration. *ACS Appl Mater Interfaces*. 2023;15:32121–35.
  254. Li H, Li J, Jiang J, Lv F, Chang J, Chen S, Wu C. An osteogenesis/angiogenesis-stimulation artificial ligament for anterior cruciate ligament reconstruction. *Acta Biomater*. 2017;54:399–410.
  255. Yang B, Song J, Jiang Y, Li M, Wei J, Qin J, Peng W, Lopez Lasaoa F, et al. Injectable adhesive self healing multicross-linked double-network hydrogel facilitates full-thickness skin wound healing. *ACS Appl Mater Interfaces*. 2020;12:57782–97.
  256. Wang L, Wang J, Zhou X, Sun J, Zhu B, Duan C, Chen P, Guo X, et al. A new self-healing hydrogel containing hucMSC-derived exosomes promotes bone regeneration. *Front Bioeng Biotechnol*. 2020;8: 564731.
  257. Chen L, Yu C, Xiong Y, Chen K, Liu P, Panayi AC, Xiao X, Feng Q, et al. Multifunctional hydrogel enhances bone regeneration through sustained

- release of stromal cell-derived factor-1alpha and exosomes. *Bioact Mater.* 2023;25:460–71.
258. Bai H, Zhao Y, Wang C, Wang Z, Wang J, Liu H, Feng Y, Lin Q, et al. Enhanced osseointegration of three-dimensional supramolecular bioactive interface through osteoporotic microenvironment regulation. *Theranostics.* 2020;10:4779–94.
  259. Pariza G, Mavrodin CI, Antoniac I. Dependency between the porosity and polymeric structure of biomaterials used in hernia surgery and chronic mesh - infection. *Mater Plast.* 2015;1:4.
  260. Zhao Y, Wang Z, Jiang Y, Liu H, Song S, Wang C, Li Z, Yang Z, et al. Biomimetic composite scaffold to manipulate stem cells for aiding rheumatoid arthritis management. *Adv Funct Mater.* 2019;29:1807860.
  261. Qiao S, Wu D, Li Z, Zhu Y, Zhan F, Lai H, Gu Y. The combination of multi-functional ingredients loaded hydrogels and three-dimensional printed porous titanium alloys for infective bone defect treatment. *J Tissue Eng.* 2020;11:2041731420965797.
  262. Wang K, Li Y, Xie LH, Li X, Li JR. Construction and application of base-stable MOFs: a critical review. *Chem Soc Rev.* 2022;51:6417–41.
  263. Stanley PM, Haimerl J, Shustova NB, Fischer RA, Warnan J. Merging molecular catalysts and metal-organic frameworks for photocatalytic fuel production. *Nat Chem.* 2022;14:1342–56.
  264. Zhou HC, Kitagawa S. Metal-organic frameworks (MOFs). *Chem Soc Rev.* 2014;43:5415–8.
  265. Mallakpour S, Nikkhoo E, Hussain CM. Application of MOF materials as drug delivery systems for cancer therapy and dermal treatment. *Coord Chem Rev.* 2022;451:214262.
  266. Ma X, Ren X, Guo X, Fu C, Wu Q, Tan L, Li H, Zhang W, et al. Multi-functional iron-based metal organic framework as biodegradable nanozyme for microwave enhancing dynamic therapy. *Biomaterials.* 2019;214: 119223.
  267. Zhu ZH, Liu Y, Song C, Hu Y, Feng G, Tang BZ. Porphyrin-based two-dimensional layered metal-organic framework with sono-/ photocatalytic activity for water decontamination. *ACS Nano.* 2022;16:13461357.
  268. Meng J, Liu X, Niu C, Pang Q, Li J, Liu F, Liu Z, Mai L. Advances in metal-organic framework coatings: versatile synthesis and broad applications. *Chem Soc Rev.* 2020;49:3142–86.
  269. Ma L, Cheng Y, Feng X, Zhang X, Lei J, Wang H, Xu Y, Tong B, et al. A janus-ROS healing system promoting infectious bone regeneration via sono-epigenetic modulation. *Adv Mater.* 2024;36: e2307846.
  270. Yan B, Tan J, Zhang H, Liu L, Chen L, Qiao Y, Liu X. Constructing fluorine-doped Zr-MOF films on titanium for antibacteria, anti-inflammation, and osteogenesis. *Biomater Adv.* 2022;134: 112699.
  271. Karakecili A, Topuz B, Ersoy FS, Sahin T, Gunyakti A, Demirtas TT. UiO-66 metal-organic framework as a double actor in chitosan scaffolds: antibiotic carrier and osteogenesis promoter. *Biomater Adv.* 2022;136: 212757.
  272. Yang X, Chai H, Guo L, Jiang Y, Xu L, Huang W, Shen Y, Yu L, et al. In situ preparation of porous metal-organic frameworks ZIF-8@Ag on poly-ether-ether-ketone with synergistic antibacterial activity. *Colloids Surf B Biointerf.* 2021;205: 111920.
  273. Karakecili A, Topuz B, Korpayev S, Erdek M. Metal-organic frameworks for on-demand pH controlled delivery of vancomycin from chitosan scaffolds. *Mater Sci Eng C Mater Biol Appl.* 2019;105: 110098.
  274. Fandzloch M, Augustyniak AW, Trzcinska-Wencel J, Golinska P, Roszek K. A new MOF@bioactive glass composite reinforced with silver nanoparticles—a new approach to designing antibacterial biomaterials. *Dalton Trans.* 2024;53:10928–37.
  275. Tao B, Lin C, He Y, Yuan Z, Chen M, Xu K, Li K, Guo A, et al. Osteoimmunomodulation mediating improved osteointegration by OGP-loaded cobalt-metal organic framework on titanium implants with antibacterial property. *Chem Eng J.* 2021;423:130176.
  276. Wang B, Chen H, Peng S, Li X, Liu X, Ren H, Yan Y, Zhang Q. Multi-functional magnesium-organic framework doped biodegradable bone cement for antibacterial growth, inflammatory regulation and osteogenic differentiation. *J Mater Chem B.* 2023;11:2872–85.
  277. Kaya S, Cresswell M, Boccaccini AR. Mesoporous silica-based bioactive glasses for antibiotic-free anti bacterial applications. *Mater Sci Eng C Mater Biol Appl.* 2018;83:99–107.
  278. Han L, Huang Z, Zhu M, Zhu Y, Li H. Drug-loaded zeolite imidazole framework-8-functionalized bioglass scaffolds with antibacterial activity for bone repair. *Ceram Int.* 2022;48:6890.
  279. Xiao T, Fan L, Liu R, Huang X, Wang S, Xiao L, Pang Y, Li D, et al. Fabrication of dexamethasone-loaded dual-metal-organic frameworks on poly(ether ether ketone) implants with bacteriostasis and angiogenesis properties for promoting bone regeneration. *ACS Appl Mater Interf.* 2021;13:50836–50.
  280. Shou P, Yu Z, Wu Y, Feng Q, Zhou B, Xing J, Liu C, Tu J, et al. Zn(2+) doped ultrasmall prussian blue nanotheranostic agent for breast cancer photothermal therapy under MR imaging guidance. *Adv Healthc Mater.* 2020;9: e1900948.
  281. Li ZH, Chen Y, Sun Y, Zhang XZ. Platinum-doped prussian blue nanozymes for multiwavelength bioimaging guided photothermal therapy of tumor and anti-inflammation. *ACS Nano.* 2021;15:5189–200.
  282. Han D, Li Y, Liu X, Li B, Han Y, Zheng Y, Yeung KW, Li C, Cui Z, Liang Y, Li Z. Rapid bacteria trapping and killing of metal-organic frameworks strengthened photo-responsive hydrogel for rapid tissue repair of bacterial infected wounds. *Chem Eng J.* 2020;396:125194.
  283. Zhao C, Shu C, Yu J, Zhu Y. Metal-organic frameworks functionalized biomaterials for promoting bone repair. *Mater Today Bio.* 2023;21: 100717.
  284. Li J, Song S, Meng J, Tan L, Liu X, Zheng Y, Li Z, Yeung KW, et al. 2D MOF periodontitis photodynamic ion therapy. *J Am Chem Soc.* 2021;143:15427–39.
  285. Dang W, Ma B, Li B, Huan Z, Ma N, Zhu H, Chang J, Xiao Y, et al. 3D printing of metal-organic framework nanosheets-structured scaffolds with tumor therapy and bone construction. *Biofabrication.* 2020;12: 025005.
  286. Xu W, Jambhulkar S, Zhu Y, Ravichandran D, Song K. 3D printing for polymer/particle-based processing: A Review. *Compos Part B Eng.* 2021;223:109102.
  287. Ghosh C, Sarkar P, Issa R, Halder J. Alternatives to conventional antibiotics in the era of antimicrobial resistance. *Trends Microbiol.* 2019;27:323–38.
  288. Lee J, Byun H, Madhurakkt Perikamana SK, Lee S, Shin H. Current advances in immunomodulatory biomaterials for bone regeneration. *Adv Healthc Mater.* 2019;8: e1801106.
  289. Mo S, Tang K, Liao Q, Xie L, Wu Y, Wang G, Ruan Q, Gao A, et al. Tuning the arrangement of lamellar nanostructures: achieving the dual function of physically killing bacteria and promoting osteogenesis. *Mater Horiz.* 2023;10:881–8.
  290. Bogatcheva E, Dubuisson T, Protopopova M, Einck L, Nacy CA, Reddy VM. Chemical modification of capuramycins to enhance antibacterial activity. *J Antimicrob Chemother.* 2011;66:578–87.
  291. Yavari SA, Croes M, Akhavan B, Jahanmard F, Eigenhuis CC, Dadbakhsh S, Vogely HC, Bilek MM, et al. Layer by layer coating for bio-functionalization of additively manufactured meta-biomaterials. *Add Manuf.* 2020. <https://doi.org/10.1016/j.addma.2019.100991>.
  292. Grayson WL, Bunnell BA, Martin E, Frazier T, Hung BP, Gimble JM. Stromal cells and stem cells in clinical bone regeneration. *Nat Rev Endocrinol.* 2015;11:140–50.
  293. Wang H, Li X, Lai S, Cao Q, Liu Y, Li J, Zhu X, Fu W, et al. Construction of vascularized tissue engineered bone with nHA-coated BCP bioceramics loaded with peripheral blood-derived MSC and EPC to repair large segmental femoral bone defect. *ACS Appl Mater Interfaces.* 2023;15:249–64.
  294. Wang M, Li H, Yang Y, Yuan K, Zhou F, Liu H, Zhou Q, Yang S, et al. A 3D-bioprinted scaffold with doxycycline-controlled BMP2-expressing cells for inducing bone regeneration and inhibiting bacterial infection. *Bioact Mater.* 2021;6:1318–29.
  295. Kuang Z, Dai G, Wan R, Zhang D, Zhao C, Chen C, Li J, Gu H, et al. Osteogenic and antibacterial dual functions of a novel levofloxacin loaded mesoporous silica microspheres/nano-hydroxyapatite/polyurethane composite scaffold. *Genes Dis.* 2021;8:193–202.
  296. Lin Liang Z, Chen L, Quan WY. 3D printed PLGA scaffold with nano-hydroxyapatite carrying linezolid for treatment of infected bone defects. *Biomed Pharmacother.* 2024;172:116228.



297. Qayoom I, Teotia AK, Panjla A, Verma S, Kumar A. Local and sustained delivery of rifampicin from a bioactive ceramic carrier treats bone infection in rat tibia. *ACS Infect Dis*. 2020;6:2938–49.
298. Yuan J, Wang B, Han C, Huang X, Xiao H, Lu X, Lu J, Zhang D, et al. Nanosized-Ag-doped porous beta-tricalcium phosphate for biological applications. *Mater Sci Eng C Mater Biol Appl*. 2020;114: 111037.
299. Alves APN, Arango-Ospina M, Oliveira R, Ferreira IM, de Moraes EG, Hartmann M, de Oliveira APN, Boccacini AR, et al. 3D-printed beta-TCP/S53P4 bioactive glass scaffolds coated with tea tree oil: coating optimization, in vitro bioactivity and antibacterial properties. *J Biomed Mater Res B Appl Biomater*. 2023;111:881–94.
300. Hu X, Chen J, Yang S, Zhang Z, Wu H, He J, Qin L, Cao J, et al. 3D printed multifunctional biomimetic bone scaffold combined with TP-Mg nanoparticles for the infectious bone defects repair. *Small*. 2024;20: e2403681.
301. Ji Y, Yang S, Sun J, Ning C. Realizing both antibacterial activity and cytocompatibility in silicocarnotite bioceramic via germanium incorporation. *J Funct Biomater*. 2023;14:154.
302. Rumian L, Tiainen H, Cibor U, Krok-Borkowicz M, Brzychczy-Wloch M, Haugen HJ, Pamula E. Ceramic scaffolds enriched with gentamicin loaded poly(lactide-co-glycolide) microparticles for prevention and treatment of bone tissue infections. *Mater Sci Eng C Mater Biol Appl*. 2016;69:856–64.
303. Cheng T, Qu H, Zhang G, Zhang X. Osteogenic and antibacterial properties of vancomycin-laden mesoporous bioglass/PLGA composite scaffolds for bone regeneration in infected bone defects. *Artif Cells Nanomed Biotechnol*. 2018;46:1935–47.
304. Sun H, Hu C, Zhou C, Wu L, Sun J, Zhou X, Xing F, Long C, et al. 3D printing of calcium phosphate scaffolds with controlled release of antibacterial functions for jaw bone repair. *Mater Des*. 2020;189:108540.
305. Kargozar S, Montazerian M, Hamzehlou S, Kim HW, Baino F. Mesoporous bioactive glasses: promising platforms for antibacterial strategies. *Acta Biomater*. 2018;81:1–19.
306. Ke D, Tarafder S, Vahabzadeh S, Bose S. Effects of MgO, ZnO, SrO, and SiO<sub>2</sub> in tricalcium phosphate scaffolds on in vitro gene expression and in vivo osteogenesis. *Mater Sci Eng C Mater Biol Appl*. 2019;96:10–9.
307. Xu Q, Chang M, Zhang Y, Wang E, Xing M, Gao L, Huan Z, Guo F, et al. PDA/Cu bioactive hydrogel with “hot ions effect” for inhibition of drug-resistant bacteria and enhancement of infectious skin wound healing. *ACS Appl Mater Interfaces*. 2020;12:31255–69.
308. Zhang Y, Zhai D, Xu M, Yao Q, Zhu H, Chang J, Wu C. 3D-printed bioceramic scaffolds with antibacterial and osteogenic activity. *Biofabrication*. 2017;9: 025037.
309. Baino F, Potestio I, Vitale-Brovarone C. Production and physicochemical characterization of cup-doped silicate bioceramic scaffolds. *Materials (Basel)*. 2018;11:1524.
310. Sugimoto H, Biggemann J, Fey T, Singh P, Kakimoto KI. Lead-free piezoelectric (Ba, Ca)(Ti, Zr)O<sub>3</sub> scaffolds for enhanced antibacterial property. *Mater Lett*. 2021;297: 129969.
311. Wang X, Han X, Li C, Chen Z, Huang H, Chen J, Wu C, Fan T, et al. 2D materials for bone therapy. *Adv Drug Deliv Rev*. 2021;178: 113970.
312. Zhao Y, Kang H, Xia Y, Sun L, Li F, Dai H. 3D printed photothermal scaffold sandwiching bacteria inside and outside improves the infected micro environment and repairs bone defects. *Adv Healthc Mater*. 2024;13: e2302879.
313. He Y, Liu X, Lei J, Ma L, Zhang X, Wang H, Lei C, Feng X, et al. Correction: bioactive VS4-based sonosensitizer for robust chemodynamic, sonodynamic and osteogenic therapy of infected bone defects. *J Nanobiotechnology*. 2024;22:46.
314. Huang Y, Li J, Yu Z, Li J, Liang K, Deng Y. Elaborated bio-heterojunction with robust sterilization effect for infected tissue regeneration via activating competent cell-like antibacterial tactic. *Adv Mater*. 2024;36: e2414111.
315. Zhang L, Zhang H, Zhou H, Tan Y, Zhang Z, Yang W, Zhao L, Zhao Z. A Ti(3)C(2) MXene-integrated near-infrared-responsive multifunctional porous scaffold for infected bone defect repair. *J Mater Chem B*. 2023;12:79–96.
316. Jing X, Xu C, Su W, Ding Q, Ye B, Su Y, Yu K, Zeng L, et al. Photosensitive and conductive hydrogel induced innervated bone regeneration for infected bone defect repair. *Adv Healthc Mater*. 2023;12: e2201349.
317. Wu Y, Liao Q, Wu L, Luo Y, Zhang W, Guan M, Pan H, Tong L, et al. ZnL(2)-BPs integrated bone scaffold under sequential photothermal mediation: a win-win strategy delivering antibacterial therapy and fostering osteogenesis thereafter. *ACS Nano*. 2021;15:17854–69.
318. Li Y, Liu C, Cheng X, Wang J, Pan Y, Liu C, Zhang S, Jian X. PDA-BPs integrated mussel-inspired multifunctional hydrogel coating on PPENK implants for anti-tumor therapy, antibacterial infection and bone regeneration. *Bioact Mater*. 2023;27:546–59.
319. Zhu C, He M, Sun D, Huang Y, Huang L, Du M, Wang J, Wang J, et al. 3D-printed multifunctional polyetheretherketone bone scaffold for multimodal treatment of osteosarcoma and osteomyelitis. *ACS Appl Mater Interfaces*. 2021;13:47327–40.
320. Fu M, Li J, Liu M, Yang C, Wang Q, Wang H, Chen B, Fu Q, et al. Sericin/nano-hydroxyapatite hydrogels based on graphene oxide for effective bone regeneration via immunomodulation and osteoinduction. *Int J Nanomedicine*. 2023;18:1875–95.
321. Wu S, Gan T, Xie L, Deng S, Liu Y, Zhang H, Hu X, Lei L. Antibacterial performance of graphene oxide/alginate-based antisense hydrogel for potential therapeutic application in *Staphylococcus aureus* infection. *Biomater Adv*. 2022;141: 213121.
322. Jin L, Wu S, Mao C, Wang C, Zhu S, Zheng Y, Zhang Y, Li Z, et al. Rapid and effective treatment of chronic osteomyelitis by conductive network-like MoS<sub>2</sub>/CNTs through multiple reflection and scattering enhanced synergistic therapy. *Bioact Mater*. 2024;31:284–97.
323. Parajuli D, Murali N, Cad K, Karki B, Samatha K, Kim AA, Park M, Pant B. Advancements in MXene polymer nanocomposites in energy storage and biomedical applications. *Polymers (Basel)*. 2022;14:3433.
324. Yin J, Han Q, Zhang J, Liu Y, Gan X, Xie K, Xie L, Deng Y. MXene-based hydrogels endow polyetheretherketone with effective osteogenicity and combined treatment of osteosarcoma and bacterial infection. *ACS Appl Mater Interfaces*. 2020;12:45891–903.
325. Wu M, Liu H, Zhu Y, Chen F, Chen Z, Guo L, Wu P, Li G, et al. Mild photothermal-stimulation based on injectable and photocurable hydrogels orchestrates immunomodulation and osteogenesis for high performance bone regeneration. *Small*. 2023;19: e2300111.
326. Vergara A, Fernandez-Pittol MJ, Munoz-Mahamud E, Morata L, Bosch J, Vila J, Soriano A, Casals Pascual C. Evaluation of lipocalin-2 as a biomarker of periprosthetic joint infection. *J Arthroplasty*. 2019;34:123–5.

## Publisher's Note

Springer Nature remains neutral with regard to jurisdictional claims in published maps and institutional affiliations.